POLYCYCLIC AZINES: SYNTHESIS AND THE USE OF NUCLEAR MAGNETIC RESONANCE TECHNIQUES FOR STRUCTURAL, MECHANISTIC, AND KINETIC ELUCIDATION

By

CARLTON D. DILL

A DISSERTATION PRESENTED TO THE GRADUATE SCHOOL
OF THE UNIVERSITY OF FLORIDA IN PARTIAL FULFILLMENT
OF THE REQUIREMENTS FOR THE DEGREE OF
DOCTOR OF PHILOSOPHY

UNIVERSITY OF FLORIDA

1997

This work is lovingly dedicated to my parents, Robert and Brenda Dill, and my sisters, Carren and Connie. Such a family is truly a blessing from God.

This dedication is also extended to my grandparents, aunts, uncles, cousins, and friends who have all been so very understanding and supportive.

ACKNOWLEDGEMNTS

The author wishes to extend tremendous gratitude to Dr. John A. Zoltewicz for his guidance, patience, and encouragement throughout the course of these studies. Dr. Zoltewicz made this a pleasurable learning experience that will extend into many facets of life. Appreciation is also extended to the members of the supervisory committee, Dr. J. E. Enholm, Dr. K. S. Schanze, Dr. R. J. Hanrahan, and Dr. W. R. Kem, as well as Dr. Roy King and Dr. Khalil Abboud.

Special thanks are due to Dr. Michael Cruskie, Dr. Norbert Maier, and Sophie Lavieri for camaraderie and encouragement in the laboratory.

To all my friends too numerous to mention, I wish to say thanks, but especially to Tony Dribben, Nagraj Bokinkere, and Lucian Boldea. It has been fun. Tony, thanks for putting up with me as a roommate.

From the teaching lab, Dr. Merle A. Battiste, Julie Ann Steffens, all of the teaching assistants and stockroom assistants, and all my students, I owe you all a great debt of gratitude.

Financial support from the Chemistry Department, Division of Sponsored Research, Taiho Pharmaceutical Co., and the Department of Pharmacology is gratefully acknowledged.

Finally, Honor and thanks to God, without whom none of this would be possible.

TABLE OF CONTENTS

page

ACKNOWLEDGEMNTS iii

LIST OF TABLES vii

LIST OF FIGURES x

ABSTRACT. xiii

CHAPTERS

1 INTRODUCTION. 1

2 STRUCTURE AND KINETIC STUDIES OF DIHYDROTHIAMIN ISOMERS BY NMR AND X-RAY CYRSTALLOGRAPHY 13

- Introduction 13
- Results and Discussion 15
  - Preparation of Dihydrothiamin Isomers 15
  - Structure Determinations of Normal-Dihydrothiamin and Iso-Dihydrothiamin. . 17
  - Structure Determination for Pseudo-Dihydrothiamin 25
  - NMR Scale Conversions of 2-3 to 2-4 29
  - Kinetics of Trapping with Hydride 31
  - Mechanism of Ring-Opening and Ring-Closing. . 39
- Conclusions 42

3 INTER-RING DIRECTED *ORTHO* LITHIATION BY THE 2-PYRIDYL GROUP IN BIPYRIDINES 44

- Introduction 44
- Results and Discussion 46
  - Lithiation and Electrophilic Substitution . . 46
  - Palladium-Catalyzed Cross-Coupling of Stannanes. 46
  - Structure Determination of BPYs 48
  - Structure Determination of Terpyridines . . . 51
- Conclusions 56

4 DIRECT PREPARATION OF N-QUATERNIZED POLYCYCLIC AZINES BY PALLADIUM-CATALYZED CROSS-COUPLING 57

Introduction 57
Results and Discussion 61
Preparation of the Representative Compounds . 61
Structure Determinations. 62
Conclusions 64

5 RELAXATION AND METAL-SUBSTRATE COMPLEX LIFETIME INFLUENCES ON NUCLEAR RELAXATION RATES OF FUNCTIONALIZED BIPYRIDINES. 66

Introduction 66
Results and Discussion 71
Preparation of Substances and Stock Solutions 71
Measurement of T_1 Relaxation Values 75
Data Manipulation of the Relaxation Values. . 78
Example with MEBPY. 83
Substrate Summaries 84
Temperature Considerations. 95
Interpretation of the Results 97
Conclusions 100

6 EXPERIMENTAL 102

APPENDIX T_1 RELAXATION DATA 135

REFERENCES. 152

BIOGRAPHICAL SKETCH 160

LIST OF TABLES

Table page

2-1. Concentrations and Rate Constants from the Respective Kinetic Experiments. 38

5-1. T_1 Relaxation Values and Rate Constants for the Respective Protons of MEBPY in the Absence of $NiCl_2$ at 25 °C 83

5-2. Corrected Rate Constant Values for the Protons at Several Nickel Concentrations at 25 °C in D_2O. . 83

5-3. Second-order Relaxation Rate Constants (k_2, M^{-1}-s^{-1}) for MEBPY in Several Solvents Containing Paramagnetic Salts at 25 °C 85

5-4. Relaxation Rate Constants (k_2) for the Carbon Atoms in MEBPY and Distances Between These Atoms and Bound Ni(II) in D_2O at 25 °C 89

5-5. Relaxation Rate Constants (k_2) for the Protons in STRBPY and Distances Between These Atoms and Bound Ni(II) in D_2O at 25 °C 90

5-6. Relaxation Rate Constants (k_2) for the Protons in BPYNOX and Distances Between These Atoms and Bound Ni(II) in D_2O at 25 °C 93

5-7. Relaxation Rate Constants (k_2) for the Protons in MEPOX and Distances Between These Atoms and Bound Ni(II) in D_2O at 25 °C 93

5-8. Relaxation Rate Constants (k_2) for the Protons in MEPYR and Distances Between These Atoms and Bound Ni(II) in D_2O at 25 °C 94

5-9. Temperature Dependence of k_{corr} Values for MEBPY in the Presence of 0.0143 M $NiBr_2$ in D_2O. 95

5-10. Energies of Activation for Relaxation of MEBPY Protons and Correlation Coefficients 96

5-11. Values from the Data Manipulation of k_2 Values of MEBPY in $NiCl_2$ at 25 °C to Demonstrate the Solomon-Bloembergen Correlation 99

6-1. Fractional Coordinates and Equivalent Isotropic Thermal Parameters ($Å^2$) for the Carbon, Nitrogen, Oxygen, and Sulfur Atoms of 2-3 107

6-2. Bond Lengths (Å) and Angles (°) for the Carbon, Nitrogen, Oxygen, and Sulfur Atoms of 2-3 108

6-3. Fractional Coordinates and Equivalent Isotropic Thermal Parameters ($Å^2$) for the Carbon, Nitrogen, Oxygen, and Sulfur Atoms of 2-4 109

6-4. Bond Lengths (Å) and Angles (°) for the Carbon, Nitrogen, Oxygen, and Sulfur Atoms of 2-4 109

A-1. T_1 Relaxation Rate Constants for MEBPY in D_2O in $NiCl_2$ at 25 °C. 136

A-2. Second-Order Rate Constants (k_2) for MEBPY in D_2O in $NiCl_2$ at 25 °C. 137

A-3. T_1 Relaxation Rate Constants for MEBPY in D_2O in $NiCl_2$ and Acetic Acid at 25 °C. 138

A-4. Second-Order Rate Constants (k_2) for MEBPY in D_2O in $NiCl_2$ and Acetic Acid at 25 °C. 139

A-5. T_1 Relaxation Rate Constants for MEBPY in D_2O in $NiBr_2$ at 25 °C. 140

A-6. Second-Order Rate Constants (k_2) for MEBPY in D_2O in $NiBr_2$ at 25 °C. 140

A-7. T_1 Relaxation Rate Constants for MEBPY in DMSO-d_6 in $NiCl_2$ at 25 °C. 140

A-8. Second-Order Rate Constants (k_2) for MEBPY in DMSO-d_6 in $NiCl_2$ at 25 °C. 141

A-9. T_1 Relaxation Rate Constants for MEBPY in CD_3OD in $NiCl_2$ at 25 °C. 142

A-10. Second-Order Rate Constants (k_2) for MEBPY in CD_3OD in $NiCl_2$ at 25 °C 142

A-11. T_1 Relaxation Rate Constants for MEBPY in D_2O in $CoCl_2$ at 25 °C 143

A-12. Second-Order Rate Constants (k_2) for MEBPY in D_2O in $CoCl_2$ at 25 °C 143

A-13. T_1 Relaxation Rate Constants for MEBPY in D_2O in $NiBr_2$ at 25 °C 144

A-14. Second-Order Rate Constants (k_2) for MEBPY in D_2O in $NiBr_2$ at 25 °C 144

A-15. T_1 Relaxation Rate Constants for STRBPY in D_2O in $NiCl_2$ at 25 °C 145

A-16. Second-Order Rate Constants (k_2) for STRBPY in D_2O in $NiCl_2$ at 25 °C 146

A-17. T_1 Relaxation Rate Constants for MEPYR in D_2O in $NiCl_2$ at 25 °C 147

A-18. Second-Order Rate Constants (k_2) for MEPYR in D_2O in $NiCl_2$ at 25 °C 147

A-19. T_1 Relaxation Rate Constants for MEPOX in D_2O in $NiCl_2$ at 25 °C 148

A-20. Second-Order Rate Constants (k_2) for MEPOX in D_2O in $NiCl_2$ at 25 °C 149

A-21. T_1 Relaxation Rate Constants for BPYNOX in D_2O in $NiCl_2$ at 25 °C 149

A-22. Second-Order Rate Constants (k_2) for BPYNOX in D_2O in $NiCl_2$ at 25 °C 150

A-23. T_1 Relaxation Times and Rate Constants for MEBPY in D_2O with $NiBr_2$, Temperature Dependence 150

LIST OF FIGURES

Figure page

1-1. Inversion-Recovery Experiment for T_1 Relaxation Measurements 3

1-2. Spectra Resulting from an Inversion-Recovery Experiment for T_1 Relaxation Measurements. 5

1-3. General Reaction for Directed-*Ortho* Lithiation. . . 9

1-4. Catalytic Cycle of Palladium-Catalyzed Stille and Suzuki Cross-Coupling. 10

1-5. Generalized Stille and Suzuki Coupling Reactions . . . 11

2-1. Proposed Dihydrothiamin Structures and Other Structures of Interest. 16

2-2. Crystal Structure of 2-3. 18

2-3. High Field Region of the Proton NMR of 2-3 21

2-4. COSY Spectrum of the High Field Region of 2-3 . . . 22

2-5. NOE and Chemical Shift Data Summary for 2-3 25

2-6. Crystal Structure of 2-4. 26

2-7. High Field Region of the Proton NMR of 2-4 28

2-8. NOE and Chemical Shift Data Summary for 2-4 29

2-9. Reduction of 2-3 with [2-3] = 0.011 M, [$NaBH_4$] = 0.064 M and pD = 9.77 at 25 °C 34

2-10. Reduction of 2-3 with [2-3] = 0.011 M, [$NaBH_4$] = 0.029 M and pD = 9.77 at 25 °C 34

2-11. Reduction of 2-3 with [2-3] = 0.021 M, [$NaBH_4$] = 0.056 M and pD = 10.71 at 25 °C. 35

2-12. Reduction of 2-4 with [2-4] = 0.012 M, $[Na(CN)BH_3]$ = 0.064 M and pD = 5.75 at 25 °C . . . 35

2-13. Reduction of 2-4 with [2-4] = 0.010 M, $[Na(CN)BH_3]$ = 0.030 M and pD = 5.75 at 25 °C . . . 36

2-14. Reduction of 2-4 with [2-4] = 0.012 M, $[Na(CN)BH_3]$ = 0.091 M and pD = 5.75 at 25 °C . . . 36

2-15. Reduction of 2-4 with [2-4] = 0.037 M, $[Na(CN)BH_3]$ = 0.091 M and pD = 6.25 at 25 °C. . . . 37

2-16. Mechanisms of Conversion to Tetrahydrothiamin From 2-3 and 2-4. 41

3-1. Reactions of 2,2′-BPY and 2,4′-BPY with LTMP and the Respective Electrophiles. 47

3-2. Stille Cross-Couplings of 3-3b and 3-4 with 3-Iodopyridine. 48

3-3. Aromatic Region of the Proton NMR of 3-3c 49

3-4. Carbon-13 NMR of 3-4 52

3-5. Proton NMR of 3-6 54

3-6. COSY Spectrum of 3-6. 55

4-1. Successful Suzuki Coupling Reaction with Prequaternized Hetarenes. 59

5-1. Illustration of Spin Polarization 67

5-2. Pyridine Systems Studied by T_1 Relaxation 71

5-3. Low Temperature Preparation of Tributyl-(4-pyridyl)-stannane. 74

5-4. Preparation of STRBPY 75

5-5. Plot of k_{corr} versus $[Ni^{+2}]$ for MEBPY with $NiCl_2$ in D_2O for Proton H-2. 84

5-6. MEBPY Proton Relaxation Rate Constants (k_2) as Correlated with Inverse Distance Between the Protons and Bound $NiCl_2$ in D_2O 87

5-7. MEBPY Proton Relaxation Rate Constants (k_2) as Correlated with Inverse Distance Between the Protons and Bound $NiCl_2$ in DMSO-d_6 87

5-8. MEBPY Proton Relaxation Rate Constants (k_2) as Correlated with Inverse Distance Between the Protons and Bound $NiCl_2$ in CD_3OD 88

5-9. Correlation Between Relaxation Rate Constants for MEBPY in DMSO and CD_3OD Solvents Containing $NiCl_2$. . 88

5-10. MEBPY Carbon Relaxation Rate Constants (k_2) as Correlated with Inverse Distance Between the Carbons and Bound $NiBr_2$ in D_2O. 90

5-11. STRBPY Proton Relaxation Rate Constants (k_2) as Correlated with Inverse Distance Between the Protons and Bound $NiCl_2$ in D_2O 91

5-12. Comparison of Comparable Protons of STRBPY and MEBPY 92

5-13. Correlation of the $S_{3'-X}$ Factor with the Inverse Sixth Power of the Nuclei to Metal Distance for MEBPY in D_2O with $NiCl_2$ 100

Abstract of Dissertation Presented to the Graduate School
of the University of Florida in Partial Fulfillment of the
Requirements for the Degree of Doctor of Philosophy

POLYCYCLIC AZINES: SYNTHESIS AND THE USE OF NUCLEAR MAGNETIC RESONANCE TECHNIQUES FOR STRUCTURAL, MECHANISTIC, AND KINETIC ELUCIDATION

By

Carlton D. Dill

August, 1997

Chairperson: John A. Zoltewicz
Major Department: Chemistry

Two dihydrothiamin isomers were prepared from thiamin according to known literature preparations, and their heretofore incorrect structures in solution and in the crystalline form are corrected using nuclear magentic resonance (NMR) spectroscopic techniques and X-ray crystallography. Kinetic studies of the reduction of the isomers by hydrides to tetrahydrothiamin show the isomers to be kinetic and thermodynamic dihydro products.

Inter-ring directed *ortho* lithiation by the 2-pyridyl group of 2,2′- and 2,4′-bipyridines followed by electrophilic derivatization results in the formation of 3 (3′) substituted bipyridines.

Two of the newly formed stannane derivatives are utilized in palladium-catalyzed cross-coupling to afford two novel terpyridines. Structures are determined by NMR spectroscopy.

Palladium-catalyzed cross-coupling reactions between a hetarylborane and N-quaternized hetaryl halides provide polyazines of unequivocal structure in terms of the location of the N-quaternized group. The scope and limitations of this new synthetic method are established by preparing examples of several ring systems.

Proton and carbon relaxation times (T_1) of compounds containing pyridine rings in the presence of paramagnetic nickel(II) and cobalt(II) salts are determined by an inversion recovery NMR experiment. The possibility of constructing a correlation between relaxation rate constants and distance between the relaxing ring nucleus and the metal-center is studied. Factors such as solvent and temperature are also explored to gain further insight.

CHAPTER 1
INTRODUCTION

Open any chemistry journal, organic or otherwise, and it is very likely that much of the chemistry involves heterocyclic compounds. Whether synthetic, spectroscopic, mechanistic, computational, or some other type of study, heterocyclic chemistry is a very large part of chemical research. In fact, many journals are dedicated specifically to heterocyclic chemistry. Therefore, when one begins research in heterocyclic chemistry it should be no surprise that many avenues of study present themselves. Not being intently focused on one goal, this work is an illustration of such an idea of diversity. There are studies involving synthetic methodology of heterocyclic compounds, and other studies which glean information about such compounds using nuclear magnetic spectroscopy (NMR) and other technological means.

Chapters 2 and 5 are dedicated to the NMR studies. Chapter 2 uses some of the well known, powerful, one-dimensional (^{1}H, ^{13}C, APT) and two-dimensional (COSY) NMR techniques to elucidate the structures of dihydrothiamin isomers, which have been somewhat controversial for more than forty years.[1-9]

The crystal structures of the isomers are also presented as substantial evidence for their proof of structure. NMR is also used to follow the reduction of the isomers to tetrahydrothiamin to obtain mechanistic and kinetic information.

Chapter 5 is dedicated to T_1 relaxation studies of functionalized pyridines in the presence of paramagnetic metals. A few introductory definitions are now presented to clarify the results obtained in this and other research involving T_1 relaxation times. In the NMR process, magnetic nuclei become aligned with an external magnetic field (B_0), and an application of radio-frequency (rf) energy (B_1) brings about a spin "flip". The NMR experiment is sustained when energy is passed from the excited spins to the surrounding "lattice" so the nuclei can return to the lower spin state and are thus available for another spin excitation cycle. This process is known as spin-lattice relaxation. A steady state value (M_{z0}) of the magnetization (M_z) results when the spins are at equilibrium in the magnetic field. The equilibrium is disturbed when the B_1 field is applied, and M_z is no longer at equilibrium. Spin-lattice relaxation is any process that returns the magnetization to the equilibrium state. The time it takes to return to equilibrium magnetization is called the spin-lattice relaxation time or T_1 relaxation time.

Relaxation is a first-order kinetic process with rate constant T_1^{-1}. Often, the term longitudinal relaxation is used because the changes in magnetization occur along the z-axis of the NMR experiment.[10,11,12]

T_1 relaxation times are typically measured by a specialized experiment known as inversion recovery involving a 180° pulse, and time delay (τ), and a 90° pulse.[10] This sequence is illustrated in Figure 1-1.

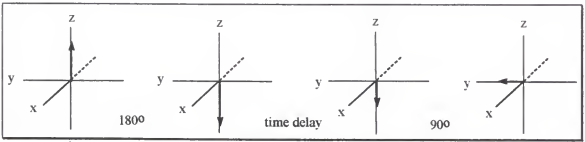

Figure 1-1. Inversion Recovery Experiment for T_1 Relaxation Measurements.

The net magnetization is aligned along the z-axis at equilibrium, and in a typical NMR experiment, the rf energy, B_1, is applied perpendicular to the magnetization so to tip the magnetization in the y direction where the detection coils are located. Often, the B_1 pulse is set to be 90° to cause an alignment in the y direction. However, if the B_1 pulse time is twice as long, the net magnetization will be aligned in the -z direction, opposite to the B_0 field. This latter pulse is termed a 180° pulse. At this point, if a 90° pulse were applied, then the spins would be rotated into the -y direction, and negative signals would be detected. An inverted spectrum would result. Typically, a time delay, τ, is applied prior to the 90° pulse allowing the magnetization to partially or fully recover to the equilibrium state depending on the length of the delay. An inversion recovery experiment utilizes an array of the τ delay times, short to long, resulting in several spectra. The first few spectra are inverted due to the short delay times during which magnetization does not return to equilibrium, while the latter spectra return to normal with longer delays (Figure 1-2). The relaxation time is calculated by an exponential fit of the peak intensities.

Nuclear relaxation is aided by a number factors including, fluctuating magnetic fields of other nuclei and unpaired electrons, if present. These are dipole-dipole interactions.[13] Important to this work is the interaction with the unpaired electrons of paramagnetic substances, specifically metal ions such as nickel (II) and cobalt (II). Paramagnetic ions have significantly more intense magnetic fields associated with them than carbon and hydrogen nuclei and therefore are very efficient at causing relaxation.

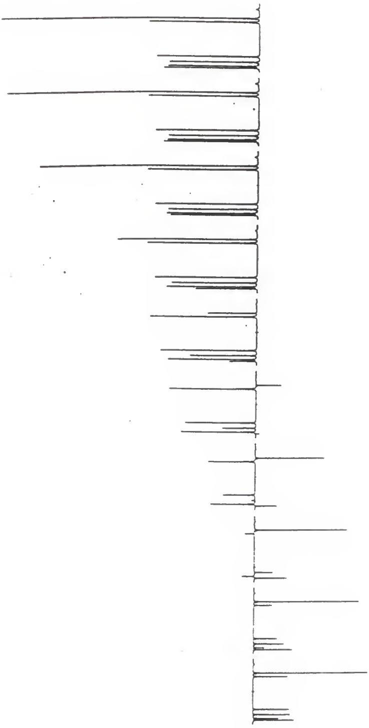

Figure 1-2: Spectra Resulting from an Inversion-Recovery Experiment for T_1 Relaxation Time Measurements

Dissolved oxygen is also a source of unpaired electrons, and therefore, degassing of NMR solvents is often necessary for the success of certain experiments.[13]

In the 1950s, Solomon and Bloembergen established the relationship between the rate constant for relaxing nuclei and a paramagnetic component resulting in the equation

$$T_1^{-1} = 2/15\ (\mu^0/4\pi)^2\ \mu^2\mu^2 S(S+1) r^{-6}\ f(\tau_c,\omega) \qquad \text{(Eq. 1-1)}$$

where T_1^{-1} is the associated rate constant, μ^2 is the nuclear magnetic moment, μ^2 is the electron magnetic moment, r is the distance from the relaxing nucleus to the paramagnetic center, and $f(\tau_c,\omega)$ is a function based on the correlation time and Larmor frequencies as shown in Equation 1-2.[14-19]

$$f(\tau_c,\omega) = [(7\tau_c/1+\omega_s^2\tau_c^2) + (3\tau_c/1+\omega_I^2\tau_c^2)] \qquad \text{(Eq. 1-2)}$$

The nuclear and electron Larmor frequencies are represented by ω_s and ω_I, respectively, and τ_c is the correlation time. The correlation time is a time constant typical of the system being studied and may be based on one or more of three components; electron relaxation, τ_s, rotational correlation time, τ_r, and chemical exchange, τ_m.

$$\tau_c^{-1} = \tau_r^{-1} + \tau_s^{-1} + \tau_m^{-1} \qquad \text{(Eq. 1-3)}$$

When more than one of the above processes is operative, the fastest process is dominant.[13] In this work, electron relaxation and chemical exchange are the more dominant correlation time processes.

The major factor drawn from these equation for this work is the proportionality of the relaxation rate to the inverse sixth power of the distance. There are several instances in the literature where this distance relationship was utilized to determine the structures of molecules in the presence of paramagnetic substances.[20,21,22] The addition of a paramagnetic species may also be used to enhance the sensitivity of certain nuclei such as ^{13}C.[10]

More recently, attention has been given to the relaxation of metal complexes that do not follow the Solomon-Bloembergen relationship. Here, unpaired spin density may be delocalized onto an attached ligand by direct delocalization or spin polarization and may be associated with the atomic orbitals of the ligand.[23,24,25] This phenomenon is appropriately termed ligand-centered effect, and although the equations are quite involved, consideration is given to the delocalized spin density. It is important to remember that these effects are still dipolar in nature, and the overall relaxation rate constant can be written as the sum of three terms,

$$T_1^{-1} = T_{1M}^{-1} + T_{1L}^{-1} + T_{1LM}^{-1} \quad \text{(Eq. 1-4)},$$

where T_{1M}^{-1} is due to the metal-centered relaxation (Solomon-Bloembergen) for metal-nuclear distances exceeding 4 Å, T_{1L}^{-1}

is the ligand-centered term, and T_{1LM}^{-1} is a cross term that is generally neglected because it is much less than T_{1L}^{-1}. Using ratios of distances (r_a^6/r_b^6) to approximate Solomon-Bloembergen predictions and ratios of observed relaxation rate constants (T_{1b}^{-1}/T_{1a}^{-1}), comparisons can be made to demonstrate the correlation with or deviation from Solomon-Bloembergen predictions.[24] This may be done for proton and carbon relaxation.

Another scenario which appears to demonstrate deviation from the Solomon-Bloembergen predictions involves situations where a substrate may exist in two states, bound and unbound to the paramagnetic metal. In such cases, the lifetime of the metal-substrate complex (time bound) is an influential factor in the measured relaxation rates.[26,27] This is discussed in greater detail in Chapter 5.

The studies in Chapters 3 and 4 are more synthetically oriented. Chapter 3 illustrates the preparation of several 3 (3′) substituted bipyridines. Using the 2-pyridyl group as a directing agent, *ortho* lithiation, and subsequent electrophilic substitution, is accomplished regiospecifically. Figure 1-3 gives the general reaction for directed-*ortho* lithiation.[28] Such chemistry with pyridines has been known for some time, but this is the first illustration of the use of the 2-pyridyl group as the directing group. Also, the possible utility of such compounds was established by preparing two novel terpyridines from two of the newly formed stannyl bipyridines making use of palladium-catalyzed cross-coupling (Stille coupling reactions, discussed subsequently).

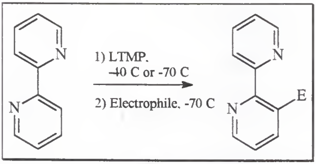

Figure 1-3: General Reaction for Directed-*Ortho* Lithiation

Palladium-catalyzed cross-coupling chemistry is utilized in three of the four studies in this work. The two main types of coupling used in this work are the Stille[29] and Suzuki couplings.[30] The catalytic process consists of an oxidative addition, transmetallation, and reductive elimination, Figure 1-4.[31,32,33]

The Stille coupling reaction utilizes a palladium catalyst to accomplish a cross-coupling between organic electrophiles, such as organic halides or triflates, and organostannanes. The organic halide or triflate oxidatively adds to the palladium catalyst and the organostannane is involved in the transmetallation. The Suzuki coupling reaction employs an organoborane or boronic acid in the transmetallation step.

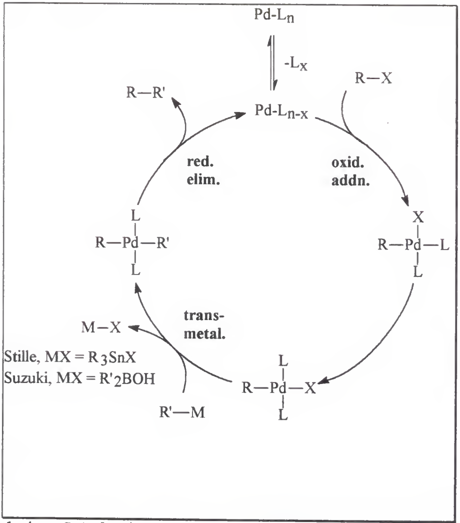

Figure 1-4. Catalytic Cycle of Palladium-Catalyzed Stille and Suzuki Cross-Couplings

The ready availability and general stability of organostannanes and boranes, the usually mild and variable reaction conditions, and the compatibility of this chemistry with most functional groups, have made the Stille and Suzuki couplings quite popular. Figure 1-5 illustrates the general Stille and Suzuki coupling reactions.

$$R{-}X \quad + \quad R'{-}SnR''_3 \xrightarrow{\text{Pd(0) or Pd(II) complex}} R{-}R'$$

$$R{-}X \quad + \quad R'{-}BY_2 \xrightarrow[\text{THF, dioxane, DMF; Aqueous Base}]{\text{Pd(0) or Pd(II) complex}} R{-}R'$$

R, R' = alkene, alkyne, aryl, hetaryl
X = I, Br, Cl, OTf
R" = n-butyl, methyl
Y = ethyl, OH, BBN

Figure 1-5. Generalized Stille and Suzuki Coupling Reactions.

The oxidative addition of organic halides or triflates to Pd(0) complexes proceeds through an unsaturated 14-electron Pd(0) intermediate.[34,35,36] Open coordination sites on palladium due to ligand dissociation leads to a species which can now allow the halide or triflate compound to initially coordinate to the Pd(0) intermediate. The relative rate at which organic halides or triflates oxidatively add to palladium is generally on the order of I > Br > Cl > OTf.[37] Taking advantage of the ligand dissociation may also improve the reaction.

In the Stille coupling, transmetallation involves a nucleophilic substitution process at a square-planar Pd(II) complex, where the organostannane is the nucleophile and the leaving group is the halide or triflate ion that resulted from the oxidative addition. The reaction might be expected to proceed through a classical associative process[38] in which the nucleophile approaches the plane of the complex perpendicularly. An unstable pentacoordinated intermediate results, which then releases the leaving group.[39]

The Suzuki coupling uses an organoborane or boronic acid in the transmetallation step. The reaction is usually done under aqueous alkaline conditions. The use of an alkaline medium for such coupling reactions seems to be necessary in order to give an intermediate "ate" complex of the boron reagent on addition of hydroxide ion.[30] This "ate" complex then transfers an organic ligand to the oxidative addition complex in the transmetallation step.[30,40,41,42,43] Though the aqueous alkaline conditions have become a somewhat standard procedure in this type of reaction, there are examples of coupling reactions with organoboranes or boronic acids under alternate conditions.[44,45,46]

Both of these reactions are employed in these studies. Chapter 3 utilizes Stille couplings to prepare novel terpyridines from two of the newly formed bipyridine compounds. Chapter 5 also contains examples of Stille couplings to prepare substrates that were studied further by T_1 relaxation. Chapter 4 focuses on the use of the Suzuki reaction between functionalized hetaryl halides with boranes to accomplish regiospecific functionalization of the products.

CHAPTER 2
STRUCTURE AND KINETIC STUDIES OF DIHYDROTHIAMIN ISOMERS BY NMR AND X-RAY CRYSTALLOGRAPHY

Introduction

Four decades ago, much attention was given to the group of compounds known as dihydrothiamines.[1] In 1950, Karrer and Krishna gave the first reported synthesis using lithium aluminum hydride to afford the sparingly water soluble thiazoline, 2-2, by the addition of hydride to position 2 of the thiazolium ring of thiamin.[2,3,47] They reported the structure to be that given by 2-2 with a melting point of 150 °C. In 1955 and 1957, scientists at the Takeda Pharmaceutical Industries, Ltd. in Japan reported the synthesis of three dihydro isomers giving them the designations of "normal-dihydrothiamine" (mp = 150 °C), "iso-dihydrothiamine" (mp = 160 °C), and "pseudo-dihydrothiamine" (mp = 175 °C).[4,5,6,7,8] Their syntheses were accomplished by a variety of routes including hydride reduction of thiamin and cyclization reactions that made derivatives of the reduced materials. It should be noted that the synthesis of normal-dihydrothiamin and that of iso-dihydrothiamin differed only by a workup under alkaline conditions. Iso-dihydrothiamine was formed when normal-dihydrothiamine was subjected to alkaline conditions. Pseudo-dihydrothiamin was formed when either of the previous isomers was dissolved in hot water. Using infrared spectroscopy, the structures of the isomers were tentatively assigned. Normal-dihydrothiamin and iso-dihydrothiamin were assigned to be the *trans* and *cis* diastereomers, respectively, of bicyclic perhydrofuro[2,3-d]thiazole adducts as shown by 2-3. Pseudo-dihydrothiamin was assigned to be a fused tricyclic pyrimido[4,5-d]thiazol-[3,4-a]-pyrimidine as shown in 2-4, an amino adduct.

In 1957, the Americans, Bonvicino and Hennessy, reported that the use of sodium trimethoxyborohydride to reduce thiamin (2-1) led to an isomer which melted at 151 °C. When heated in water, this material gave an isomer which melted at 175 °C.[9] Being unaware of the earlier Japanese work, they reported structures 2-2, the thiazoline of Karrer and Krishna, and 2-3, the same furo[2,3]thiazole as the Japanese, for the respective isomers, relying on infrared and ultraviolet spectroscopy to make structural assignments. Thus, the Japanese and American groups did not make the same assignments for compounds with similar melting points.

Others have simply accepted the American results and therefore may have given erroneous information. For example, Hadjiladas reported proton and carbon NMR data for the 150 °C isomer assuming the American structure, but the data are questionable if the Japanese structure is correct.[48]

The current work involves the preparation of the three reported isomers, and the determination of their actual structures by NMR spectroscopic analysis and X-ray crystallography. Also, the further reduction of the respective isomers to tetrahydrothiamin, 2-5, is studied kinetically as another distinguishing factor.[9]

Results and Discussion

Preparation of Dihydrothiamin Isomers

The three reported forms of dihydrothiamin were prepared according to the literature.[4,9] The first isomer (mp 149-151 °C) was made by the mild reduction of neutralized thiamin hydrochloride with $Na(OCH_3)_3BH$ under aqueous conditions (-12 °C), and a second isomer (mp 173-175 °C) was prepared by dissolving the first isomer in hot water followed by addition of Na_2CO_3 and extraction into $CHCl_3$. The third form was not prepared in exact accordance with the literature but was prepared more easily by dissolving the first isomer (mp 149-151 °C) in methanol and adding a 10% NaOH solution to it. Subsequent stirring quickly afforded a white precipitate (mp 156-158 °C).

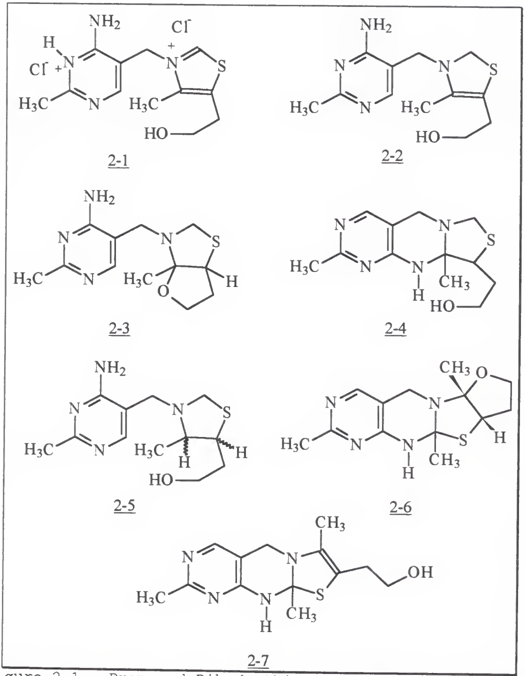
2-1
2-2
2-3
2-4
2-5
2-6
2-7

Figure 2-1. Proposed Dihydrothiamin Structures and Other Structures of Interest.

The mixed melting point with the 151 °C isomer was found to be between the two, 152-154 °C, just as reported by the Japanese authors.[4] The structures of the normal-dihydrothiamin and pseudo-dihydrothiamin were determined by NMR analysis and X-ray crystallography, while the structure of the third form was determined by NMR analysis.

Structure Determinations of Normal-Dihydrothiamin and Iso-Dihydrothiamin

Crystal structure of 2-3. Slow solvent evaporation from an ethyl acetate solution of the isomer melting at 151 °C resulted in the formation of crystals that were submitted for analysis by X-ray crystallography. Figure 2-2 shows the resulting crystal structure having a unit cell containing both of the enantiomers establishing it as structure 2-3. It is a racemic compound and not a racemic mixture or conglomerate.[49] The most notable feature is the *cis*-fused five-membered rings having the bicyclic perhydrofuro[2,3-d]thiazole structure that lie somewhat perpendicular to the pyrimidine ring. The methyl and the methinyl CH are not eclipsed and both are outside the envelope of the fused rings, while the N-**CH_2**-S and O-**CH_2**-CH_2 groups are inside the envelope. The bridging CH_2 protons have different chemical environments.

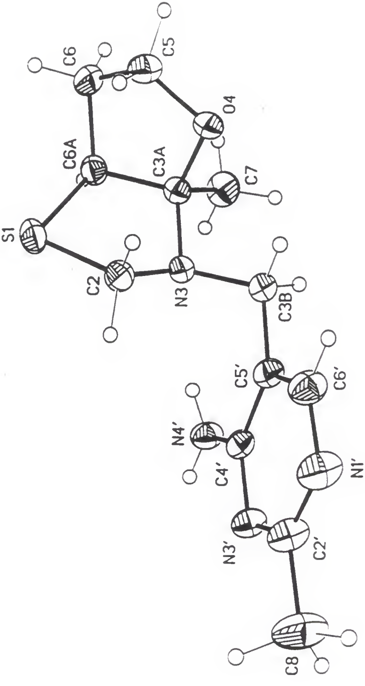

Figure 2-2: Crystal Structure of 2-3.

(Kindly provided by Dr. Khalil Abboud)

One is nearer to the methyl group of the *cis*-fused rings by 0.69 Å, and the other is nearer to the pyrimidine proton by 0.93 Å. This is of significance in the subsequent NOE experiments. One of the protons of the NH_2 is directed toward the N-atom of the thiazolidine ring forming a bent H-bond with a distance of 2.29 Å between the two sites. The resultant 6-membered ring is a common feature of crystal structures.[50]

The molecular structure of 2-3 has some resemblance to the crystal structure of tetracyclic 2-6, formed by simple deprotonation of thiamin, 2-1, under mild conditions.[51,52] Again, the *cis* perhydrofuro[2,3-d]thiazole unit is present, now as a consequence of the addition of the amino group to the 2 position of the thiazolium ring to produce tricyclic 2-7, followed by additional cyclization.

Attempted crystal growth of iso-dihydrothiamin. The isomer with mp 156-158 °C was dissolved in a mixture of ethanol, hexanes, and ethyl acetate for possible crystal growth. However, the crystals that formed had a lower melting point (mp 149-151 °C) corresponding to the isomer from which it was made. The higher melting material reverted back to the lower melting one.

NMR analysis of normal-dihydrothiamin. At first glance, the complexity of the ^{1}H NMR spectrum (Figure 2-3) of 2-3 raises serious doubts about the existence of an unsaturated thiazole ring, as originally proposed by the Americans. The obvious presence of diastereotopic protons, indicative of chiral centers, immediately invalidated the originally proposed structure (2-2) and made peak assignment somewhat challenging. The aromatic (7.96 ppm) and methyl (2.48 and 1.56 ppm) protons were easily assigned based on chemical shifts and integration, as was the NH_2 peak (5.79 ppm). The **CH_2**-CH_2O methylene protons of the furan ring were assigned to those at 2.41 and 2.09 ppm, being at higher field since they were not directly deshielded by any of the heteroatoms. The remaining peaks between 3.62 and 4.03 ppm were more complex and required more involved experimentation.

A COSY experiment (Figure 2-4) indicated that the two proton multiplet at 4.03 ppm was coupled with the high field methylene protons (2.41, 2.09 ppm). Thus, these protons were given the assignment O-**CH_2**-CH_2. The one proton doublet at 3.92 ppm was coupled (14 Hz) to the one proton doublet at 3.62 ppm. The one proton doublet at 3.77 ppm was coupled (8 Hz) to the one proton doublet at 3.62 ppm. These methylene protons exhibit geminal coupling and correspond to the bridging methylene and the N-**CH_2**-S methylene, respectively.

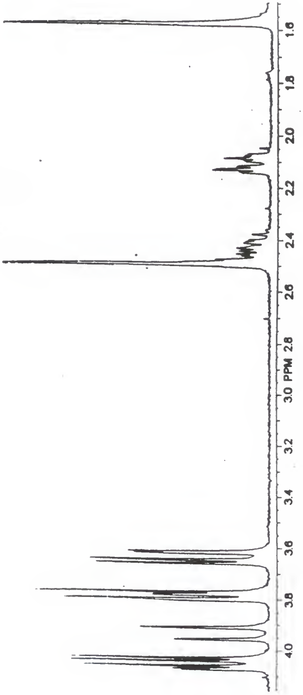

Figure 2-3: High Field Region of the Proton NMR of 2-3 ($CDCl_3$).

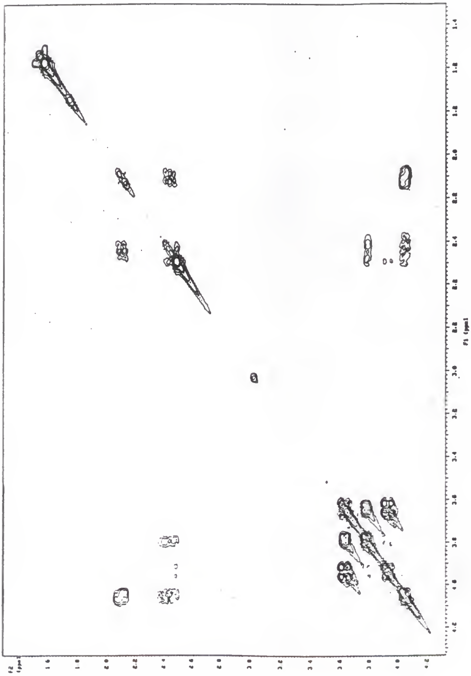

Figure 2-4: COSY Spectrum of the High Field Region of 2-3 $(CDCl_3)$.

Distinguishing between the two was accomplished by preparing 2-3 in D_2O, first allowing the thiazole proton N=**CH**-S to exchange to N=**CD**-S,[53,54] followed by the reduction with $Na(OCH_3)_3BH$. This resulted in a deuterium labeled compound with a loss of geminal coupling at the exchanged methylene. It was quite obvious that the 8 Hz doublets at 3.77 and 3.62 ppm had collapsed to singlets. Thus, these were assigned as N-$\mathbf{CH_2}$-S group, and the more highly coupled methylene protons (14 Hz) were assigned to the bridging methylene unit. Also, the one proton doublet at 3.78 ppm was determined to be the proton bound to the methinyl carbon; it was coupled to the proton at 2.41 ppm and was also largely exchanged (>85%) in the deuterium labeling experiment. The deuterium labeling experiment showed that the signal at 2.41 ppm lost some of its multiplicity whereas the 2.09 ppm signal did not, suggesting different coupling constants.

Isotope exchange at the N-$\mathbf{CH_2}$-S methylene resulted in an interesting spectral change. The newly formed chiral center, N-**CHD**-S present equally in both configurations, caused the bridging methylene to assume slightly different chemical shifts; the signal for each proton was split into two additional lines with separations of 2-4 Hz, giving an apparent dd pattern. However, the magnitude of the new separation was different for each of the methylene protons, and the magnitude also changed with field strength (300 versus 500 MHz). This demonstrated that the new multiplicity was not due to spin coupling but rather to differential shielding by the chiral center as would be expected with diastereomers.

Nuclear Overhauser effect (NOE) experiments helped in making peak assignments. Upon irradiation of the aromatic proton signal (7.96 ppm), enhancement of both protons of the methylene bridge was expected. However, only one (3.62 ppm, 14 Hz) was enhanced (5.2%). Upon irradiation of the methyl signal at 1.56 ppm, the other proton of the methylene bridge (3.92 ppm) was enhanced (8.7%), along with the doublet at 3.78 ppm (12.9%) associated with the methinyl proton. Moreover, since each of the methylene bridge protons was enhanced separately, the pyrimidine ring was determined not to be a free rotor in $CDCl_3$. There may be significant hydrogen bonding between the NH_2 protons and the thiazolidine nitrogen atom preventing such rotation. This geometry was quite similar to the orientation exhibited in the crystal structure. Figure 2-5 provides a pictorial summary of the NOE and chemical shift data for 2-3.

NMR analysis of iso-dihydrothiamin. The ^1H NMR spectrum of this higher melting isomer in $CDCl_3$ was found to be exactly the same as that of the lower melting (151 °C) isomer, indicating that the two compounds with different melting points have the same structure in solution. This structure is that established by the X-ray and NMR analyses of 2-3.

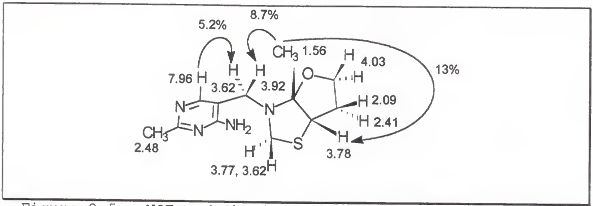

Figure 2-5. NOE and Chemical Shift Data Summary for 2-3.

Structure Determination for Pseudo-Dihydrothiamin

Crystal structure of pseudo-dihydrothiamin. The atom connectivity of a crystal grown from $CDCl_3$ has molecular structure 2-4, containing three fused rings that do not include the hydroxyethyl group (Figure 2-6). The three stereocenters defined by atoms NCC are *cis-cis*. The central ring is slightly puckered, and the 5-membered ring has a slightly puckered envelope-like conformation. The hydroxyethyl group is expected to be a free rotor in solution.

NMR analysis of pseudo-dihydrothiamin. With the structure of 2-3 established, determination of the structure of this isomer became simpler because the NMR data for the

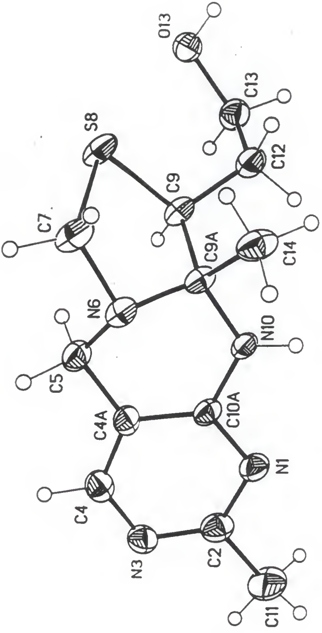

Figure 2-6: Crystal Structure for 2-4.
(Kindly provided by Dr. Khalil Abboud.)

two could be compared and contrasted (Figure 2-7). Again, the aromatic (7.94 ppm) and methyl (2.38 and 1.45 ppm) protons were easily assigned by their chemical shifts and integrated areas. Also, the high field methylene protons of **CH_2**-CH_2-O were readily distinguished(2.18 and 1.69 ppm), and although a different solvent was used, the upfield shift, relative to that in 2-3, and the multiplicity were indicative of a ring-opened furan.[11] The O-**CH_2** protons also exhibited an upfield shift and more complex multiplicity, again no longer being deshielded by a ring. The N-**CH_2**-S methylene doublets shifted downfield, 4.16 and 3.84 ppm, with a 9 Hz coupling constant, similar to that in 2-3. The bridging methylene protons are also shifted downfield, 3.98 and 3.88 ppm, and each had a 16 Hz coupling constant, compared to 14 Hz in 2-3. The proton associated with the methinyl carbon was easily observed at 3.43 ppm as a one proton doublet.

NOE experiments for this isomer were less informative. Irradiation of the methyl signal (1.45 ppm) enhanced signals at 4.16 (11%), 3.98 (6.5%), 3.43 (3.9%), 2.18 (3.9%), and 1.69 ppm (4.3%).

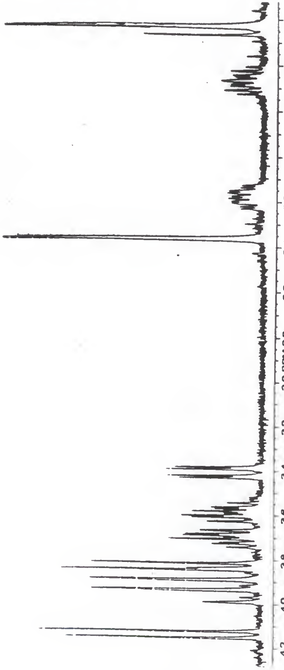

Figure 2-7: High Field Region of the Proton NMR for 2-4 (D_2O).

As expected, irradiation of the aromatic proton signal enhanced both of the bridging methylene protons, each by 3.1%. Figure 2-8 summarizes the NOE and chemical shift data for 2-4.

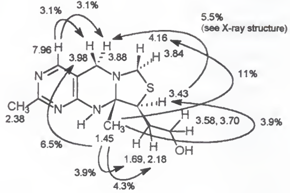

Figure 2-8. NOE and Chemical Shift Data Summary for 2-4.

The ^{13}C attached proton test spectrum demonstrated four CH, CH_3 types and eight C, CH_2 types, in agreement with the structure which is now established as that corresponding to 2-4. Also, the N-**C**-N carbon was present at 84 ppm, 20 ppm higher than the analogous carbon (N-**C**-O) in 2-3.

NMR Scale Conversion of 2-3 to 2-4

In a study of the conversion of 2-3 into 2-4, the substrates were dissolved in acidic phosphate buffer (pD = 6.25) and alkaline carbonate buffer (pD = 9.77) solutions, and the changes in the ^1H NMR spectra were observed. The samples were kept at room temperature for 22 h before spectra were recorded. At pD = 6.25, 2-3 had converted to 2-4 with deuterium exchange of the thiazole methyl and the methinyl proton, 2-4 experienced similar deuterium exchange. Also, new peaks, possibly corresponding to a diastereomer of 2-4, were observed, most noticeably at 3.88 (d) and 4.2 (d) ppm.

Obviously, both isomers must ring-open to allow deuterium exchange and conversion of 2-3, the kinetic isomer, to 2-4, the thermodynamic isomer. The fact that the methinyl proton exchanged gave excellent evidence for the existence of the first structure proposed by Bonviccino and Hennesey (2-2) as an intermediate, which had not been seen previously.

Inversion of configuration at the stereogenic nitrogen atom is expected to be facile, leading to equilibrating *cis* and *trans* ring-fused structures.[55] A change in configuration at the thiazolidine methyl site is also possible by way of a pH-dependent ring-opening and ring-closing process, as revealed subsequently, providing *cis* and *trans* methyl and hydroxyethyl side-chains. Hence, two diastereomers are possible in solution, perhaps seen in the above mentioned spectra and in the spectrum of the crude material resulting from the preparation of 2-4 from 2-3.

At pD = 9.77, 2-3 had begun to undergo similar conversion to 2-4 but change was incomplete, and 2-4 was completely unchanged. This was evidence that the ring-opening of both compounds is acid-catalyzed, an observation further substantiated by the following kinetic experiments.

Kinetics of Trapping with Hydride

Knowing that further reduction of both dihydrothiamin isomers results in the formation of tetrahydrothiamin (2-5),[9,54,56,57] and that hydride is a carbocation trapping agent,[58] the reactivity of the isomers toward hydride reduction served as another way to distinguish between the two. Preliminary qualitative experiments gave some clues to the reactivity, and quantitative experiments gave further insight.

When 2-3 was allowed to react with $NaBH_4$ in aqueous solution (pH = 10), no starting material remained (by TLC) after five hours, and the formation of tetrahydrothiamin was confirmed by NMR. It should be noted that tetrahydrothiamin has two diastereomeric forms, *cis* and *trans*, that are distinguishable by NMR. The thiazolidine ring methyl substituent appears as a doublet at either 1.30 ppm (minor, *trans*[56]) or 1.05 ppm (major, *cis*[56]) depending on the diastereomer. In the reduction of 2-3, one diastereomer is formed preferentially in a 3:2 ratio (*cis*:*trans*). This was the case for all reductions of 2-3. The same reaction run in a borax buffer (pH = 9.2) was qualitatively determined to be slightly faster.

When 2-4 was treated with $NaBH_4$ in aqueous solution, no reaction occurred and only starting material remained after several hours. However, when 2-4 was allowed to react with $Na(CN)BH_3$ in phthalic acid buffer (pH = 4.2), tetrahydrothiamin formation was complete (by TLC) after 3 hours. NMR spectra confirmed product formation, but the opposite diastereomer was present in slight excess with a 9:11 ratio (*cis*:*trans*). Typically, the *cis* isomer is expected to predominate.[54,56] However, this was not the case for 2-4 with $Na(CN)BH_3$.

These preliminary experiments led to more quantitative kinetic experiments where the respective compounds were reduced, and the disappearance of 2-3 or 2-4 and the appearance of tetrahydrothiamin were monitored by ^1H NMR over time. First-order rate constants, k_{obs}, could then be determined from the collected data.

Under the present conditions, the rate of reaction of both hydrides with water is negligible,[59,60] although some bubbles were always evolved on mixing. The cyano hydride is some 10^8 times less reactive than the parent hydride toward water.[60] No attempt was made to control the ionic strength of the medium, which was generally high from the buffer.

As a start, 2-3 was allowed to react in an unbuffered solution of $NaBH_4$. The plot of the collected data, log [% substrate remaining] versus time (min), showed unexpected curvature because the pD of solution increased from 10.4 to 11.3. Just as in the qualitative experiments, the more alkaline conditions slowed the reaction.

Compound 2-3 was allowed to react in a buffered solution (pD = 9.7) of $NaBH_4$. Again, a curved plot resulted, and again, the pD had increased. Even an increase in the HCO_3^- buffer concentration (pD = 9.0) was not effective in maintaining a constant pH with $NaBH_4$ resulting in a curved plot. Finally, the more concentrated Buffer C was used (pD = 9.77). Figures 2-9 and 2-10 illustrate the data from the two runs with differing BH_4^- concentrations and no observed pD changes. Figure 2-11 illustrates the data from a run with a higher pD and higher substrate concentration. An attempted reduction of 2-3 with $Na(CN)BH_3$ at high pD resulted in only a meager amount of tetrahydrothiamin along with ring degradation products.

The reduction of 2-4 with $Na(CN)BH_3$ was also studied quantitatively. At pD = 5.75, the reductions with differing concentrations of reducing agent were quite successful. Figures 2-12, 2-13, and 2-14 illustrate the plotted data. Similar reductions of 2-4 were also done at pD = 6.25 (Figure 2-15).

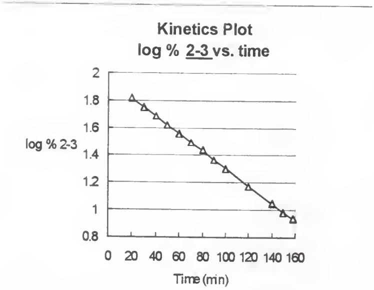

Figure 2-9. Reduction of 2-3 with [2-3] = 0.011 M, $[NaBH_4]$ = 0.064 M and pD = 9.77 at 25 °C.

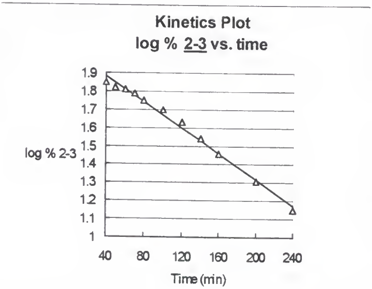

Figure 2-10. Reduction of 2-3 with [2-3] = 0.011 M, $[NaBH_4]$ = 0.029 M and pD = 9.77 at 25 °C.

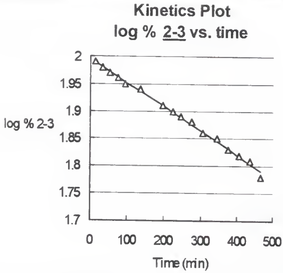

Figure 2-11. Reduction of 2-3 with [2-3] = 0.021 M, [$NaBH_4$] = 0.056 M and pD = 10.71 at 25 °C.

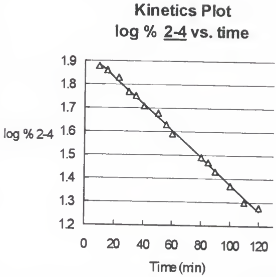

Figure 2-12. Reduction of 2-4 with [2-4] = 0.012 M, [$Na(CN)BH_3$] = 0.064 M and pD = 5.75 at 25 °C.

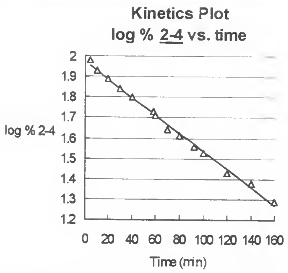

Figure 2-13. Reduction of 2-4 with [2-4] = 0.010 M, $[Na(CN)BH_3]$ = 0.030 M and pD = 5.75 at 25 °C.

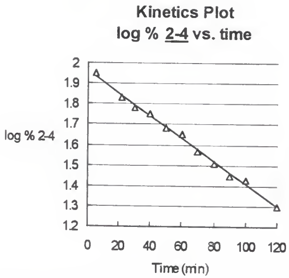

Figure 2-14. Reduction of 2-4 with [2-4] = 0.012 M, $[Na(CN)BH_3]$ = 0.091 M and pD = 5.75 at 25 °C.

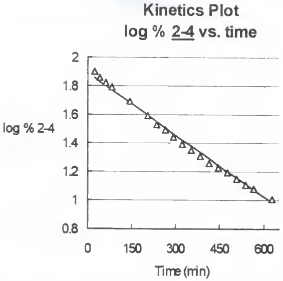

Figure 2-15. Reduction of 2-4 with [2-4] = 0.037 M, [Na(CN)BH_3] = 0.091 M and pD = 6.25 at 25 °C.

From the plots, the first-order rate constants of the reactions could be calculated from the slopes.

$$k_{obs} = (-slope / 60) \times 2.3 \quad (Eq.\ 2\text{-}1)$$

Division by 60 was necessary to convert minutes to seconds and 2.3 is for the conversion of $\log_{10}$ to ln. Table 2-1 gives the data for the rate constant determinations from the kinetic experiments. In order to appreciate the difference between 2-3 and 2-4, the kinetic data for both substrates should be considered simultaneously.

The data in Table 2-1 show: (1) changing the substrate concentration for 2-3 and 2-4 had no effect on the rate. (2) the reduction of 2-3 was clearly first-order in hydride ion concentration, and (3) the reactions of both substrates were clearly first-order in hydronium ion concentration. For 2-3, the apparent third-order rate constants could be calculated by

$$k_3 = k_{obs} / [D_3O^+][NaBH_4] \quad \text{(Eq. 2-2)}$$

since the rate was affected by changes in the pH and reducing agent concentration. The third entry in Table 2-1 for 2-3 shows a k_3 value 35% smaller than the average of the first two, perhaps because the initial ionic strength was twice as large. Otherwise, the values were determined to be in reasonable agreement.

With substrate 2-4, changing the reducing agent concentration had no effect on the rate, but a change in pD did. Therefore, apparent second-order rate constants were calculated by

$$k_2 = k_{obs} / [D_3O^+] \quad \text{(Eq. 2-3)},$$

again showing reasonable agreement among the values.

Table 2-1. Concentrations and Rate Constants from the Respective Kinetic Experiments.

Substrate (2-3 or 2-4)	[2-3] or [2-4], (M)	[H-](M)	pD	k_{obs} (s^{-1})	k_3 or k_2
2-3	1.1×10^{-2}	6.4×10^{-2} a	9.77 c	2.45×10^{-4}	2.6×10^{7} h
2-3	1.1×10^{-2}	2.9×10^{-2} a	9.77 c	1.36×10^{-4}	2.3×10^{7} h
2-3	2.1×10^{-2}	5.6×10^{-2} a	10.71 d	1.71×10^{-5}	1.6×10^{7} h
2-4	2.3×10^{-2}	6.4×10^{-2} b	6.25 e	5.07×10^{-4}	90 i
2-4	1.2×10^{-2}	6.4×10^{-2} b	5.75 f	2.19×10^{-4}	123 i
2-4	1.0×10^{-2}	3.0×10^{-2} b	5.75 f	1.68×10^{-4}	94 i
2-4	1.2×10^{-2}	9.1×10^{-2} b	5.75 f	2.12×10^{-4}	119 i
2-4	3.7×10^{-2}	9.1×10^{-2} b	6.25 g	5.56×10^{-4}	99 i

(a) $NaBH_4$, (b) $Na(CN)BH_3$, (c) Buffer C, (d) Buffer D, (e) Buffer E, (f) Buffer F, (g) Buffer G, (h) k_3 (M^{-2} s^{-1}), (i) k_2 (M^{-1} s^{-1})

Mechanism of Ring-Opening and Ring-Closing

From the qualitative and quantitative experiments with 2-3 and 2-4, the mechanisms for the reduction are quite similar in that both are acid catalyzed, and the same products are formed, whether from deuterium exchange or hydride trapping (2-5). This suggests a common set of ring-opened intermediates. Figure 2-16 illustrates the mechanism from both substrates which involves protonation of the furan oxygen in 2-3 and a nitrogen atom in 2-4, ring-opening to the reactive intermediate cation, and hydride trapping. That intermediate was determined to be the ring-opened iminium ion, 2-8. The presence of enamine 2-2, as proposed by the two groups of early workers is also a possibility, as indicated by the deuterium exchange experiments, although it was never isolated.

There is some question about where to locate the protonation site in 2-4. In the case of 2-1, protonation is known to take place at the aromatic ring nitrogen 1 as shown in 2-1.[61] However, favored here is protonation at the amino nitrogen atom of 2-4, because this site departs in the cleavage process, the microscopic reverse of the likely step of amino addition in the forward direction.

Cyclization to form a five-membered ring, here 5-*exo-trig*, generally is much faster than closure to form a six-membered ring, 6-*exo-trig*.[62] Moreover, the rotation and rehybridization of the pyrimidyl amino group to give the six-membered ring should contribute to the energy barrier. Therefore, 2-3 is a kinetic product, and 2-4 is a thermodynamic product. Apparently, cyclization back to 2-3 is faster than hydride trapping, and there is, therefore, a kinetic dependence on the [BH_4^-], reduction becoming the rate limiting step in the forward direction to 2-5.

Cyclization back to 2-4 is sufficiently slow so that trapping by the less reactive $(CN)BH_3^-$ is more rapid. Thus, in the forward process involving the reduction of 2-4 to 2-5, ring-opening of protonated 2-4 becomes the rate limiting step. At lower pH, any conversion of 2-4 to 2-3 by way of the ring-opened intermediate should be rapidly reversible, giving back the lower energy 2-4.

The tetrahydrothiamin product ratio from the respective isomers (3:2 for 2-3, 9:11 for 2-4; *cis*:*trans*) was a point of interest in that neither gave the product ratio of approximately 3:1 (*cis*:*trans*) that results from the direct reduction of thiamin with $NaBH_4$ as reported and confirmed here.[17] This indicates that the mechanism of reduction of thiamin directly to tetrahydrothiamin is not exactly the same as that for the reduction of dihydrothiamin to tetrahydrothiamin. It is known that thiamin assumes a tricyclic form, 5-7 (Figure 1), near neutral pH.[63-66]

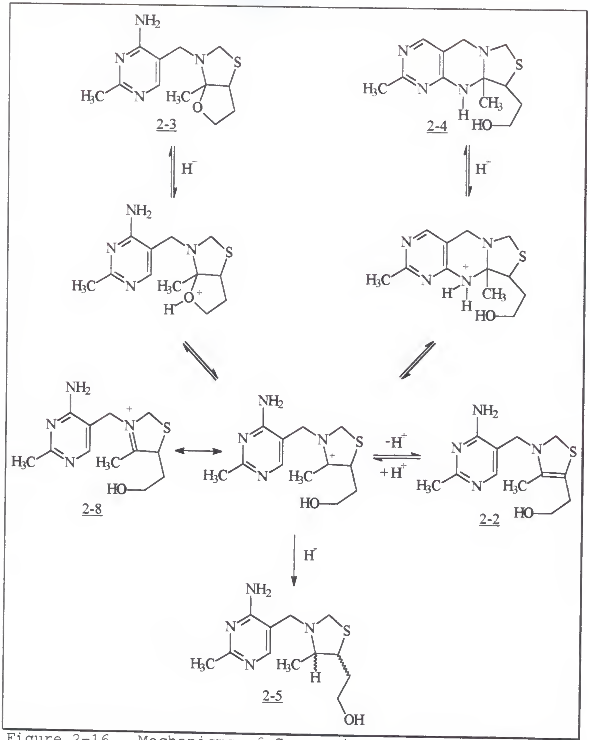

Figure 2-16. Mechanisms of Conversion to Tetrahydrothiamin from 2-3 and 2-4.

In this form, the order of hydride addition is likely to be the reverse of that of dihydrothiamin. The first hydride attack will occur at the iminium-enamine carbon on the face of the ring opposite to the hydroxyethyl group. Therefore, providing a reasonable explanation for the different *cis* to *trans* ratio is possible.

Conclusions

Bonvicino and Hennessy misidentified both of the isomers of dihydrothiamin, attributing structure 2-2, now known to be 2-3, to the isomer melting at 150 °C. The Japanese scientists correctly identified the isomer melting at 175 °C as 2-4, but misidentified the materials melting at 150 °C and 160 °C as the *trans* and *cis* isomers of 2-3, respectively.

Normal-dihydrothiamin (mp 149-151 °C) is assigned as 2-3, a *cis*-fused five membered ring furan adduct. Iso-dihydrothiamin (mp 156-158 °C) is most likely the same compound as normal-dihydrothiamin but involves a different crystal packing to account for the difference in melting point.[12] Pseudo-dihydrothiamin (mp 173-175 °C) is assigned as the *cis-cis* diastereomer of 2-4, a tri-cyclic amino adduct.

Kinetic experiments of the further reduction of 2-3 and 2-4 to tetrahydrothiamin, 2-5, give excellent evidence for acid-catalyzed ring-opening mechanisms not only for the reductions, but also for the conversion of 2-3 to 2-4. Thus, 2-3 is the kinetic product, and 2-4 is the thermodynamic product of the reduction of thiamin to dihydrothiamin.

CHAPTER 3

INTER-RING DIRECTED *ORTHO* LITHIATION BY THE 2-PYRIDYL GROUP IN BIPYRIDINES

Introduction

Heteroatom-containing substituents on an aromatic ring can direct lithiation to an *ortho* position and may have a strong rate accelerating effect on deprotonation.[67] In fact, Gilman, using aromatic ethers, observed a "pronounced tendency of metalation to take place *ortho* to an ether linkage."[68] Much of the research in this area has focused on finding different metallating conditions to improve yields and selectivity and to discover effective directing substituents.[28] More recently, methodology has been developed for selective directing conditions applied to disubstituted aromatic compounds.[69]

The phenomenon has been called a "directed *ortho* metallation"[70,71] and a "complex induced proximity effect".[72] Initial coordination of a lithium atom to the lone electron pair of the heteroatom brings the metallating agent into close proximity of the *ortho* hydrogen atom that is removed. Often this is said to be a ground state effect but the results of recent computations suggest the phenomenon to be a transition state effect, more adequately described as "kinetically enhanced metalation."[73] Stronger stabilization of the transition state rather than the ground state accounts for the directing and accelerating capabilities of such substituents.

For monosubstituted pyridines, Queguiner has been a major contributor to the methodology that has been concerned largely with substituents that direct metallation to an *ortho* site on the same ring.[28] The use of a 2-pyridyl substituent to effect inter-ring kinetically enhanced metallation is far less common.[72]

Reported here is the use of the 2-pyridyl group in bipyridines (BPYs) to direct lithiation and subsequent electrophilic substitution to the adjacent ring, thereby providing a facile route to the synthesis of 3- or 3′-substituted bipyridines. Two of the newly formed stannyl products were cross-coupled under Stille conditions[74] in the presence of tetrakis(triphenylphosphine) palladium ($Pd(PPh_3)_4$) to afford two novel terpyridines.

Results and Discussion

Lithiation and Electrophilic Substitution

Figure 3-1 illustrates the reactions in which 2,2′-BPY (3-1) or 2,4′-BPY (3-2) was mono-lithiated with lithium 2,2,6,6-(tetramethyl)piperidide (LTMP)[75] at -40 °C or -70 °C and then quenched with several illustrative electrophiles. Bu_3SnCl, Et_2BOMe, I_2, or CH_3CHO and 3-1 gave substituted 2,3′-BPYs 3-3a-e and Bu_3SnCl with 3-2 gave 2,4′-BPY 3-4. Mixtures of mono- (3-3b) and distannylated (3-3a) BPYs resulted from the same reaction but were easily separated by column chromatography, the latter in low yield (14%).

Palladium-Catalyzed Cross-Coupling of Stannanes

To demonstrate the utility of the stannylated BPYs for cross-coupling reactions, two novel terpyridines, 2,2′:3′,3″-terpyridine (3-5) and 2,4′:3′,3″-terpyridine (3-6), were prepared when 3-3b and 3-4 were treated with 3-iodopyridine in the presence of $Pd(PPh_3)_4$ under Stille coupling conditions,[29] respectively. While 3-6 was formed in high yield (80%), various attempts to improve the outcome (21%) for 3-5 consistently failed. Figure 3-2 shows the cross-coupling reactions.

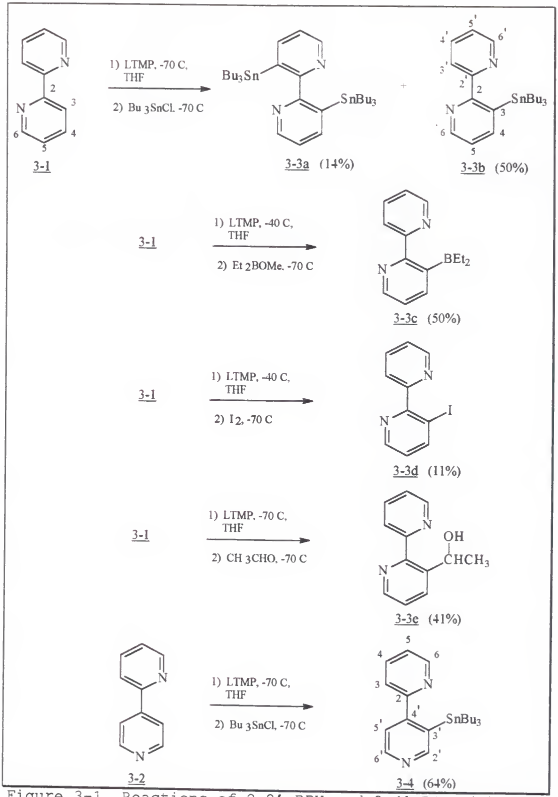

Figure 3-1. Reactions of 2,2'-BPY and 2,4'-BPY with LTMP and the Respective Electrophiles.

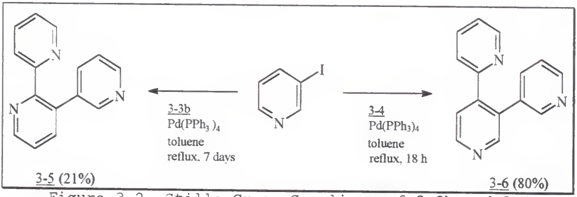

Figure 3-2. Stille Cross-Couplings of 3-3b and 3-4 with 3-Iodopyridine.

Structure Determination of BPYs

NMR analysis provided the means for structure determination to verify that the site of lithiation, and therefore electrophilic substitution, was indeed the 3 or 3′ position. As an example, Figure 3-3 gives the aromatic region of the ^{1}H NMR for 3-3c. For 2,2′-BPYs 3-3a-e, positions 4 and 5 were easily excluded as sites of lithiation due to the absence of a characteristic singlet in the aromatic region. The same spin-spin coupling patterns would arise from substitution at either the 3 or 6 positions, but these are easily distinguished. If substitution were to occur at position 3, H-5 would couple with H-4 and H-6, thus giving a dd splitting pattern with coupling constants of about 8 and 5 Hz, respectively, with signals appearing at approximately 7.3-7.4 ppm.

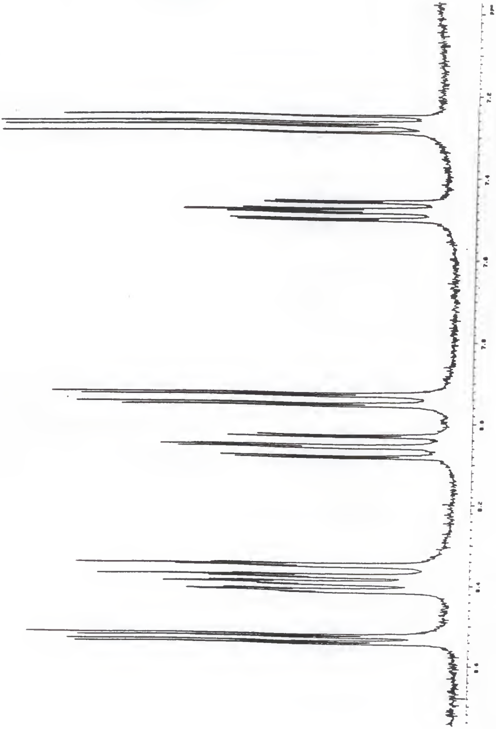

Figure 3-3: Aromatic Region of the Proton NMR of 3-3c ($CDCl_3$).

This was observed. Had substitution occurred at position 6, H-4 would be coupled with H-3 and H-5, and a similar dd (or t) splitting pattern would be found but with coupling constants of about 8 Hz for both sites.[76] This was not the case. Also, the typical shift of H-4 is downfield compared to H-5, as found here, providing further confirmation.

The simple three proton spectrum of the aromatic portion of disubstituted BPY 3-3a due to its symmetry indicates that substitution took place at the same site on each ring, again at the 3 (3′) positions as ascertained above. Moreover, the presence of small side bands resulting from the coupling of ^{117}Sn and ^{119}Sn isotopes identifies the adjacent protons as those at the 4 and 4′ positions in 3-3a and 3-3b and further supports the structures.[77]

The ethyl chains of borane 3-3c show diastereotopic protons for the methylene groups; these are present as *two* sets of multiplets at 0.81 and 0.57 ppm thus indicating the presence of a BN inter-ring bond and restricted rotation of the boryl group, as observed by others.[78]

In the case of product 3-4 from 2,4′-BPY, substitution occurred on the 4′-pyridyl ring as indicated by the absence of two multiplets, each containing two protons, typically associated with a symmetrical 4-substituted pyridyl ring. However, the proton spectrum was not especially informative about the two possible reaction sites, but the ^{13}C spectrum provided substantial information (Figure 3-4).[74] Knowing that an *ipso* carbon is deshielded by tin, as are the *ortho* carbons but to a lesser degree, the reaction site could be identified.[8] An APT experiment indicated the signals at 146.5 (C-4′) and 154.8 (C-2) ppm to be those of the proton-free carbons of starting material 3-2 while the APT spectrum of 3-4 contained proton-free signals at three sites, 150.8 (C-4′), 155.7 (C-2) and 136.4 (C-3′) ppm. The high field position of this latter signal identifies it as a 3′ and not a 2′ carbon atom, having been shifted from 121.2 ppm in the starting material.

Structure Determination of Terpyridines

NMR also provided the means to determine the structures of the novel terpyridines, 3-5 and 3-6. Since both compounds were isolated as the dihygrogen perchlorate salts, many of the signals were more downfield, as expected. For 3-5, the protons on the carbons adjacent to the annular nitrogen atoms gave the most useful information. The one proton singlet at 8.90 ppm (H-2″) indicated the presence of a 3-substituted pyridine as expected from the coupling reaction. The downfield one proton doublets at 8.96, 8.85, and 8.71 ppms for positions H-6″, H-6′, and H-6 each had the expected coupling constants from 5-6 Hz. A few of the remaining peaks could be tentatively assigned, but this was complicated by overlapping signals.

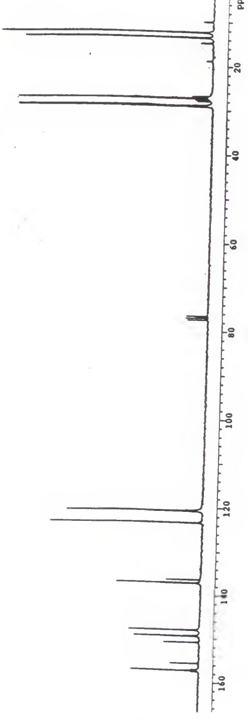

Figure 3-4: Carbon-13 NMR of 3-4 ($CDCl_3$).

The proton spectrum Figure 3-5) of 3-6 (DMSO-d_6) was deceptive in that accidental signal overlap at two low field positions indicated the presence of an unsubstituted 4-pyridyl ring. However, a COSY analysis (Figure 3-6) confirmed that simple cross-coupling did occur to give the expected product. The COSY indeed showed that the two low field signals were not coupled to each other, and therefore, there was no unsubstituted 4-pyridyl ring. In fact, these signals (9.04 and 8.87 ppms) were due to the overlap of the expected singlets and doublets from the protons H-2′, H-6′ and H-2″, H-6″. The doublet in the overlap at 9.04 ppm was more specifically assigned as H-6′ due to the coupling (6 Hz) with H-5′ at 8.12 ppm, and the signal at 8.12 ppm was shown not to have any further coupling. This was significant because the H-6″ doublet in the overlap at 8.87 ppm was coupled to H-5″ which was part of the multiplet at 7.95 ppm. However, there was further coupling (8 Hz) of H-5″ to H-4″ at 8.24 ppm. The doublet at 8.52 ppm was assigned as H-6, being coupled (5 Hz) to H-5 at 7.49 ppm. H-4 was determined to be part of the multiplet at 7.95 ppm, being coupled to H-3 (8 Hz) and H-5 (7 Hz).

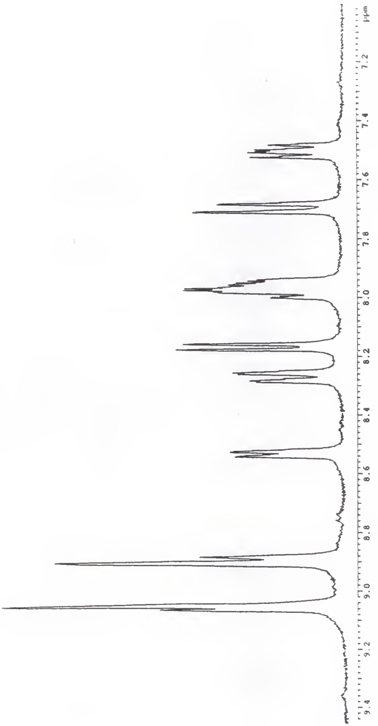

Figure 3-5. Proton NMR of 3-6 (DMSO-d_6).

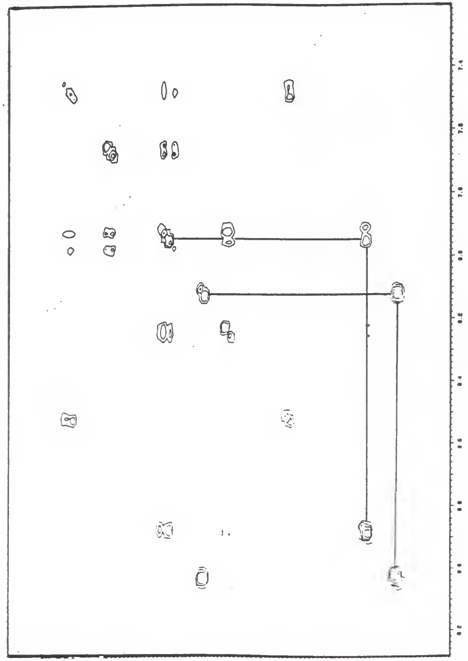

Figure 3-6. COSY Spectrum of 3-6 (DMSO-d_6).

Conclusions

Directed *ortho* lithiation of bipyridines was found to be an effective means for the preparation of 3- and 3′-substituted BPYs directly from the parent BPYs, which has not been common.[80,81] The approach presented here gives some insight into the scope and limitations of such methodology with bipyridines.[82] Several electrophiles could be utilized, but yields were only moderate, although optimization was not explored. Also, these compounds were illustrated to be of use by reacting them further in palladium-catalyzed cross-coupling reactions. With bipyridines and related compounds being extremely important as ligands, this methodology could lead to compounds that contribute much to such an area of study.[83,84,85]

CHAPTER 4
DIRECT PREPARATION OF N-QUATERNIZED POLYCYCLIC AZINES BY PALLADIUM-CATALYZED CROSS-COUPLING

Introduction

When quaternizing nitrogen atoms in polycyclic azines, the success of the reaction is often determined by steric and electronic factors.[86,87,88] If perhaps several similarly reactive nitrogen atoms are available, selectively directing N-quaternization to one of the nitrogens is synthetically challenging and generally is unsuccessful. Mixtures are often formed which may be tedious to separate,[89] as well as making identification of the resultant isomers quite difficult. An even more challenging aspect arises when functionalization of the less reactive site is desired, and so special methods are required to achieve the selectivity. One such method, for example, involves a multistep route employing a removable protecting group at the more reactive annular nitrogen atom in 2,3′-bipyridine. After protection, the sterically hindered, less reactive nitrogen atom could be mono-N-methylated to form 1-methyl-2,3′-bipyridnium ion.[90]

This report includes examples using palladium-catalyzed cross-coupling with "prequaternized" hetaryl compounds to achieve selective functionalization and unequivocal isomers. This approach serves as model for syntheses where selective N-quaternization, as well as other types of N-functionalization of several rings is now possible in a regiocontrolled manner.[91]

Although the number of recently reported transition metal-catalyzed cross-coupling reactions used to prepare polyaryl and polyhetaryl compounds has grown extensively, palladium being the metal of choice,[29,71,92,93,94] the preparation of N-quaternized polyhetaryls by such coupling reactions using quaternized starting materials seems not to have been exploited at all.

In this report, a boronic acid or a hetarylborane and a halogenated, N-quaternized heteroaromatic compound are employed to effect coupling under aqueous alkaline conditions in the presence of a palladium catalyst, a standard procedure known as the Suzuki reaction.[29,92,95] Figure 4-1 illustrates the successful reactions. An alkaline medium seems to be a necessity for such couplings in order to afford an intermediate "ate" complex of the boron reagent on addition of hydroxide ion.[39] The "ate" complex then transfers its aromatic ligand to the palladium

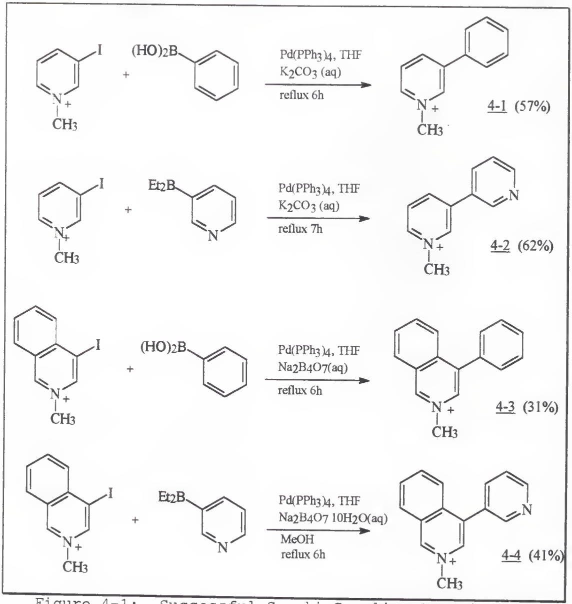

Figure 4-1: Successful Suzuki Coupling Reaction with Prequaternized Hetarenes.

oxidative addition product of the halide prior to product formation in a final reductive elimination step.[40-43]

Nonaqueous solvents such as DMF and triethylamine have also been effective for the cross-coupling of pyridylboronic acids in the presence of a palladium catalyst.[44]

Boranes are known to couple with triflates with a palladium catalyst in a suspension of Na_3PO_4 in dry dioxane.[39] Oxidative addition complexes have been isolated and characterized but such was beyond the scope of this study.[41,96,97]

In selecting reaction conditions for coupling, it is worth remembering that N-quaternization activates a halogenated hetarene for nucleophilic substitution by displacement of the halogen atom.[98,99] For example, nucleophilic substitution of 2-chloro- and 4-chloro-1-methylpyridinium ions is about 10^{21} and 10^{19} time faster, respectively, than substitution of chlorobenzene.[98,99] Moreover, the alkaline conditions may also give rise to degradation of quaternized hetarenes by ring cleavage reactions.[100] While nucleophilic substitution by the S_NAr mechanism is largely insensitive to the identity of the halogen nucleofuge,[98] cross-coupling rates decrease in the order I > Br > Cl. Special considerations, such as the halogen atom and reaction conditions (especially pH), should be made for the cross-coupling reactions of hydrolytically labile substrates to be successful.

Results and Discussion

Preparation of the Representative Compounds

The compounds selected for preparation were designed to illustrate the power of the approach and to establish some scope and limitations. Consider the syntheses of 3-phenyl-1-methyl-pyridinium ion[100] (4-1) and 1-methyl-3,3′-bipyridinium ion (4-2). 3-Iodo-1-methylpyridinium ion,[101] the quaternized starting material for the reactions, was obviously activated for nucleophilic substitution and ring cleavage by hydroxide ion. However, 4-1 was successfully prepared using phenylboronic acid and the 3-iodide, and 4-2 was formed from the same iodide and diethyl(3-pyridyl) borane. While the quaternizations of 3-phenylpyridine to give 4-1 and 3,3′-bipyridine to yield 4-2 would be simple and unequivocal reactions, the current coupling method illustrates the principle that even quaternized substrates very highly activated for nucleophilic substitution and ring cleavage may be cross-coupled successfully under aqueous alkaline conditions.

The reactivity of N-methylisoquinolinium salts were also examined. Nucleophilic substitution[102] and ring cleavage[99,103] reactions of these bicyclic materials are often many times more facile than that of the pyridinium ions. It was, therefore, necessary to make several attempts to find the proper alkaline conditions to minimize side reactions.

Borate, phosphate, and bicarbonate buffers were examined in order to lower successively the reaction pH.

It was possible to prepare the 4-phenylated isoquinolinium ion, 4-3, by employing 4-bromo-2-methylisoquinolinium ion[104] and phenyl boronic acid with borate base, but attempts to make the 4-pyridylated isoquinolinium ion using borate, phosphate, or bicarbonate buffers were unsuccessful due to ring degradation of the heterocyclic cation when the reaction was run with two phases, the aqueous alkaline layer containing the isoquinolinium ion. However, the addition of methanol to make the mixture homogeneous allowed 4-4 to be formed and isolated in 43% yield in the presence of borate buffer. The unquaternized precursor of 4-4 has been prepared by a palladium coupling route.[105]

Structure Determinations

Simple inspection of the proton NMR of the prepared compounds provided sufficient evidence for the actual structures in that several of the non-quaternized substrates are known.[106,107] For 4-1, the presence of a singlet at 9.38 ppm indicated a 3-substituted pyridine. A doublet at 8.93 ppm was assigned to H-6 of the pyridine ring having a coupling constant of 6 Hz, common for that position coupling to H-5. A doublet at 8.17 ppm was assigned to H-4 having an 8 Hz coupling to H-5.

The dd splitting pattern at 8.17 ppm could then be assigned to H-5 having the 6 and 8 Hz couplings to the above mentioned proton. The remaining aromatic peaks were easily assigned to the phenyl because they were at higher field, and the three proton singlet at 4.39 ppm was given to the N-methyl group.

For 4-2, there should be two signals corresponding to the isolated protons in a 3,3′-bipyridine system, and this was indeed the case, the difference between the two pyridyl rings being that one was quaternized. The singlet at 9.47 ppm was assigned to H-2, and the doublet (1 Hz long range coupling) at 9.07 ppm was given to H-2′ of the non-quaternized ring. Corresponding to 4-1, there were two doublets at 8.95 ppm with 6 and 8 Hz couplings. Thus, these were given assignments of H-6 and H-4, respectively. A doublet at 8.73 ppm with 5 Hz coupling was assigned to H-6′, as expected for an unquaternized pyridine ring. At 8.25 ppm there were two overlapping triplets assigned to H-5 and H-4′. At 7.63 ppm there was a dd splitting pattern with 5 and 8 Hz couplings, and this was assigned to H-5′. The quaternizing methyl proton signals appeared at 4.39 ppm.

The most easily assigned signals for 4-3 were the three proton singlet for the N-methyl at 4.50 ppm and the five proton multiplet associated with the phenyl ring at 7.65 ppm.

There was a singlet at 10.00 ppm associated with H-1, and there was a doublet with a 1 Hz coupling at 8.78 ppm. These two peaks are associated with the quaternized isoquinolinium ring. The remaining signals at 8.55, 8.23, and 8.09 ppm could then be assigned to the other isoquinoline protons, H-5, H-6, H-7, and H-8.

With a pyridyl ring bonded to the isoquinolinium system, the spectrum of 4-4 became somewhat more complicated. The three proton signal at 4.51 ppm was, of course, assigned to the N-methyl group, and the singlet at 10.07 ppm was assigned to H-1 of the isoquinolinium ion. The three proton multiplet at 8.85 ppm was assigned to H-3 of isoquinolinium, along with the H-2′ and H-6′ protons of the pyridine ring. Analogous to 4-3, there were signals for H-5, H-6, H-7, and H-8 at 8.58 ppm, 8.26 ppm, and 8.10 ppm, a multiplet which also included H-4′ of the pyridyl ring. The signal at 7.72 ppm was assigned to H-5′ of the pyridyl ring with characteristic couplings of 6 and 9 Hz.

Conclusions

Preparation of N-quaternized polycyclic azines of unequivocal structure may be accomplished by palladium-catalyzed cross-coupling under aqueous conditions. Starting with funtionalized starting materials allows the steric and electronic factors that control such functionalizations to be overcome. Other types of nitrogen derivatives, such as N-oxides[1], are also found to be successful. Following this work, similar methodology was established for Stille coupling reactions.[108]

---

[1] N-Oxide compounds were prepared by Michael Cruskie.

CHAPTER 5

RELAXATION AND METAL-SUBSTRATE COMPLEX LIFETIME INFLUENCES ON NUCLEAR RELAXATION RATES OF FUNCTIONALIZED BIPYRIDINES

Introduction

Pyridine and pyridine N-oxide compounds have been the focus of many studies which seek to probe the magnetic interactions between unpaired electrons on transition metal ions and magnetic nuclei coordinated to these ions.[13,109,110,111] By observing ^{13}C and ^{1}H chemical shift and relaxation patterns, the delocalization of spin density onto pyridine ligands has been appreciated. Early work focused on changes in chemical shifts produced by these ions while more recent studies have employed the more sensitive proton and carbon T_1 relaxation methods.

Spin density is delocalized by direct delocalization and spin polarization.[13] Direct delocalization is self-explanatory, while spin polarization is not as easily understood. If spin density is present in a p_π orbital of an sp^2 hybridized atom, spin polarization induces spin density at the nucleus through the 1s and 2s orbitals. Spin density is then introduced to the nuclei of attach atoms through the σ covalent bond but with a sign opposite that of the spin density in the p_π orbital. This is illustrated in Figure 5-1.

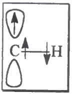

Figure 5-1. Illustration of Spin Polarization

In the presence of paramagnetic metal ions such as d^8 Ni(II) and d^7 Co(II), an alternating pattern of proton chemical shifts for pyridine N-oxide is observed, *ortho* signals shift upfield, *meta* downfield, and *para* upfield.[13,109] This type of pattern is characteristic of π delocalization which induces spin polarization of the *meta* carbon. Proton signals of pyridine with Ni(II), on the other hand, are all shifted downfield with the order *ortho* shift > *meta* > *para*.[13,110,111] This is indicative of direct delocalization of σ spin density. When unpaired electrons are in the metal orbitals of octahedral complexes which have the correct symmetry to form a σ bond with a nitrogen or oxygen lone pair, for example, direct delocalization of spin density is observed.[13] Spin polarization is required to induce spin density onto ligands when unpaired electrons reside in metal orbitals that cannot contribute to σ delocalization.

Pyridine N-oxide does form a σ bond with Ni(II) and Co(II), but the non-orthogonality between the coordination bond and the π system induces the spin density into the π system.[13,109]

However, things are not always so simple, and the magnitude and direction of chemical shifts indicate that more than one delocalization process is possible. For example, Cramer and Drago determined that σ and π delocalization of spin density are quite probable in order to explain the observed proton chemical shifts of octahedral Ni(II) complexes of pyridine.[110] In another study, Doddrell and Roberts came to similar conclusions for Ni(II) and Co(II) complexes of pyridine but determined that delocalization onto ^1H and ^{13}C is not necessarily the same within a compound. In addition, they found that delocalization for Ni(II) and Co(II) complexes are not likely to be the same.[111] Bertini, Luchinat, and Scozzafava determined that more than one spin delocalization mechanism is also in effect for pyridine N-oxide, with dissimilarities for proton and carbon as well.[109]

Nuclear relaxation times for such compounds have led to similar conclusions regarding the delocalization of spin density.[13,109] Relaxation times reflect, in part, the amount of spin density which is delocalized onto a ligand from a paramagnetic metal ion. Since chemical shifts may be used to determine the amount of spin density residing in ligand orbitals, equations for relaxation which also take this into account have been derived.[23,24,25] Thus, the breakdown of the Solomon-Bloembergen prediction, as it relates relaxation rate constants to distance ($T_1^{-1} \propto R^{-6}$), has been observed in several instances.

Another case in which the Solomon-Bloembergen prediction appears to breakdown presents itself when a substrate exists in two states, unbound and bound to a paramagnetic metal. In this situation, the relaxation phenomenon as predicted by Solomon-Bloembergen (T_1) and the lifetime of the metal-substrate complex (τ) influence the measured rate of relaxation ($1/(T_1 + \tau)$).[26,27] Since the relative amounts of these two effects vary with distance between the nuclei and the metal-center, the influence of the two phenomena are different for each nucleus. For example, a nucleus in close proximity to the metal-center would be expected to have a small T_1 value ($T_1 < \tau$) such that τ dominates the measured rate of relaxation. The opposite ($T_1 > \tau$) is true for nuclei much farther from the metal-center. Since there are two processes, it is obvious that the Solomon-Bloembergen prediction may not adequately explain the measured relaxation rates. This is demonstrated more definitively in a later discussion.

In a recent publication, Zoltewicz and Bloom found an unusual relationship between nickel(II) induced relaxation rate constants for protons and distances between these protons and nickel bound to a nitrogen atom in a quaternized bipyridine system.[112] Relaxation rate constants were corrected to reflect only the change caused by the Ni(II) and then were plotted against the inverse distance in Angstroms between the nitrogen coordination site and the annular protons, "a slightly concave curve that is very well approximated by a simple linear relationship (correlation coefficient r = 0.994)" resulted. This finding led to the idea that perhaps a new, unusual phenomenon involving relaxation rate constants and distances was found. However, this idea was based only on one simple plot.

Our new work focuses mainly on the proton and carbon relaxation data obtained for the compound 1-methyl-4-(4′-pyridyl)pyridinium iodide (MEBPY, 5-1), as used by Zoltewicz and Bloom, in the presence of paramagnetic salts, mainly nickel(II), but also cobalt(II). Variables such as solvent and temperature are also explored. Furthermore, the proton relaxation data for a few other pyridine-containing compounds are studied to provide more insight into the observed relationships. Figure 5-2 illustrates all of the molecules studied. The compounds, excluding MEPYR, are chosen because of their cylindrical symmetry with respect to the site of coordination to the respective metal ions. The intent of this new work is to obtain relaxation data, determine obvious and general trends, and to compare and contrast the results with those from the literature.

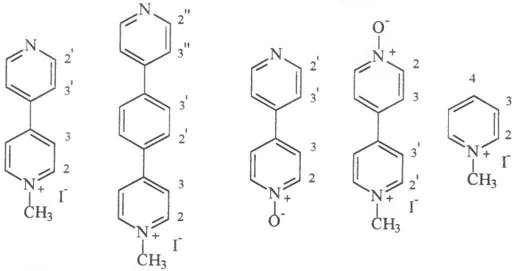

MEBPY 5-1 | STRBPY 5-2 | BPYNOX 5-3 | MEPOX 5-4 | MEPYR 5-5

Figure 5-2: Pyridine Systems Studied by T_1 Relaxation.

Results and Discussion

Preparation of Substances and Stock Solutions

MEBPY (5-1), BPYNOX (5-3), and MEPOX (5-4) were all prepared in accordance with known procedures, and MEPYR (5-5) was available in our laboratory.[113,114] MEBPY was easily prepared by a mono-N-methylation of 4,4'-bipyridine

(4,4′-BPY) with methyl iodide and was recrystallized from ethanol. BPYNOX was made by oxidizing 4,4′-BPY with H_2O_2 in acetic acid, and MEPOX was prepared by mono-N-methylation of BPYNOX with methyl iodide.

The synthesis of STRBPY (5-2) was somewhat more challenging because the compound to be quaternized was not readily available. A suitable synthesis for bis-(4-pyridyl)benzene had to be found. A few examples involving palladium-catalyzed cross-coupling exist in the literature, and it was from these that a successful synthesis eventually resulted.[115,116]

The first attempted method involved the coupling of diethyl(4-pyridyl)borane with para-dibromobenzene, an example of the Suzuki reaction.[29] However, the preparation of the borane by lithiation of 4-bromopyridine proved unsuccessful. This was attributed to the self-quaternization of 4-bromopyridine and the inability to fully dry it, since it had to be isolated from its more stable hydrochloride salt.

Next, the possibility of tin reagents was explored due to the success of Stille reactions which involve, in this case, the cross-coupling of an aryl halide and an aryl stannane in the presence of a palladium catalyst.[28]

Firstly, the preparation of 1,4-bis-(tributylstannyl)-benzene, for possible coupling with 4-bromopyridine, was attempted but proved unsuccessful. Finally, tributyl-(4-pyridyl)stannane was prepared but by a procedure not previously reported. Similar compounds had been prepared by a reaction between 4-pyridyl sodium and a tin halide reagent,[117] but the method presented here was found to be simpler and to provide good yields (60-80%). The hydrochloride salt of 4-bromopyridine was simply added to diethyl ether forming a slurry, with some slight solubility. After cooling to -40 °C, two equivalents of butyllithium (BuLi) were added, the first to remove the hydrochloride proton and the second to accomplish a metal-halogen exchange. The reaction mixture, now containing 4-lithiopyridine, was cooled further to -70 °C and was quenched with tributyltin chloride (Bu_3SnCl). The desired compound was isolated by solvent evaporation after aqueous washings and was purified by column chromatography with silica gel. Figure 5-3 shows this procedure.

After the stannane was isolated, it was then allowed to react with para-dibromobenzene in the presence of a palladium catalyst to form the 1,4-bis-(4-pyridyl)benzene. When using tetrakis(triphenylphosphine)palladium as the catalyst, the reaction had mixed success. Some of the 1,4-bis-(4-pyridyl)benzene could be isolated, but often, mono-coupled product, p-(4-pyridyl)bromobenzene, was isolated exclusively or in competitive yields. However, the mono-coupled product was allowed to react further to obtain the desired dicoupled product.

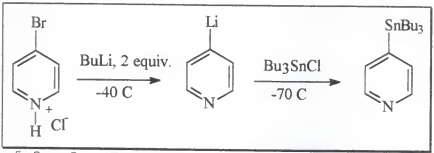

Figure 5-3: Low Temperature Preparation of Tributyl-(4-pyridyl)stannane. (The lithium compound was not isolated.)

Prequaternization of the mono-coupled product with methyl iodide formed 4-(4-(1′-methylpyridin-1′-ium-4′-yl) bromobenzene iodide, and using the methodology outlined in Chapter 4, further coupling of the stannane was attempted. This unsuccessful reaction would have resulted in the desired quaternized product.[86]

The most successful coupling occurred using *trans*-di-(acetato)-bis[*o*-(di-*o*-tolylphosphino)benzyl]palladium as the catalyst.[118,119] The 1,4-bis-(4-pyridyl)benzene was isolated in 82% yield. The material was then quaternized with methyl iodide to prepare 1-methyl-4-((4′-pyridyl)phenyl)pyridinium iodide. Figure 5-4 illustrates these reactions.

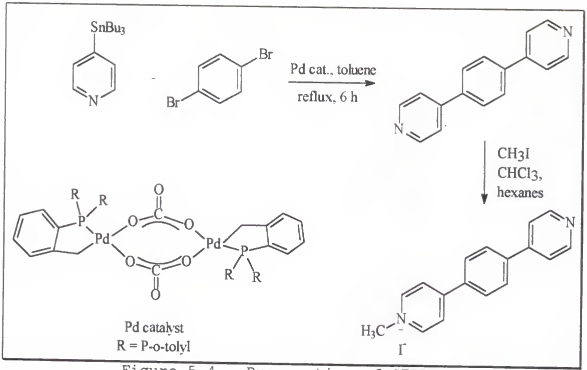

Figure 5-4. Preparation of STRBPY.

Stock solutions of MEBPY, BPYNOX, MEPOX, MEPYR (0.10 M), and STRBPY (0.060 M) were prepared in degassed deuterated solvents, D_2O, DMSO-d_6, CD_3OD, or a combination thereof. Corresponding stock solutions of $NiCl_2$, $NiBr_2$, and $CoCl_2$ (0.30 M) were also prepared. Degassing of the solvents with nitrogen was necessary to remove dissolved paramagnetic oxygen.

Measurement of T_1 Relaxation Values

Relaxation values for each of the protons or carbons were determined by the inversion-recovery method on the Gemini 300 MHz or Unity 500 MHz NMR machines. In a typical experiment, 700 μl of the substrate stock solution

(0.10 M or 0.060 M) was placed in an NMR tube, and the T_1 relaxation values were determined for the substrate in the absence of paramagnetic substances at 25 °C. These values were used for correction terms. Subsequently, a small amount of the stock solution of the paramagnetic substance (0.30 M) was added, and the relaxation values were again determined at 25 °C. Additions of the paramagnetic substance continued, each time increasing the paramagnet concentration followed by measurement of the relaxation values. The substrate concentrations were 0.98-0.82 M in D_2O with NiX_2 (MEBPY, MEPOX, BPYNOX, and MEPYR), 0.099-0.98 M in DMSO-d_6 and CD_3OD with $NiCl_2$ (MEBPY), 0.099-0.098 M in D_2O with $CoCl_2$ (MEBPY), and 0.059-0.53 M in D_2O/DMSO-d_6 with $NiCl_2$ (STRBPY). The metal salt concentrations were 0.0059-0.053 M for $NiCl_2$ and $NiBr_2$ in D_2O (MEBPY, MEPOX, BPYNOX, and MEPYR), 0.0017-0.0063 M for $NiCl_2$ in DMSO-d_6 (MEBPY), 0.0013-0.0051 M for $NiCl_2$ in CD_3OD (MEBPY), 0.0017-0.0071 M for $CoCl_2$ in D_2O (MEBPY), and 0.0036-0.033 M for $NiCl_2$ D_2O/DMSO-d_6 (STRBPY).

Changes in the ^1H NMR spectra of the respective compounds were observed upon addition of the metal ions. There was line broadening which resulted in the loss of coupling patterns and slight shifts on the order of 0.1-0.2 ppm, but at the highest nickel concentrations there was significant overlap of signals which made determination of relaxation time difficult, especially for the proton closest to the coordination site. In the extreme case these data could not be collected, but this was rare. The proton closest to the coordinating nitrogen or oxygen atom was the first to exhibit the effect, but as metal ion concentration increased, subsequent protons began to exhibit the same effect. Small broadening effects are also observed in ^{13}C spectra.

No attempt was made to control the ionic strength of the solutions for the experiments. Ionic strength is determined by

$$I = \tfrac{1}{2}\,\Sigma[X^{+/-}]z^2 \quad \text{(Eq. 5-1)}$$

where $[X^{+/-}]$ is the concentration of any ion in solution and z is the charge on the ion. In the present experiments, there is a contribution from the substrate and the metal salt. The substrate contribution is given by

$$I_{subst} = \tfrac{1}{2}\,([S^+]1^2 + [X^-]1^2) \quad \text{(Eq. 5-2),}$$

and since substrate ion concentration $[S^+]$ equals the counter-ion concentration $[X^-]$, the equation collapses to

$$I_{subst} = [S] \quad \text{(Eq. 5-3).}$$

The metal salt contribution is given by

$$I_{salt} = \tfrac{1}{2}\,([M^{+2}]2^2 + [X^-]1^2) \quad \text{(Eq. 5-4),}$$

and since halide ion concentration is twice the metal ion concentration, the equation may be rewritten as

$$I_{salt} = \tfrac{1}{2}\,([M^{+2}]2^2 + 2[M^{+2}]) \quad \text{(Eq. 5-5).}$$

The equation then collapses to

$$I_{salt} = 3[MX_2] \quad \text{(Eq. 5-6)}.$$

So the overall ionic strength of the solutions in these experiments is given by

$$I = [S] + 3[MX_2] \quad \text{(Eq. 5-7)}.$$

Experiments in D_2O have an ionic strength range of 0.10 - 0.24 M since greater concentrations of metal salts are used. In DMSO-d_6 and CD_3OD, the range is 0.10-0.11 M, and the change is insignificant.

Data Manipulation of the Relaxation Values

After the measurement of the relaxation values, the data were handled in the following manner. First, the relaxation values were converted to the corresponding rate constants (k) according to the equation

$$k = 1 / T_1 \quad \text{(Eq. 5-8)}.$$

Then, the rate constants for the substrates in the presence of paramagnetic material were corrected for relaxation in the absence of this ion. This was done by subtracting the rate constant for substrate without paramagnetic material (k_{solv}) from the observed rate constant values in the presence of paramagnetic salt (k_{obs}) such that

$$k_{corr} = k_{obs} - k_{solv} \quad \text{(Eq. 5-9)}.$$

The corrected relaxation rate constants for each specific proton were then plotted versus the paramagnetic salt concentration to obtain the value k_2 from the slope of such a plot according to the equation

$$k_{corr} = k_2[M^{+2}] + b \quad \text{(Eq. 5-10)}$$

where k_2 is the apparent second-order rate constant for relaxation resulting from the following equilibrium (Equation 5-11) and b is the intercept which is considered in greater detail at the end of this section. For carbon atoms, k_{obs} versus the paramagnetic salt concentration was used to determine k_2. This was done because obtaining k_{solv} values, in the absence of paramagnetic salt, would require an exorbitant amount of time, and k_{solv} for carbon is expected to be rather insignificant due to typically long relaxation times for carbon.

$$M^{+2}(Solv)_6 + S \overset{K}{\rightleftharpoons} M^{+2}S(Solv)_5 + Solv \quad \text{(Eq. 5-11)}$$

In this equilibrium S is free substrate, Solv is solvent, $M^{+2}S(Solv)_5$ is substrate bound to the paramagnetic substance, and K is the equilibrium constant. The metals used in this study are known to form hexacoordinate, octahedral species with the solvents chosen.[120-128] Since each of the substrates studied has a free nitrogen or oxygen atom as a coordination site, excluding MEPYR, the metal ion is expected to form a covalent bond with the substrates. It is assumed that only one substrate at a time binds to the metal due to the low concentration of the metal ion and the known, modest binding constant for pyridine and Ni(II).[129]

Moreover, Chachaty states that it seems that relaxation rates of ligands in a coordination sphere are not very dependent on the number of bound ligands.[130] The presence of this equilibrium also indicates that substrate-solvent exchange should have a significant influence on the T_1 value provided that exchange is faster than relaxation. The equilibrium constant may be given by

$$K = [M^{+2}S(Solv)_5] \;/\; [S]\;[M^{+2}] \qquad \text{(Eq. 5-12)}$$

Accordingly,

$$k_{corr} = k_1 \text{ x (fraction of bound substrate)}$$

$$= k_1 \; [M^{+2}S(Solv)_5] \;/\; ([M^{+2}S(Solv)_5] + [S]) \qquad \text{(Eq. 5-13)}$$

where k_1 is the true first-order rate constant for the relaxation of mono-coordinated complex. Substitution into Equation 5-13 by Equation 5-12 gives

$$k_{corr} = k_1[Ni^{+2}]K \;/\; ([Ni^{+2}]K + 1) \qquad \text{(Eq. 5-14)}$$

There would then be two limiting cases. If $[Ni^{+2}]K < 1$, then Equation 5-14 collapses to

$$k_{corr} = k_1[Ni^{+2}]K \qquad \text{(Eq. 5-15)}$$

or

$$k_{corr} = k_2[Ni^{+2}] \qquad \text{(Eq. 5-16)}$$

If $[Ni^{+2}]K > 1$, then the substrate is essentially completely bound, and Equation 5-14 becomes

$$k_{corr} = k_1 \qquad \text{(Eq. 5-17)}$$

This latter saturation binding was not observed.

Thus, k_2 is composed of two terms, k_1, a first-order term, and an equilibrium binding constant, K. The product of these two terms gives second-order units, 1/M-s.

Once the k_2 value for each atom was determined, plots of k_2 versus the inverse distance from the metal ion to each nucleus were used to illustrate the deviation from the Solomon-Bloembergen prediction, as well as giving credence to the existence of other relaxation processes such as ligand-centered effects.

A distance of 2.5 Å between the coordinating nitrogen or oxygen atom and the metal-center is chosen based on distances that have been determined for pyridine complexes with Ni(II) and Co(II), 2.0-2.2 Å.[120-128] This bond length may be slightly longer than that in reality, but whether the bond length was 0 Å (metal located on the coordination site), as used by Zoltewicz and Bloom, or even longer than 2.5 Å had no effect on the magnitude of the correlation coefficient for the observed correlation between relaxation rate constants and metal to nucleus distance.

When considering the intercept value (b) in Equation 5-10, the above manipulation of the data does not fully reflect the results from all of the experiments. The intercept value generally is zero within the error limits of one standard deviation for D_2O solvent, with an occasional exception. But this is not the case when the solvents are DMSO-d_6 and CD_3OD. For experiments in DMSO-d_6 and CD_3OD, there are large values for the intercept which are often several times larger than a single standard deviation indicating that the values were finite and of significance.

The observation is interpreted to mean that mixed forms of the solvated metal ion are present in the non-aqueous solvents; these include those from bulk solvent as well as those from residual D_2O, $M(Solv)_{6-y}(D_2O)_y$. Moreover, if there is a significant difference in the metal ion species in terms of binding or turn-over rates, certain species may have little or no effect on the relaxation rate constants. So, the data are treated in the following way making the assumption that the total nickel ion concentration has to be corrected to reflect the presence of an unreactive form. Thus, the intercept value was divided by the slope to generate a constant, *a*, that is the same for all of the positions in the substrate as in Equation 5-13.

$$k_{corr} = k_2([M^{+2}] + a) \qquad \text{(Eq. 5-18)}$$

The *a* values are determined to be -8.5×10^{-4} M for DMSO-d_6 and -6.5×10^{-4} M for CD_3OD. Thus, the total paramagnetic ion concentration is reduced to reflect the presence of millimolar amounts of a relaxation non-active form of the metal ion, presumably a hydrate.

Example with MEBPY

As an example of the above manipulation, the data obtained for the protons of MEBPY in D_2O in the presence of $NiCl_2$ are presented. Table 5-1 lists the T_1 values and corresponding rate constants (k_{solv}) for MEBPY in the absence of paramagnetic nickel (II).

Table 5-1. T_1 Relaxation Values and Rate Constants for the Respective Protons of MEBPY in the Absence of $NiCl_2$ at 25 °C.

Proton	Shift (δ ppm)	T_1 (s) (±Error)[a]	k_{solv} (s^{-1})
H-2′	8.79	3.83 (±0.31)	0.261
H-3′	7.94	2.98 (±0.28)	0.336
H-3	8.42	2.84 (±0.23)	0.352
H-2	8.95	3.16 (±0.18)	0.316
Me	4.50	1.53 (±0.04)	0.654

a) Error based on one standard deviation.

Table 5-2 gives the values of the corrected rate constants (k_{corr}) for each proton resulting from the observed T_1 values in the presence of a low concentration of nickel (II). Similar data were then collected with increasing Ni^{+2} concentrations, also listed in Table 5-2. Error limits for all of the data may be found in the Appendix.

Table 5-2. Corrected Rate Constants for the Protons of MEBPY at Several Nickel Concentrations at 25 °C in D_2O.

$[Ni^{+2}]$ (M)	k_{corr} H-2′ (s^{-1})	k_{corr} H-3′ (s^{-1})	k_{corr} H-3 (s^{-1})	k_{corr} H-2 (s^{-1})	k_{corr} H-Me (s^{-1})
0.00588	6.07	4.11	1.97	0.645	0.392
0.0103	11.4	7.54	3.38	1.09	0.682
0.0143	14.3	10.2	4.86	1.59	0.957
0.0222	22.4	16.2	7.52	2.56	1.52
0.0273	22.7	19.4	8.82	3.14	1.96
0.0529	34.8	39.5	16.8	5.43	3.40

Figure 5-5 shows the plot of k_{corr} versus $[Ni^{+2}]$ for the determination of k_2 for proton H-2. The k_2 (next section) values were then plotted versus the inverse of the distance from the metal ion to each proton.

These types of experiments and data manipulation were done for all of the mentioned compounds. Each of the compounds are discussed individually.

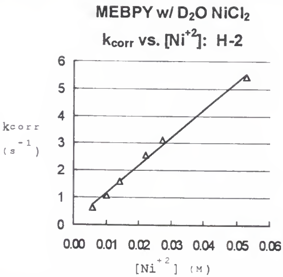

Figure 5-5. Plot of k_{corr} versus $[Ni^{+2}]$ for MEBPY with $NiCl_2$ in D_2O for Proton H-2. Slope(k_2) = 102 (±4.17), Intcpt. = 0.14 (±0.11), Correlation Coeff. = 0.997.

Substrate Summaries

Summary and discussion of relaxation data for MEBPY. Much of the experimentation focused on MEBPY, and nuclear relaxation data were collected under different conditions: ^1H, D_2O with $NiCl_2$; ^1H, D_2O with $NiCl_2$ and acetic acid; ^1H and ^{13}C, D_2O with $NiBr_2$ (also used for the temperature study);

^{1}H, D_2O with $CoCl_2$; ^{1}H, DMSO-d_6 with $NiCl_2$; ^{1}H, CD_3OD with $NiCl_2$. See the Appendix for all of the data from these experiments. Table 5-3 gives the k_2 values for the protons of MEBPY under the specific conditions.

Table 5-3. Second-order Relaxation Rate Constants (k_2, M^{-1}-s^{-1}) for MEBPY in Several Solvents containing Paramagnetic Salts at 25 °C

^{1}H	Shift (ppm)	D_2O $NiCl_2$	D_2O $NiCl_2$^{a}	D_2O $NiBr_2$	DMSO-d_6 $NiCl_2$	CD_3OD $NiCl_2$	D_2O $CoCl_2$
2′	8.79	979	879	999	21600	13300	1390
3′	7.94	750	668	800	4570	2790	118
3	8.42	314	286	314	1060	613	42.9
2	8.95	102	95.0	165	264	186	28.8
Me	4.50	64.5	64.2	105	153	120	17.3

a) Containing acetic acid to lower the pD to about 4.

There are some obvious trends. The protons closest to the nitrogen atom coordinated to the metal ion had the largest rate constants. There was a fall off in the value of the rate constants as the distance between the hydrogen nuclei and the metal-center increased. Importantly, all of the data with Ni^{+2} in D_2O gave relatively consistent values, demonstrating good reproducibility. Changing the counterion or the pD did not seem to affect the results.

Significantly, DMSO-d_6 and CD_3OD solvents gave very large rate constants for the protons closest to the metal-center as well as an especially fast decline in the values with respect to distance.

Cobalt was unusual. A fall off pattern for the rate constants similar to that for the nickel substrates was not observed in that $CoCl_2$ in D_2O resulted in a faster fall off of the rate constants.

Solvent effects are perhaps more easily understood. Solvent viscosity affects relaxation values in that molecules should experience less rotation in a more viscous solvent. Thus, there is a greater interaction with the surroundings and more opportunity for relaxation; shorter relaxation times are observed. The correction values (k_{solv}) for MEBPY in DMSO-d_6, D_2O, and CD_3OD showed this to be true with the respective viscosities being 2.2, 1.0, and 0.55 mPa-s. However, this effect was subtracted out for the respective corrected rate constants (k_{corr}) when measuring the effect of nickel ion. Perhaps some consideration should be given to the relative dielectric constants for the solvents as a factor in the efficiency of spin delocalization, D_2O (78.0), DMSO (48.0), and CD_3OD (32.0) and for the degree of metal-substrate binding as affected by solvent polarity.

Plots of the k_2 values versus the inverse distances from the metal-center illustrate the fall off in the respective solvents (Figures 5-6, 5-7, 5-8). These plots are not linear, but the relaxation rates also do not show a linear relationship with the inverse sixth power of the distance. However, a plot of the k_2 values for DMSO-d_6

versus the k_2 values for CD_3OD shows considerable linearity, suggesting the effects of the paramagnetic ion are similar in the two solvents (Figure 5-9).

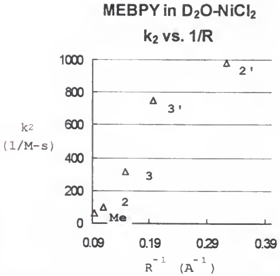

Figure 5-6. MEBPY Proton Relaxation Rate Constants (k_2) as Correlated with the Inverse Distance between the Protons and Bound $NiCl_2$ in D_2O.

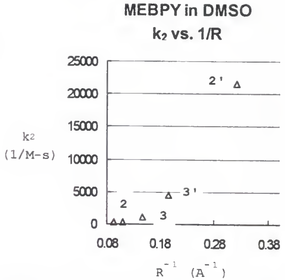

Figure 5-7. MEBPY Proton Relaxation Rate Constants (k_2) as Correlated with the Inverse Distance between the Protons and Bound $NiCl_2$ in DMSO-d_6.

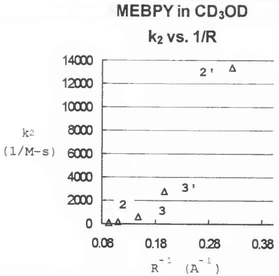

Figure 5-8. MEBPY Proton Relaxation Rate Constants (k_2) as Correlated with the Inverse Distance between the Protons and Bound $NiCl_2$ in CD_3OD.

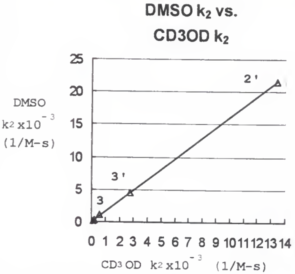

Figure 5-9: Correlation Between Relaxation Rate Constants for MEBPY in DMSO and CD_3OD Solvents Containing $NiCl_2$ (Slope = 1.6, Correlation Coefficient = 0.999).

The relaxation data for the carbon atoms of MEBPY was also determined. Table 5-4 lists the k_2 values, and Figure 5-10 gives the plot of k_2 versus the inverse distance between the carbon atoms and the metal-center. This plot shows seen there is no distinct pattern with respect to distance. In fact, the two pyridine rings seem to exhibit quite different relaxation behavior; the top and bottom portions seem to have their own relationship. Again, the inverse sixth power relationship between the relaxation rate constants and distance was not observed.

Table 5-4: Relaxation Rate Constants (k_2) for the Carbon Atoms in MEBPY and Distances Between These Atoms and Bound Ni(II) in D_2O at 25 °C.

Carbon	k_2 (M^{-1}-s^{-1})	R (Å)
C-2′	864	3.0
C-3′	725	4.3
C-4′	435	4.8
C-4	72.3	6.3
C-3	47.4	7.1
C-2	35.5	8.4
C-Me	21.0 [a]	10.4

a) Value corrected for number of protons (3) on the carbon.

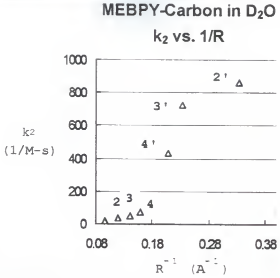

Figure 5-10. MEBPY Carbon Relaxation Rate Constants (k_2) as Correlated with the Inverse Distance between the Carbons and Bound $NiBr_2$ in D_2O.

Summary and discussion of relaxation data for STRBPY. Table 5-5 gives the observed second-order rate constants (k_2) for the protons of STRBPY, as well as the chemical shifts and the respective through space distances [R] from the metal-center to the protons.

Table 5-5: Relaxation Rate Constants (k_2) for the Protons in STRBPY and Distances Between These Atoms and Bound Ni(II) in D_2O at 25 °C.

Proton	k_2 (M^{-1}-s^{-1})	R (Å)
H-2″	1250	3.1
H-3″	1010	5.1
H-3′	549	6.8
H-2′	271	9.1
H-3	170	10.8
H-2	199	13.1
H-Me	236	14.9

This compound was of interest because of its longer length compared to any of the other substrates, and this offered the possibility of measuring an effect over longer distances. The k_2 values were found to be slightly larger than those of MEBPY in D_2O for equivalent positions with the same distances. The binding constant for STRBPY may well be larger than that of MEBPY due to the expected smaller effect of the more distant positively charged nitrogen atom on binding. The k_2 values seemed to follow the same fall off pattern as that of MEBPY except for the farthest protons, H-2 and Me, where the paramagnetic effect may be weakest (Figure 5-11).

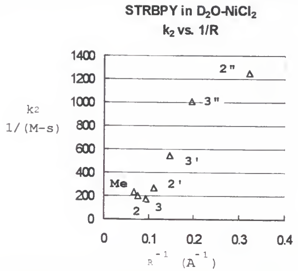
STRBPY in D_2O-$NiCl_2$
k_2 vs. 1/R

Figure 5-11. STRBPY Proton Relaxation Rate Constants (k_2) as Correlated with the Inverse Distance between the Protons and Bound $NiCl_2$ in D_2O.

There seemed to be a limitation of approximately 11 Å for the observed effects. A plot of the k_2 values for STRBPY versus those of MEBPY for the comparable protons illustrated the similarity between the molecules (Figure 5-12).

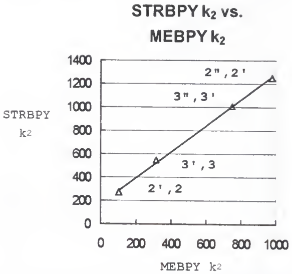

Figure 5-12. Comparison of Comparable Protons of STRBPY and MEBPY (Slope = 1.1, Correlation Coefficient = 0.999). Position numbers on the left are for STRBPY, and position numbers on the right are for MEBPY.

Summary and discussion of relaxation data for BPYNOX. Table 5-6 gives the observed second-order rate constants (k_2) for the protons of BPYNOX, as well as the chemical shifts and the respective through space distances [R] from the metal-center to the protons.

Table 5-6: Relaxation Rate Constants (k_2) for the Protons in BPYNOX and Distances Between These Atoms and Bound Ni(II) in D_2O at 25 °C.

Proton	k_2 (M^{-1}-s^{-1})	R (Å)
H-2′	2150	3.1
H-3′	1380	5.1
H-3	615	6.8
H-2	967	9.1

This compound has two possible sites for coordination with the metal ion. In fact, the k_2 values seemed to illustrate this possibility. Proton H-2′,closest to the free nitrogen atom, had the largest k_2 value, and proton H-2, closest to the N-oxide, had the third largest, indicating a significant degree of coordination to the oxide. However, whether the coordination was greater at the nitrogen atom or oxygen atom was not determined.

Summary and discussion of relaxation data for MEPOX. Table 5-7 gives the observed second-order rate constants (k_2) for the protons of MEPOX, as well as the chemical shifts the respective through space distances [R] from the metal-center to the protons.

Table 5-7: Relaxation Rate Constants (k_2) for the Protons in MEPOX and Distances Between These Atoms and Bound Ni(II) in D_2O at 25 °C.

Proton	k_2 (M^{-1}-s^{-1})	R (Å)
H-2	199	4.3
H-3	56.3	6.5
H-3′	48.0	8.2
H-2′	35.7	10.6
H-Me	33.7	12.3

The coordination site for this compound was the N-oxide, and the proton closest to it had the largest k_2 value which was considerably smaller than those for a proton next to a free nitrogen atom. There was not a distinct pattern with respect to distance.

Summary and discussion of relaxation data for MEPYR. Table 5-8 gives the observed second-order rate constants (k_2) for the protons of MEPYR, as well as the chemical shifts and the respective through space distances [R] from the metal-center to the protons.

Table 5-8: Relaxation Rate Constants (k_2) for the Protons in MEPYR in D_2O at 25 °C.

Proton	k_2 (M^{-1}-s^{-1})
H-2	31.8
H-3	31.1
H-4	31.5
H-Me	28.4

This compound was chosen as a control substance because there is no obvious site of coordination with the paramagnetic ion. The k_2 values for all of the protons were essentially the same indicating that there was no central location for the coordinated of the metal ion, relaxation perhaps taking place in a collision complex.

Temperature Considerations

Relaxation times for MEBPY in D_2O were determined at three temperatures (30, 40, and 50 °C) in the absence of a paramagnetic metal and then in the presence of $NiBr_2$, 0.0143 M. Table 5-9 gives the corrected relaxation rate constants at the respective temperatures.

Table 5-9. Temperature Dependence of k_{corr} Values for MEBPY in the Presence of 0.0143 M $NiBr_2$ in D_2O.

Proton	δ (ppm)	30 °C	40 °C	50 °C
H-2′	8.81	13.4	23.3	38.9
H-3′	7.95	9.14	12.3	13.3
H-3	8.43	4.21	3.88	3.27
H-2	8.96	1.35	1.10	0.869
Me	4.52	0.821	0.677	0.540

There is a difference in the response between the protons of the two rings. The k_{corr} values for the protons (H-2′ and H-3′) on the ring which binds to the nickel ion clearly increase with temperature, whereas the protons on the more distant ring (H-3, H-2, and Me) decrease slightly in their k_{corr} values with temperature.

In order for these two different responses to be explained, the assumptions implicit in the derivations from Equation 5-13 need to be reconsidered. Not only must the relaxation phenomenon be considered, but also the lifetime of the metal-substrate complex, Equation 5-19, as demonstrated by others.[26,27]

$$k_1 = 1 / (T_{1M} + \tau_M) \quad \text{(Eq. 5-19)}$$

In this equation, T_{1M} is the relaxation time of a nucleus as influenced by the paramagnetic metal, and τ_M is the lifetime of the metal-substrate complex.

There are two limiting cases with respect to T_{1M} and τ_M, relaxation being faster than complex dissociation, $T_{1M} < \tau_M$, and relaxation being slower than complex dissociation, $T_{1M} > \tau_M$. In the former, k_1 is equal to τ_M according to Equation 5-19, and in the latter, k_1 is equal to T_{1M}. Nuclei very close to the paramagnetic species would be dominated by τ_M, and nuclei farther from the paramagnetic species would be dominated by T_{1M}. Unfortunately, T_{1M} and τ_M cannot be determined without the knowledge of the fraction of the substrate bound, here, an unknown quantity

The temperature dependence for MEBPY is a good example of the above consideration. Table 5-10 gives the activation energies for several positions of MEBPY from Arrhenius plots of ln k_{corr} versus inverse temperature (K^{-1}), as well as the quality of the correlation as expressed by the correlation coefficient.

Table 5-10. Energies of Activation for Relaxation of MEBPY Protons and Correlation Coefficients.

Position	E_a	Correlation
H-2′	1.06×10^4	0.999
H-3′	--	0.965
H-3	--	0.962
H-2	-0.433×10^4	0.995
Me	-0.412×10^4	0.995

The good correlation coefficients for protons 2′, 3, and Me suggest that relaxation for these positions is dominated by only one of the aforementioned phenomena. The positive activation energy for proton 2′ indicates that the rate increases with increasing temperature, and since complex lifetime, τ_M, decreases with increasing temperature, it is the dominate process. Conversely, the negative activation energy for protons 2 and Me indicates that the rate decreases with increasing temperature, and the dominate process is relaxation, T_{1M}, since it increases with increasing temperature. The poor correlation coefficients for protons 3′ and 3 do not allow activation energies to be determined for these positions. However, it does suggest that both of the competitive phenomena, T_{1M} and τ_M, are influencing the rates of relaxation of protons 3′ and 3.

Interpretation of the Results

Now that it is clear that two phenomena are affecting the measured relaxation rates, it becomes possible to correct the data for each proton site such that the contribution of the relaxation term, T_{1M}, may be realized and correlated with the inverse sixth power of the distance. This, however, requires further derivation.

By substituting Equation 5-19 into Equation 5-10, a new expression of k_{corr} is obtained.

$k_{corr} = [1 / (T_{1M} + \tau_M)]\ K\ [Ni^{2+}] + b$ (Eq. 5-20)

Therefore, a new expression for k_2 is also obtained.

$k_2 = K / (T_{1M} + \tau_M)$ (Eq. 5-21).

With MEBPY as an example, and utilizing the limiting cases described in the temperature consideration, Equation 5-21 gives the k_2 expression for proton 2′, closest to the coordinating nitrogen atom, as

$k_{2-2'} = K / \tau_M$ (Eq. 5-22),

where as proton 3′ is expressed as

$k_{2-3'} = K / (T_{1M3'} + \tau_M)$ (Eq. 5-23),

now experiencing more of an effect from relaxation. Taking a ratio of these two rate constants results in

$k_{2-2'}/k_{2-3'} = [K / \tau_M] / [K / (T_{1M3'} + \tau_M)]$ (Eq. 5-24).

This, of course, eliminates the equilibrium constant, K, and may be rearranged further to

$(k_{2-2'}/k_{2-3'}) - 1 = T_{1M3'} / \tau_M$ (Eq. 5-25).

The value resulting from the left side of Equation 5-25 may be determined for each position of MEBPY, $k_{2-2'}/k_{2-X} - 1$. Since τ_M is unknown, it must be eliminated by taking another ratio,

$(k_{2-2'}/k_{2-3'} - 1)/(k_{2-2'}/k_{2-X} - 1) = T_{1M3'} / T_{1MX}$ (Eq. 5-26).

The value resulting from the left side of Equation 5-26 may be determined and define as the fractional amount relating T_{1MX} to $T_{1M3'}$. Although neither T_{1MX} nor $T_{1M3'}$ are known, we now have a term, $T_{1M3'}/T_{1MX}$, which we can correlate to the inverse sixth power of the distance since $1/T_{1M} \propto 1/R^6$. Table 5-11 gives an example of this manipulation. For simplicity within the table, new terms are introduced. The ratio of the second-order rate constants is expressed by $Q_{2'-X}$, and $S_{3'-X}$ is the fractional coefficient relating T_{1MX} to $T_{1M3'}$, such that $S_{3'-X} = T_{1M3'}/T_{1MX}$. Figure 5-13 is the plot of $S_{3'-X}$ versus the inverse sixth power of the distance to illustrate the Solomon-Bloembergen relationship.

Table 5-11. Values from the Data Manipulation of k_2 Values of MEBPY in $NiCl_2$ at 25 °C to Demonstrate the Solomon-Bloembergen Correlation.

Proton	k_2	$Q_{2'-X} - 1^a$	$S_{3'-X}\,^b$	$1/R^6$
H-2′	979	0	--	$1.13\text{x}10^{-3}$
H-3′	750	0.31	1.0	$5.68\text{x}10^{-5}$
H-3	314	2.12	0.14	$1.01\text{x}10^{-5}$
H-2	102	8.60	0.036	$1.76\text{x}10^{-6}$
Me	64.5	14.18	0.022	$6.30\text{x}10^{-7}$

a) $Q_{2'-X} = k_{2-2'}/k_{2-X}$. b) $S_{3'-X} = (k_{2-2'}/k_{2-3'} - 1)/(k_{2-2'}/k_{2-X} - 1)$

This demonstrates that when the residence lifetime (τ_m) is factored out, the Solomon-Bloembergen prediction holds for each of the proton sites of MEBPY. Plots for all conditions with MEBPY, including DMSO-d_6, CD_3OD, $CoCl_2$, and temperature, and with STRBPY for ring protons 2″ to 3 give similarly excellent correlation coefficients (0.996-0.999) suggesting that the Solomon-Bloembergen prediction holds for the studied substrates under varying conditions when the residence lifetime influence is removed from consideration.

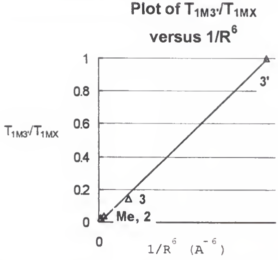

Figure 5-13. Correlation of the $S_{3'-X}$ Factor with the Inverse Sixth Power of the Nuclei to Metal Distance for MEBPY in D_2O with $NiCl_2$. Slope = $1.76 \times 10^4 (\pm 0.05 \times 10^4)$, Incpt. = $-0.004(\pm 0.015)$, Correlation Coefficient = 0.999.

Conclusions

T_1 relaxation times of functionalized pyridine molecules in the presence of paramagnetic metal salts were determined, and from the observed data, it was quite obvious that there were significant deviations from Solomon-Bloembergen prediction which correlates relaxation rate constants with the inverse sixth power of the distance from a nucleus to a paramagnetic center. This suggested that other factors influencing relaxation rates, such as the influence of the lifetime of the substrate with the metal ion, must be present.

Although, the original result of Zoltewicz and Bloom perhaps suggested a new and unusual phenomenon for relaxation none of the systems studied gave clear correlation of relaxation with a simple inverse distance relationship.

When a nucleus exists in two states, bound and unbound to a paramagnetic species, the nucleus is either in the limit of slow exchange of complex dissociation or in the limit of fast exchange. If the nucleus is close to the paramagnetic species, then the relaxation time is sufficiently small such that the lifetime of the complex has a greater effect on the measured relaxation rate. For a nucleus more distant from the paramagnetic species, the opposite is true, and the actual relaxation has the greater effect. This was demonstrated with the temperature dependence study as the nuclei closer to the metal ion experienced a relaxation rate increase with increasing temperature, and the nuclei farther from the metal ion experienced a relaxation rate decrease.

For the systems with D_2O, DMSO, and CD_3OD, not involving temperature dependence, a manipulation of the data which factors out the lifetime of the complex resulted in values which could be correlated with the inverse sixth power of the distance. Even under the different conditions, the excellent correlation indicated that the Solomon-Bloembergen relationship was in effect.

CHAPTER 6
EXPERIMENTAL

General Comments. Thiamin chloride hydrochloride, sodium (trimethoxy)borohydride, sodium borohydride, sodium cyanoborohydride, sodium carbonate, sodium bicarbonate, acetic acid-d_4, sodium acetate-d_3, dibasic sodium phosphate, deuterated monobasic potassium diphosphate, 2,2′-dipyridyl, 2,4′-dipyridyl, 2.5 M butyllithium in hexanes, 2,2,6,6-tetramethylpiperidine, tributyltin chloride, diethylmethoxy borane, iodine, acetaldehyde, 3-iodopyridine, tetrakis(triphenylphospine) palladium(0), phenylboronic acid, potassium hexafluorophosphate, diethyl-3-pyridyl-borane, 4,4′-dipyridyl, methyl iodide, 4-bromopyridine hydrochloride, para-dibromobezene, and the drying agent sodium sulfate were commercially available from Aldrich, Fisher Scientific (Acros), or Sigma Chemical and were used without further purification. Column chromatography made use of Kieselgel 20 230-240 mesh or Alumina 80-200 mesh. Thin-layer chromatography was done on Whatman polyester backed silica gel plates or Selecto Scientific Alumina plates. NMR data was collected on either the QE-300 MHz, VXR-300 MHz, Gemini 300 MHz, or Unity Varian 500 MHz.

Graphical analysis of data made use of a Microsoft Excel program.

Normal-Dihydrothiamin (2-3). This procedure follows that published in 1957.[3] Thiamin chloride hydrochloride (5.00g, 14.8 mmol), dissolved in water (15 mL) and cooled to 0 °C, was treated with 1N NaOH (15 mL, 15 mmol) and MeOH (20 mL). After cooling to -12 °C, $Na(OCH_3)_3BH$ (2.40g, 19.0 mmol) was added in small portions over 20 min. After the addition was complete, the reaction was warmed to room temperature, and a heavy white precipitate formed after several hours. The solid was collected, dried, and recrystallized from EtOAc and hexanes to afford 2.37 g (8.90 mmol, 60.1% yield, mp 149-151 °C). ^1H NMR ($CDCl_3$): δ 7.96 (1H, s), 5.79 (2H, s), 4.03 (2H, dd *J* = 4 and 9 Hz), 3.92 (1H, d *J* = 14 Hz), 3.78 (1H, dd, *J* = 2 and 6 Hz), 3.77 (1H, d, *J* = 8 Hz), 3.62 (1H, d, *J* = 14 Hz), 3.62 (1H, d, *J* = 8 Hz), 2.48 (3H, s), 2.41 (1H, m), 2.09 (1H, dtd, *J* = 1, 4, and 12 Hz), 1.56 (3H, s). ^{13}C NMR ($CDCl_3$): δ 167.1, 162.6, 154.7, 110.2, 104.3, 68.5, 55.0, 54.5, 47.7, 35.4, 25.5, 23.1. Anal. Calcd. for $C_{12}H_{18}N_4OS$: C, 54.11; H, 6.81; N, 21.03. Found: C, 54.38; H, 6.71; N, 20.95.

Iso-Dihydrothiamin (2-3b). Dihydrothiamin, from above, (50 mg, 0.19 mmol), dissolved in MeOH (3 mL), was treated with 10% NaOH (5 mL). After subsequent stirring for a few minutes, a white precipitate formed.

The solid was collected, dried, and recrystallized from EtOAc and hexanes to afford 22 mg (0.083 mmol, 43% yield, mp 156-158 °C). ^{1}H NMR ($CDCl_3$): δ 7.96 (1H, s), 5.79 (2H, s), 4.03 (2H, dd J = 4 and 9 Hz), 3.92 (1H, d J = 14 Hz), 3.78 (1H, dd, J = 2 and 6 Hz), 3.77 (1H, d, J = 8 Hz), 3.62 (1H, d, J = 14 Hz), 3.62 (1H, d, J = 8 Hz), 2.48 (3H, s), 2.41 (1H, m), 2.09 (1H, dtd, J = 1, 4, and 12 Hz), 1.56 (3H, s). Anal. Calcd. for $C_{12}H_{18}N_4OS$: C, 54.11; H, 6.81; N, 21.03. Found: C, 54.27; H, 6.71; N, 21.09. It should be noted that after the solid was dissolved in a mixture of ethanol, hexanes, and ethyl acetate for growing crystals, the crystals that formed had a lower melting point corresponding to first isomer (mp 149-151 °C).

Pseudo-Dihydrothiamin (2-4). This procedure follows that published in 1957.[9] After isomer 2-3 (0.50g, 1.9 mmol) was dissolved in boiling water (10 mL), cooled, and saturated with solid Na_2CO_3, the mixture was thoroughly extracted with $CHCl_3$, and the organic phase dried over K_2CO_3. Solvent evaporation resulted in a white residue which was recrystallized from EtOAc, hexanes, and MeOH. A white solid resulted (110 mg, 0.41 mmol, 22% yield, mp 173-175 °C). ^{1}H NMR (D_2O): δ 7.94 (1H, s), 4.16 (1H, d J = 9 Hz), 3.98 (1H, d J = 16 Hz), 3.88 (1H, d, J = 16 Hz), 3.84 (1H, d, J = 9 Hz), 3.72 (1H, m), 3.62 (1H, m), 3.43

(1H, d, J = 10 Hz), 2.38 (3H, s), 2.18 (1H, m), 1.69 (1H, m), 1.45 (3H, s). ^{13}C NMR (D_2O): δ 170.7, 161.6, 156.2, 111.4, 84.1, 65.4, 57.5, 55.7, 48.6, 38.0, 28.4, 25.5. Anal. Calcd. for $C_{12}H_{18}N_4OS$: C, 54.11; H, 6.81; N, 21.03. Found: C, 53.84; H, 6.89; N, 20.80.

Normal-Dihydrothiamin (2-3) Deuterated. Thiamin chloride hydrochloride (0.50 g, 1.5 mmol), dissolved in D_2O (3 mL) and cooled to 0 °C, was treated with Na_2CO_3 (g, mmol) and CH_3OD (2 mL). After cooling to -12 °C, $Na(OCH_3)_3BH$ (0.24 g, 1.9 mmol) was added in small portions. After the addition was complete, the reaction was warmed to room temperature, and a heavy white precipitate formed after several hours. The solid was collected, dried, and recrystallized from EtOAc and hexanes to afford 230 mg of product(0.86 mmol, 57% yield, mp 147-149 °C). ^{1}H NMR ($CDCl_3$): Same as 2-3, except the doublets at 3.77 and 3.62 collapse to singlets.

X-ray Crystal Structure Information. Slow solvent evaporation of a solution of 2-3 in EtOAc resulted in the formation of needles, mp 149-151 °C, that were submitted for X-ray analysis. Chloroform was used to grow a crystal of 2-4, mp 173-175 °C.

Compound 2-3: $C_{12}H_{18}N_4OS$, M_r = 266.36, Monoclinic, P2(1)/n, a = 6.3749(1) Å, b = 23.1887(3) Å, c = 9.724 Å,

α = 90°, β = 106.94°, γ = 90°, V = 1375.04(3) $Å^3$, Z = 4, $D_{calc.}$ = 1.287 g-cm^{-3}, Mo Kα(λ = 0.71073 Å), T = 173 K.

Compound 2-4: $C_{12}H_{18}N_4OS$, M_r = 266.36, Orthorhombic, Pbca, a = 6.7405(1) Å, b = 16.9618(1) Å, c = 23.0344 Å, α = 90°, β = 90°, γ = 90°, V = 2633.55(5) C^3, Z = 8, Dcalc. = 1.344 g-cm-3, Mo K_α(λ = 0.71073 Å), T = 173 K.

Data for both compounds were collected at 173 K on a Siemens CCD SMART PLATFORM equipped with a CCD are detector and a graphite monochromator utilizing Mo K_α radiation (λ = 0.71073 Å). Cell parameters were refined using 5969 (compound 2-3) and 6943 (compound 2-4) reflections from each data set. A hemisphere of data (1381 frames) was collected using the T-scan method (0.3E frame width). The first 50 frames were remeasured at the end of data collection to monitor instrument and crystal stablilty (maximum correction on I was < 1%). Absorption corrections were applied based on the psi scan using the entire data sets.

Both structures were solved by Direct Methods[131] in *SHELXTL* and refined using full-matrix least squares on F^2. The non-H atoms were refined with anisotropic thermal parameters except for the disordered C atoms. All of the H atoms were included in the final cycle of refinement and were riding on the atoms to which they are bonded. In each compound there was one methyl H atoms disordered and were refined in riding models in two parts with 50% occupancy for each part. For compound 2-3, 173 parameters were refined in the final cycle of refinement using 2658 reflections with I > 2σI to yield R_1 and wR_2 of 3.82% and 8.99%, respectively. For compound 2-4, 173 parameters were refined in the final cycle of refinement using 2280 reflections with I > 2σ(I) to yield R_1 and wR_2 of 4.82% and 9.26%, respectively. Refinement was done using F^2.

Table 6-1. Fractional Coordinates and Equivalent Isotropic[a] Thermal Parameters (Å^2) for the Carbon, Nitrogen, Oxygen and Sulfur Atoms of 2-3.

Atom	x	y	z	U
S1	2970(1)	2075(1)	3097(1)	37(1)
C2	1826(2)	1824(1)	1267(2)	27(1)
C3A	-943(2)	1531(1)	2307(2)	23(1)
C3B	-984(2)	1152(1)	-53(2)	27(1)
N3	375(2)	1349(1)	1377(1)	22(1)
O4	-2611(2)	1942(1)	1572(1)	29(1)
C5	-2169(3)	2497(1)	2242(2)	34(1)
C6	-883(3)	2371(1)	3779(2)	33(1)
C6A	541(2)	1863(1)	360(2)	26(1)
C7	-2097(3)	1025(1)	2760(2)	36(1)
C8	3869(4)	460(1)	-3868(2)	52(1)
N1′	987(3)	1027(1)	-3354(2)	40(1)
C2′	2611	652(1)	-2855(2)	34(1)
N3′	3252(2)	424(1)	-1527(1)	29(1)
N4′	2739(2)	351(1)	718(2)	28(1)
C4′	2136(2)	583(1)	-604(2)	25(1)
C5′	366(2)	980(1)	-1025(2)	26(1)
C6′	-97(3)	1183(1)	-2405(2)	34(1)

a) For anisotropic atoms, the U value is U_{eq}, calculated as $U = 1/3 \Sigma_i \Sigma_j U_{ij} a_i \times a_j \times A_{ij}$, where A_{ij} is the dot product of theC4′ i^{th} and j^{th} direct space unit cell vectors.

Table 6-2. Bond Lengths (Å) and Angles (°) for the Carbon, Nitrogen, Oxygen and Sulfur Atoms of 2-3.

1	2	3	1-2	1-2-3
C2	S1	C6A	1.812(2)	92.69(7)
C6A	S1		1.823(2)	
N3	C2	S1	1.462(2)	104.62(10)
C2	N3	C3A		108.51(11)
C2	N3	C3B		111.88(11)
C3A	N3	C3B	1.464(2)	112.66(11)
O4	C3A	N3	1.451(2)	110.81(11)
O4	C3A	C7		107.62(12)
N3	C3A	C7		111.72(12)
O4	C3A	C6A		105.16(11)
N3	C3A	C6A		108.80(11)
C7	C3A	C6A	1.517(2)	112.54(12)
N3	C3B	C5′	1.480(2)	112.74(12)
C5′	C3B		1.506(2)	
C5	O4	C3A	1.433(2)	110.31(11)
O4	C5	C6		104.67(13)
C5	C6	C6A	1.510(2)	101.95(12)
C6	C6A	C3A	1.527(2)	103.53(12)
C6	C6A	S1		113.70(11)
C3A	C6A	S1	1.542(2)	106.40(10)
C2′	N1′	C6′	1.330(2)	115.12(14)
N1′	C2′	N3′		126.4(2)
N1′	C2′	C8		117.4(2)
C8	C2′		1.507(2)	
N3′	N3′	C8	1.344(2)	116.2(2)
C2′	N3′	C4′		117.40(13)
N4′	C4′	N3′	1.343(2)	117.89(13)
N4′	C4′	C5′		121.19(14)
N3′	C4′	C5′	1.349(2)	120.92(14)
C6′	C5′	C4′	1.371(2)	115.55(14)
C6′	C5′	C3B		121.58(14)
C4′	C5′	C3B	1.421(2)	122.83(14)
N1′	C6′	C5′	1.354(2)	124.6(2)

Table 6-3. Fractional Coordinates and Equivalent Isotropic[a] Thermal Parameters (Å^2) for the Carbon, Nitrogen, Oxygen and Sulfur Atoms of 2-4.

Atom	x	y	z	U
N1	12207(3)	108(1)	3331(1)	27(1)
C2	12697(3)	-652(1)	3307(1)	30(1)
N3	11828(3)	-1244(1)	3596(1)	31(1)
C4	10340(3	-1032(1)	3961(1)	29(1)
C4A	9685(3)	-276(1)	4022(1)	24(1)
C5	8062(3)	-19(1)	4427(1)	28(1)
N6	8384(2)	805(1)	4606(1)	26(1)
C7	6671(3)	1093(2)	4930(1)	32(1)
S8	4775(1)	1438(1)	4393(1)	31(1)
C9	6560(3)	1388(1)	3796(1)	23(1)
C9A	8622(3)	1348(1)	4107(1)	23(1)
N10	10134(3)	1057(1)	3711(1)	24(1)
C10A	10673(3)	297(1)	3686(1)	22(1)
C11	14397(4)	-862(2)	2914(1)	45(1)
C12	6397(3)	2039(1)	3350(1)	28(1)
C13	4575(3)	2000(1)	2963(1)	30(1)
O13	2786(2)	2191(1)	3265(1)	30(1)
C14	9306(3)	2153(1)	4329(1)	31(1)

a) For anisotropic atoms, the U value is U_{eq}, calculated as $U = 1/3\ \Sigma_i\Sigma_j\ U_{ij}\ a_i \times a_j \times A_{ij}$, where A_{ij} is the dot product of theC4′ ith and jth direct space unit cell vectors.

Table 6-4. Bond Lengths (Å) and Angles (°) for the Carbon, Nitrogen, Oxygen and Sulfur Atoms of 2-4.

1	2	3	1-2	1-2-3
C2	N1	C10A	1.333(3)	116.3(2)
N1	C2	N3		126.5(2)
N1	C2	C11		116.3(2)
C11	C2		1.503(3)	
N3	C2	C11	1.340(3)	117.1(2)
C2	N3	C4		115.6(2)
N3	C4	C4A	1.356(3)	123.6(2)
C4	C4A	C10A	1.363(3)	116.0(2)
C4	C4A	C5		125.0(2)
C5	C4A		1.502(3)	
C10A	C4A	C5	1.409(3)	119.0(2)
N6	C5	C4A	1.474(3)	110.0(2)
C7	N6	C5	1.459(3)	110.1(2)
C7	N6	C9A		105.9(2)
C5	N6	C9A		112.9(2)
N6	C7	S8		107.93(14)
S8	C7		1.872(2)	
C9	S8	C7	1.831(2)	91.85(9)

Table 6-4. Continued

1	2	3	1-2	1-2-3
C12	C9	C9A	1.513(3)	114.0(2)
C12	C9	S8		115.3(2)
C9A	C9	S8	1.565(3)	103.98(13)
N10	C9A	N6	1.454(2)	110.6(2)
N10	C9A	C14		107.5(2)
N6	C9A	C14	1.481(3)	109.1(2)
N10	C9A	C9		110.5(2)
N6	C9A	C9		106.6(2)
C14	C9A	C9	1.529(3)	112.5(2)
C10A	N10	C9A	1.340(3)	122.9(2)
N10	C10A	N1		117.3(2)
N10	C10A	C4A		120.8(2)
N1	C10A	C4A	1.356(3)	121.9(2)
C9	C12	C13		115.2(2)
C13	C12		1.519(3)	
O13	C13	C12	1.429(3)	112.7(2)

General Procedure for NMR Conversions. Two small samples of 2-3 (4.0 mg) and two of 2-4 (4.0 mg) were placed in four separate NMR tubes and were dissolved in 0.1 mL CD_3OD. To each of one of the samples of 2-3 and 2-4 was added 0.6 mL of Buffer C, and to the other samples was added Buffer D. The samples were kept at room temperature for 22 h, and the ^1H NMR spectra were then obtained and the changes observed.

General Procedure for Tetrahydrothiamin Formation and Isolation (2-5). The reductions of 2-3 and 2-4 to tetrahydrothiamin were accomplished by dissolving the compounds in a small amount of MeOH followed by the addition of an aqueous solution (H_2O or buffer) of the reducing agent ($NaBH_4$ or $Na(CN)BH_3$). The reactions were monitored by thin-layer chromatography on silica gel. Tetrahydrothiamin was isolated by extracting the aqueous reaction mixtures with chloroform, then dried over K_2CO_3 and evaporated to afford the white solid product. ^{1}H NMR and melting point confirmed product formation.

The original preparation of 2-5 from 2-1 with NaBH4 under alkaline conditions at 0 °C was repeated.[54] The unrecrystallized product had *cis/trans* ratio of 3.1/1 (lit[54] 2.5:1) Under these conditions with the intermittent addition of the hydride, the solution had a yellow color indicative of the presence of 2-7 and its bicyclic sulfide ring opened derivative.[63] Attempts to reduce 2-1 with $NaBH_3CN$ in water resulted in the precipitation of a slightly soluble borohydride salt.

Tetrahydrothiamin 2-5 from 2-3 in Aqueous $NaBH_4$ (5-5). To 2-3 (0.050 g, 0.19 mmol), dissolved in MeOH (4 mL), was added $NaBH_4$ solution (0.045 g, 1.2 mmol in 20 mL H_2O). TLC showed no starting material after 5 h. Product was isolated (38 mg, 0.14 mmol, 74% yield, mp 145-149 °C). Anal. Calcd. for $C_{12}H_{20}N_4OS$.1/3H20: C, 52.53; H, 7.59; N, 20.42. Found: C, 52.27; H, 7.93; N, 20.27.

Tetrahydrothiamin from 2-3 with $NaBH_4$ in Borax Buffer (5-5). To 2-3 (0.050 g, 0.19 mmol), dissolved in MeOH (4 mL), was added $NaBH_4$ solution (0.030 g, 1.2 mmol in 20 mL borax buffer). TLC showed no starting material after 3.5 h. Product was isolated (38 mg, 0.14 mmol, 74% yield, mp 145-149 °C).

Tetrahydrothiamin from 2-4 with Na(CN)BH_3 in Phthalic Acid Buffer (5-5). To 2-4 (0.050 g, 0.19 mmol), dissolved in MeOH (4 mL), was added Na(CN)BH_3 solution (0.060 g, 1.2 mmol in 20 mL phthalic acid buffer). TLC showed no starting material after 3 h. Product was isolated (39 mg, 0.15 mmol, 79% yield, mp 145-149 °C).

Buffer A (pD = 9.77): Dilute Aqueous $Na_2CO_3/NaHCO_3$. Sodium carbonate (5.3 mg, 0.050 mmol) and sodium bicarbonate (4.2 mg, 0.050 mmol), dissolved in D_2O (2.0 mL), had $[CO_3^{-2}]$ = $[HCO_3^-]$ = 0.025 M.

Buffer B (pD = 9.10): Aqueous $Na_2CO_3/NaHCO_3$ Increased $[HCO_3^-]$. Sodium carbonate (2.6 mg, 0.025 mmol) and sodium bicarbonate (6.2 mg, 0.075 mmol), dissolved in D_2O (2.0 mL), had $[CO_3^{-2}]$ = 0.013 M and $[HCO_3^-]$ = 0.038 M.

Buffer C (pD = 9.77): Strong Aqueous $Na_2CO_3/NaHCO_3$. Sodium carbonate (53 mg, 0.50 mmol) and sodium bicarbonate (42 mg, 0.50 mmol), dissolved in D_2O (2.0 mL) had $[CO_3^{-2}]$ = $[HCO_3^-]$ = 0.25 M.

Buffer D (pD = 10.71): Strong Aqueous $Na_2CO_3/NaHCO_3$. Sodium carbonate (132.5 mg, 1.25 mmol) and sodium bicarbonate (21 mg, 0.25 mmol), dissolved in D_2O (2.0 mL) had $[CO_3^{-2}]$ = 0.625 M and $[HCO_3^-]$ = 0.125 M.

Buffer E (pD = 6.25): Aqueous Na_2HPO_4/KD_2PO_4. Dibasic sodium phosphate (14.2 mg, 0.10 mmol) and deuterated monobasic potassium diphosphate (27.6 mg, 0.20 mmol), dissolved in D_2O (2.0 mL), had $[HPO_4^{-2}] = 0.050M$ $[D_2PO_4^-] = 0.10$ M.

Buffer F (pD = 5.75): Aqueous CD_3O_2D/CD_3O_2Na. Deuterated acetic acid (17 μL, 0.30 mmol) and deuterated sodium acetate (127.5 mg, 1.50 mmol), dissolved in D_2O (2.0 mL), had $[CD_3O_2D] = 0.15$ M $[CD_3O_2^-] = 0.75$ M.

Buffer G (pD = 6.25): Aqueous CD_3O_2D/CD_3O_2Na. Deuterated acetic acid (5.7 μL, 0.10 mmol) and deuterated sodium acetate (127.5 mg, 1.50 mmol), dissolved in D_2O (2.0 mL), had $[CD_3O_2D] = 0.05$ M $[CD_3O_2^-] = 0.75$ M.

General Procedure for Kinetic Experiments with 2-3. 2-3 was placed in an NMR tube and was dissolved in a small amount (0.1 or 0.2 mL) of CD_3OD. Quickly added to this was a freshly prepared solution (unbuffered or buffered) of reducing agent ($NaBH_4$, $NaBH_3CN$). Timing began upon mixing. ^1H NMR data was collected over time, and integration and peak height of the thiazole methyl signal were observed for the disappearance of 2-3 and the appearance of tetrahydrothiamin. The percent of 2-3 remaining at each time interval was plotted versus time on a logarithmic scale.

General Procedure for Kinetic Experiments with 2-4. 2-4 was placed in an NMR tube and added to this was a freshly prepared solution (buffered) of $NaBH_3CN$. Timing began upon mixing. ^1H NMR data was collected over time, and integration and peak height of the thiazole methyl signal were observed for the disappearance of 2-4 and the appearance of tetrahydrothiamin. The percent of 2-4 remaining at each time interval was plotted versus time on a logarithmic scale.

Unbuffered Reaction of 2-3 with $NaBH_4$. $NaBH_4$ (3.3 mg, 0.087 mmol) was dissolved in D_2O (1.0 mL). As described above, 2-3 (4.2 mg, 0.016 mmol) was dissolved in CD_3OD (0.2 mL), and the $NaBH_4$ solution (0.5 mL) was added.

Reaction of 2-3 with $NaBH_4$ at pD = 9.77. Just prior to use, $NaBH_4$ (2.3 mg, 0.061 mmol) was dissolved in Buffer A (1.0 mL). As described above, 2-3 (2.0 mg, 0.0075 mmol) was dissolved in CD_3OD (0.1 mL), and the $NaBH_4$ solution (0.6 mL) was added.

Reaction of 2-3 with $NaBH_4$ at pD = 9.0. Just prior to use, $NaBH_4$ (2.3 mg, 0.061 mmol) was dissolved in Buffer B (1.0 mL). As described above, 2-3 (2.0 mg, 0.0075 mmol) was dissolved in CD_3OD (0.1 mL), and the $NaBH_4$ solution (0.6 mL) was added.

Reaction of 2-3 with $NaBH_4$ at pD = 9.77 (Run 1). Just prior to use, $NaBH_4$ (2.8 mg, 0.075 mmol) was dissolved in Buffer C (1.0 mL). As described above, 2-3 (2.0 mg, 0.0075 mmol) was dissolved in CD_3OD (0.1 mL), and the $NaBH_4$ solution (0.6 mL) was added.

Reaction of 2-3 with $NaBH_4$ at pD = 9.77 (Run 2). Just prior to use, $NaBH_4$ (1.2 mg, 0.032 mmol) was dissolved in Buffer C (1.0 mL). As described above, 2-3 (2.0 mg, 0.0075 mmol) was dissolved in CD_3OD (0.1 mL), and the $NaBH_4$ solution (0.6 mL) was added.

Reaction of 2-3 with $NaBH_4$ at pD = 10.71. Just prior to use, $NaBH_4$ (2.5 mg, 0.066 mmol) was dissolved in Buffer D (1.0 mL). As described above, 2-3 (4.0 mg, 0.15 mmol) was dissolved in CD_3OD (0.1 mL), and the $NaBH_4$ solution (0.6 mL) was added.

Reaction of 2-3 with $NaCNBH_3$ at pD = 9.77. Just prior to use, $NaCNBH_3$ (3.7 mg, 0.059 mmol) was dissolved in Buffer C (1.0 mL). As described above, 2-3 (2.0 mg, 0.0075 mmol) was dissolved in CD_3OD (0.1 mL), and the $NaCNBH_3$ solution (0.6 mL) was added.

Reaction of 2-4 with $NaCNBH_3$ at pD = 6.25. Just prior to use, $NaCNBH_3$ (4.0 mg, 0.064 mmol) was dissolved in Buffer E (1.0 mL). As described above, 2-4 (2.3 mg, 0.0086 mmol) was dissolved in the $NaCNBH_3$ solution (0.7 mL).

Reaction of 2-4 with $NaCNBH_3$ at pD = 5.75 (Run 1). Just prior to use, $NaCNBH_3$ (4.0 mg, 0.064 mmol) was dissolved in Buffer F (1.0 mL). As described above, 2-4 (2.3 mg, 0.0086 mmol) was dissolved in the $NaCNBH_3$ solution (0.7 mL).

Reaction of 2-4 with $NaCNBH_3$ at pD = 5.75 (Run 2). Just prior to use, $NaCNBH_3$ (1.9 mg, 0.030 mmol) was dissolved in Buffer F (1.0 mL). As described above, 2-4 (1.9 mg, 0.0071 mmol) was dissolved in the $NaCNBH_3$ solution (0.7 mL).

Reaction of 2-4 with $NaCNBH_3$ at pD = 5.75 (Run 3). Just prior to use, $NaCNBH_3$ (5.7 mg, 0.091 mmol) was dissolved in Buffer F (1.0 mL). As described above, 2-4 (2.3 mg, 0.0086 mmol) was dissolved in the $NaCNBH_3$ solution (0.7 mL).

Reaction of 2-4 with $NaCNBH_3$ at pD = 6.25. Just prior to use, $NaCNBH_3$ (5.7 mg, 0.091 mmol) was dissolved in Buffer G (1.0 mL). As described above, 2-4 (6.9 mg, 0.026 mmol) was dissolved in the $NaCNBH_3$ solution (0.7 mL).

Preparation of Lithium- 2,2,6,6-Tetramethylpiperidide.[76] Butyllithium and 2,2,6,6-tetramethylpiperidine were added with stirring to THF at -30 °C under nitrogen. The solution was warmed to 0 °C and stirred for 30 min. The LTMP solution was cooled to the necessary temperature prior to further reaction.

3,3′-Bis(tributylstannyl)-2,2′-bipyridine (3-3a) and 3-(Tributylstannyl)-2,2′-bipyridine (3-3b). With the LTMP (4.80 mmol) at -70 °C, 2,2′-bipyridine (0.300 g, 1.92 mmol) dissolved in THF (15 mL) was added over a period of 15 min. The reaction was stirred for 45 min, followed by slow addition of tributyltin chloride (1.35 mL, 4.99 mmol).

After stirring at -70 °C for 1h, it was then warmed to room temperature and stirred for several hours. Distilled water (5mL) was added, along with diethyl ether (30 mL). The ether phase was washed with a saturated solution of NaH_2PO_4 (2 x 50 mL), water (50 mL), and brine (50 mL, 1 M), then dried over Na_2SO_4 and evaporated to an orange oil. First, a silica gel column of the oil was eluted with hexanes: EtOAc (95:5) to remove excess tributyltin materials, and then an alumina column was eluted with hexanes, which afforded the bis(tributylstannyl) bipyridine, and the mono(tributylstannyl) pyridine was eluted with hexanes: EtOAc (90:10). After solvent evaporation both products were isolated as clear oils; bis(tributylstannyl) bipyridine 190 mg (0.20 mmol, 14% yield) and mono(tributylstannyl) bipyridine 430 mg (0.97 mmol, 50% yield). For bis(tributylstannyl) bipyridine: ^1H NMR ($CDCl_3$): δ 8.47 (2H, dd, J = 2 and 5 Hz), 8.06 (2H, dd, J = 2 and 7 Hz) 7.28 (2H, dd, J = 5 and 7 Hz), 0.83-1.43 (54 H, m). Anal. Calcd. For $C_{34}H_{60}N_2Sn_2$: C, 55.62; H, 8.24; N, 3.82. Found C, 55.87; H, 8.49; N, 4.16. For mono(tributylstannyl) bipyridine: ^1H NMR (CD_3OD): δ 8.55 (2H, dd, J = 2 and 5 Hz), 8.45 (1H, d, J = 8 Hz), 8.05 (1H, dd, J = 2 and 7 Hz), 7.90 (1H, td, J = 2 and 8 Hz), 7.40 (1H, ddd, J = 1, 5, and 8 Hz), 7.33 (1H, dd, J = 5 and 8 Hz), 0.80-1.14 (27H, m).

Anal. Calcd. For $C_{22}H_{34}N_2Sn$: C, 59.35; H, 7.70; N, 6.29. Found: C, 59.72; H, 8.01; N, 6.58.

3-(Tributylstannyl)-2,4′-bipyridine (3-4). To an LTMP (9.60 mmol) solution in THF at -70 °C was added 2,4′-bipyridine (1.00 g, 6.40 mmol) in THF over 20 min. After stirring at -70 °C for 45 min, tributyltin chloride (2.10 mL, 7.68 mmol) was added slowly. After stirring for 1 h, it was warmed slowly to room temperature and stirred for several hours. Distilled water (5 mL) was added, along with diethyl ether (50 mL). The ether phase was washed with a saturated solution of NaH_2PO_4 (2 x 50 mL), water (50 mL), and brine (50 mL, 1 M), then dried over Na_2SO_4 and evaporated to an orange oil. A silica gel column was eluted sequentially with: 100 mL hexanes: EtOAc (90:10), 100 mL hexanes: EtOAc (70:30), 100 mL hexanes: EtOAc (50:50),and finally with 100 mL hexanes: EtOAc (30:70). The product was eluted with the latter. Evaporation afforded 1.82 g of the clear oil product (4.09 mmol, 64% yield). ^{1}H NMR ($CDCl_3$): δ 8.81 (1H, d, *J* = 1 Hz), 8.59 (2H, d, *J* = 5 Hz), 7.83 (1H, d, *J* = 8 Hz), 7.78 (1H, td, *J* = 2 and 8 Hz), 7.66 (1H, dd, *J* = 1 and 5 Hz), 7.30 (1H, ddd, *J* = 2, 5 and 7 Hz), 0.80-1.14 (27H, m). Anal. Calcd. For $C_{22}H_{34}N_2Sn\bullet 1/2\ H_2O$: C, 58.17; H, 7.77; N, 6.17. Found: C, 58.34; H, 7.93; N, 5.81.

3-Diethylboryl-2,2′-bipyridine (3-3c). With the LTMP (4.80 mmol) at -40 °C, the 2,2′bipyridine (0.500 g, 3.20 mmol) dissolved in THF (10 mL) was added over a period of 1 h. After stirring for 1 h, the mixture was the cooled to -70 °C, and diethylmethoxy borane (0.63 mL, 4.96 mmol) was added over a period of 30 min. Stirring continued for 1 h, followed by warming to room temperature and stirring for several hours. Distilled water (5 mL) was added, along with diethyl ether (50 mL). The ether phase was washed with saturated solution of NaH_2PO_4 (2 x 50 mL), water (50 mL), and brine (50 mL, 1 M), then dried over Na_2SO_4 and evaporated to a dark oil. The oil, dissolved in diethyl ether (70 mL), was washed several times with a satd. solution of $FeSO_4$ until the red color of a complex with 2,2′-bipyridine was no longer observed. The ether phase was then collected, dried over Na_2SO_4, and evaporated to a dark oil. An alumina column eluted first with hexanes then with increasing EtOAc up to 30%. The product was isolated as a yellow oil (362 mg, 1.62 mmol, 50% yield). ^1H NMR ($CDCl_3$): δ 8.54 (1H, dd, J = 2 and 5 Hz), 8.40 (2H, m), 8.08 (1H, td, J = 2 and 8 Hz), 7.95 (1H, dd, J = 2 and 8 Hz), 7.50 (1H, td, J = 2 and 6 Hz), 7.28 (1H, q, J = 5 and 7 Hz), 0.81 (2H, m), 0.57 (2H, m), 0.43 (6H, t, J = 8 Hz). Anal. Calcd. For $C_{14}H_{17}N_2B \bullet 1/2\ H_2O$: C, 72.01; H, 7.72; N, 12.01. Found: C, 72.40; H, 7.97; N, 11.93.

3-Iodo-2,2'-bipyridinium diperchlorate (3-3d). With the LTMP (9.28 mmol) at -40 °C, the 2,2'bipyridine (1.00 g, 6.40 mmol), in THF (15 mL), was added slowly. After stirring for 1 h, and cooling to -70 °C, and iodine (1.62 g, 6.40 mmol), in THF (15 mL), was added over 1 h. After stirring for 1 h and warming to room temperature, stirring continued for several hours. After solvent evaporation, the resultant dark oil was dissolved in EtOAc. This solution was washed with saturated solution of NaH_2PO_4 (2 x 50 mL), water (50 mL), and several times with a satd. solution of $FeSO_4$ until the red color of a complex with 2,2'-bipyridine was no longer observed. The organic phase was collected, dried over Na_2SO_4, and evaporated to a dark oil. An alumina column eluted first with hexanes then with increasing EtOAc up to 30%. The product was isolated as an orange oil (199 mg, 0.70 mmol, 11 % yield). ^1H NMR ($CDCl_3$): δ 8.73 (1H, dt, J = 1 and 5 Hz), 8.65 (1H, dd, J = 2 and 5 Hz), 8.29 (1H, dd, J = 2 and 8 Hz), 7.82 (1H, td, J = 2 and 8 Hz), 7.70 (1H, dt, J = 1 and 8 Hz), 7.35 (1H, ddd, J = 1, 5 and 8 Hz), 7.04 (1H, dd, J = 5 and 8 Hz). Anal. Calcd. For $C_{10}H_9N_2ICl_2O_8{\bullet}1/2\ H_2O$: C, 24.41; H, 2.05; N, 5.69. Found: C, 24.18; H, 1.64; N, 5.51.

3-(1-Hydroxyethyl)-2,2'bipyridine (3-3e). With the LTMP (9.28 mmol) at -40 °C, the 2,2'bipyridine (0.500 g, 3.20 mmol),), in THF (15 mL), was added slowly.

After stirring for 1 h, and cooling to -70 °C, acetaldehyde (0.25 mL, 4.45 mmol) was added over 1 h. After stirring for 1 h and warming to room temperature, stirring continued for several hours. Distilled water (5 mL) was added, along with diethyl ether (50 mL). The ether phase was washed with saturated solution of NaH_2PO_4 (2 x 50 mL), water (50 mL), and brine (50 mL, 1 M), then dried over Na_2SO_4 and evaporated to a dark oil. An alumina column of the dark oil was eluted first with hexanes, then with increasing EtOAc up to 30%. The product was isolated as a yellow oil (260 mg, 1.30 mmol, 41% yield). ^{1}H NMR ($CDCl_3$): δ 8.62 (2H, m), 8.14 (1H, dd, *J* = 1 and 7 Hz), 7.91 (2H, m), 7.32 (2H, m), 6.97 (1H, d, *J* = 5 Hz), 4.89 (1H, q, *J* = 5 and 6 Hz), 1.54 (3H, d, *J* = 7 Hz). Anal. Calcd. For $C_{12}H_{12}N_2O \cdot 1/3\ H_2O$: C, 69.88; H, 6.19; N, 13.58. Found: C, 69.79; H, 6.21; N, 13.20.

2,2′: 3′,3″-Terpyridinium diperchlorate (3-5).

3-Iodopyridine (0.300 g, 1.46 mmol) and $Pd(PPh_3)_4$ (0.170 g, 0.146 mmol), in degassed toluene (50 mL), were stirred under nitrogen for 15 min and heated at gentle reflux. 3-3a (0.700 g, 1.57 mmol), dissolved in toluene (5 mL), was added in three equal portions over 30 min. After refluxing for 18 h, the reaction was cooled with ice and was diluted with EtOAc (30 mL). Insolubles were filtered away, and the filtrate was concentrated to a yellow oil which was dissolved in a solution of AcOH (2 mL), EtOAc (2 mL), and $NaClO_4$ (20 mg). Perchloric acid (70%) was added dropwise to this solution affording a white precipitate which was collected and washed with EtOAc and hexanes, The solid was recrystallized from EtOH and EtOAc yielding 508 mg of the white solid terpyridinium diperchlorate salt (1.17 mmol, 80% yield, m. p. > 280 °C). ^1H NMR (DMSO): δ 9.04 (2H, m), 8.87 (1H, m), 8.52 (1H, d, $J = 5$ Hz), 8.24 (1H, dd, $J = 2$ and 8 Hz), 8.12 (1H, d, $J = 6$ Hz), 7.95 (2H, m), 7.67 (1H, d, $J = 8$ Hz), 7.49 (1H, dd, $J = 5$ and 7 Hz). Anal. Calcd. For $C_{15}H_{13}Cl_2N_3O_8$: C, 41.49; H, 3.02; N, 9.68. Found: C, 41.49; H, 2.81; N, 9.39.

2,4′:3′,3″-Terpyridinium diperchlorate (3-6). 3-Iodopyridine (0.230 g, 1.12 mmol) and $Pd(PPh_3)_4$ (0.130 g, 0.112 mmol), dissolved in degassed toluene (30 mL), were stirred under nitrogen for 15 min and heated was at gentle reflux. 3-4 (0.500 g, 1.12 mmol), in toluene (5 mL), was added in three equal portions over 30 min. After refluxing for 6 days, copper iodide (5 mg, 0.03 mmol) was added and refluxing continued for another 24 h. The mixture was cooled with ice and diluted with EtOAc (30 mL). Insolubles were filtered off, and the filtrate was washed with water. The organic phase was dried over Na_2SO_4 and evaporated to a yellow oil which was dissolved in diethyl ether and extracted with 0.2 M HCl (2 x 25 mL).

The acidic aqueous phase was neutralized with Na_2CO_3 and was extracted thoroughly with $CHCl_3$. The chloroform solution was dried over K_2CO_3 and evaporated to a yellow oil which was dissolved in a solution of AcOH (2.5 mL), EtOAc (2.5 mL), and $NaClO_4$ (20 mg). Perchloric acid (70%) was added dropwise to affording a white precipitate which was collected and washed with EtOAc and hexanes. The solid was recrystallized from EtOH and EtOAc yielding 131 mg of the white solid terpyridinium diperchlorate salt (0.30 mmol, 80% yield, m. p. > 280 °C). ^1H NMR (CD_3OD): δ 8.96 (1H, d, $J = 5$ Hz), 8.90 (1H, s), 8.85 (1H, d, $J = 6$ Hz), 8.71 (1H, d, $J = 5$ Hz), 8.47 (1H, dt, $J = 2$ and 8 Hz), 8.23 (2H, m), 8.04 (1H, dd, $J = 6$ and 8 Hz) 7.87 (1H, dd, $J = 5$ and 8 Hz), 7.81 (2H, m). Anal. Calcd. For $C_{15}H_{13}Cl_2N_3O_8$: C, 41.49; H, 3.02; N, 9.68. Found: C, 41.53; H, 2.89; N, 9.54.

1-Methyl-3-phenylpyridinium Hexafluorophosphate (4-1). A mixture of 3-iodo-1-methylpyridinium perchlorate[102] (0.500 g, 1.59 mmol), phenylboronic acid (0.200 g, 1.64 mmol), and terakis(triphenylphosphine) palladium(0) (0.184 g, 0.159 mmol) in degassed tetrahydrofuran (15 mL) was allowed to stir at room temperature for 15 min. To this was added potassium carbonate (0.330 g, 2.36 mmol) in water (15 mL), and the suspension was heated at reflux under a nitrogen atmosphere.

After 6 h, the reaction was cooled to room temperature, and the precipitated catalyst was collected by filtration. To the filtrate was added EtOAc (10 mL) and water (10 mL). The aqueous layer was separated, and to it was added an excess of saturated KPF_6 solution. Upon stirring, product precipitated to give 285 mg (0.90 mmol) of a white solid (58% yield, mp 131-135 °C (lit.[102] mp no mp)). ^1H NMR (DMSO-d_6): δ 9.38 (1H,s), 8.93 (1H, d, *J* = 6 Hz), 8.86 (1H, d, *J* = 8 Hz), 8.17 (1H, dd, *J* = 6 and 8 Hz), 7.88 (2H, m), 7.58 (3H, m), 4.39 (3H, s, CH_3). Anal. Calcd. for $C_{12}H_{12}NPF_6$: C, 45.73; H, 3.84; N, 4.44. Found: C, 45.78; H, 3.80; N, 4.38.

1-Methyl-3-(3-pyridyl)pyridinium Hexafluorophosphate (4-2).

A mixture of 3-iodo-1-methylpyridinium perchlorate[102] (0.500 g, 1.59 mmol), diethyl-3-pyridylborane (0.240 g, 1.63 mmol), and terakis(triphenylphosphine) palladium(0) (0.184 g, 0.159 mmol) in degassed tetrahydrofuran (15 mL) was allowed to stir at room temperature for 15 min. To this was added potassium carbonate (0.330 g, 2.36 mmol) in water (15 mL), and the suspension was heated at reflux under a nitrogen atmosphere. After 7 h, the reaction was cooled to room temperature, and the precipitated catalyst was collected by filtration. To the filtrate was added EtOAc (10 mL) and water (10 mL). The aqueous layer was separated, and to it was added an excess of saturated KPF_6 solution. Upon stirring, product precipitated to give 310 mg (0.98

mmol) of a orange solid (62% yield, mp 210-213 °C (lit.[102] mp iodide)). ^{1}H NMR (DMSO-d_6): δ 9.47 (1H,s), 9.07 (1H, d, J = 1 Hz), 8.95 (2H, dd, J = 6 and 8 Hz), 8.73 (1H, dd, J = 5 Hz), 8.25 (2H, m), 7.63 (1H, dd, J = 5 and 8 Hz), 4.39 (3H, s, CH_3). Anal. Calcd. for $C_{11}H_{11}N_2PF_6$: C, 41.79; H, 3.51; N, 8.86. Found: C, 41.68; H, 3.47; N, 8.70.

2-Methyl-4-phenylisoquinolinium Hexafluorophosphate (4-3). A mixture of 4-bromo-2-methylisoquinolinium iodide[106] (0.500 g, 1.43 mmol), phenylboronic acid (0.292 g, 2.40 mmol), and terakis(triphenylphosphine) palladium(0) (0.277 g, 0.240 mmol) in degassed tetrahydrofuran (15 mL) was allowed to stir at room temperature for 15 min. To this was added sodium borate (1.83 g, 4.80 mmol) in water (15 mL), and the suspension was heated at reflux under a nitrogen atmosphere. After 6 h, the reaction was cooled to room temperature, and the precipitated catalyst and sodium borate were filtered away. To the filtrate was added EtOAc (10 mL) and water (10 mL). The aqueous layer was separated, and to it was added an excess of saturated KPF_6 solution. Upon stirring, product precipitated to give 160 mg (0.44 mmol) of a white solid (31% yield, mp 182-184 °C). ^{1}H NMR (DMSO-d_6): δ 10.00 (1H,s), 8.78 (1H, d, J = 1 Hz), 8.55 (1H, dd, J = 1 and 8 Hz), 8.23 (1H, dd, J = 1 and 7 Hz), 8.09 (2H, td, J = 1 and 7 Hz), 7.65 (5H, m), 4.50 (3H, s, CH_3).

Anal. Calcd. for $C_{16}H_{14}NPF_6$: C, 52.61; H, 3.86; N, 3.83. Found: C, 52.48; H, 3.84; N, 3.70.

2-Methyl-4-(3-pyridyl)isoquinolinium Iodide (4-4). A mixture of 4-bromo-2-methylisoquinolinium iodide[106] (0.500 g, 1.43 mmol), diethyl-3-pyridylborane (0.250 g, 1.70 mmol), and terakis(triphenylphosphine) palladium(0) (0.165 g, 0.143 mmol) in degassed tetrahydrofuran (15 mL) was allowed to stir at room temperature for 15 min. To this was added 7 mL of MeOH, followed by sodium borate (1.09 g, 2.86 mmol) in water (15 mL), and the suspension was heated at reflux under a nitrogen atmosphere. After 6 h, the reaction was cooled to room temperature, and the precipitated catalyst and sodium borate were filtered away. To the filtrate was added EtOAc (10 mL) and water (10 mL). The aqueous layer was separated and concentrated to an orange oil/solid which was washed with 10 mL of MeOH. The insolubles were filtered away. The product precipitated from MeOH upon addition of EtOAc to give 215 mg (0.062 mmol) of an orange solid (43% yield, mp 200-203 °C). ^1H NMR (DMSO-d_6): δ 10.07 (1H,s), 8.85 (3H, m), 8.58 (1H, d, J = 9 Hz), 8.26 (1H, m), 8.10 (3H, m), 7.72 (1H, dd, J = 6 and 9 Hz), 4.51 (3H, s, CH_3). Anal. Calcd. for $C_{15}H_{13}N_2I$: C, 51.74; H, 3.76; N, 8.05. Found: C, 51.42; H, 3.71; N, 7.68.

1-Methyl-4-(4′-pyridyl)pyridinium Iodide (MEBPY) 5-1. 4,4′-Dipyridyl (0.500 g, 3.20 mmol) was dissolved in EtOAc (3 mL) and $CHCl_3$ (3 mL). While stirring at room temperature, methyl iodide (0.30 mL, 4.82 mmol) was added. A yellow precipitate began to form, at which time, the mixture was transferred to the refrigerator and continued to stir for 2 days. The yellow solid product was collected and recrystallized from ethanol (580 mg, 2.01 mmol, 63% yield, mp 239-243 °C, lit.[113] mp 244 °C). ^1H NMR (D_2O): δ 8.95 (2H, d, J= 6 Hz), 8.82 (2H, d, J = 5 Hz), 8.43 (2H, d, J = 6 Hz), 7.96 (2H, d, J = 5 Hz), 4.49 (3H, s). Anal. Calcd. for $C_{11}H_{11}N_2I$: C, 44.32; H, 3.72; N, 9.40. Found: C, 44.51; H, 3.70; N, 9.34.

Tributyl-(4-pyridyl)stannane. A slurry of 4-bromopyridine hydrochloride (1.00 g, 5.14 mmol) freshly distilled diethyl ether (50 mL) was cooled to -45 °C under nitrogen with stirring. Butyllithium (4.12 mL, 2.5 M in hexane, 10.30 mmol) was added over a period of 10 min. The resultant yellow slurry was stirred for 20 min. The reaction was cooled to -70 °C, and the tributyltin chloride (2.09 mL, 7.71 mmol) was added. The mixture became homogeneous. After stirring for 20 min, the reaction was warmed to room temperature, and a white precipitate formed. The mixture stirred for another hour and was then poured into a separatory funnel and washed with 50 mL of water.

The organic phase was separated, and the aqueous layer was extracted with 50 mL of diethyl ether. The ethereal solutions were combined, dried over sodium sulfate, and the solvent evaporated to an oil. Flash chromatography of the oil with silica gel was accomplished by eluting first with hexanes to remove excess tributyl tin compounds, followed by 9:1 hexanes : EtOAc. Evaporation of the solvents yielded a clear oil (1.10 g, 2.99 mmol, 58 % yield). ^{1}H NMR ($CDCl_3$): δ 8.47 (2H, dd, J = 2 and 5 Hz), 7.35 (2H, dd, J = 2 and 5 Hz), 1.53 (6H, m), 1.32 (6H, m), 1.10 (6H, t), 0.88 (9H, t). Sn Side Bands. Anal. Calcd. for $C_{17}H_{31}NSn \bullet 1/8\ H_2O$: C,55.13; H,8.45; N,3.78. Found: C,54.73; H,8.85; N,3.79.

p-(4-Pyridyl)bromobenzene. Tributyl-(4-pyridyl)stannane (0.97 g, 2.63 mmol), para-dibromobezene (1.24 g, 5.27 mmol), and tetrakis(triphenylphosphine) palladium(0) (0.131 g, 0.107 mmol) were dissolved in toluene (50 mL). Under nitrogen, the mixture was heated at reflux for 6 h and then cooled to room temperature. The reaction was diluted with diethyl ether (70 mL), and insolubles were filtered away. The filtrate was extracted with 0.2 M HCl (2 x 50 mL). The acidic aqueous phases were combined and neutralized with Na_2CO_3. This solution was thoroughly extracted with ether which was dried over Na_2SO_4, and solvent evaporation of the combined organic phases yielded a pale yellow solid. The solid was recrystallized from acetone and water giving

285 mg of the pure product (1.22 mmol, 46.5% yield, mp 121-124 °C). ^{1}H NMR ($CDCl_3$): δ 8.68 (2H, dd, J = 2 and 6 Hz), 7.64 (2H, d, J = 8 Hz), 7.57 (4H, m). Anal. Calcd. for $C_{11}H_8BrN$: C, 56.44; H, 3.44; N, 5.98. Found: C, 56.45; H, 3.43; N, 5.92.

p-(4-(N-Methyl)Pyridinium iodide) bromobenzene. p-(4-Pyridyl)bromobenzene (50 mg, 0.21 mmol) was dissolved in EtOAc (5 mL), and excess methyl iodide was added. This was heated at reflux for 30 min, and 40 mg of the yellow solid product resulted (0.11 mmol, 83% yield, mp > 250 °C). ^{1}H NMR (DMSO-d_6): δ 9.04 (2H, d, J = 6 Hz), 8.50 (2H, d, J = 6 Hz), 8.02 (2H, d, J = 8 Hz), 7.85 (2H, d, J = 8 Hz), 4.33 (3H, s). Anal. Calcd. for $C_{12}H_{11}BrNI$: C, 38.33; H, 2.95; N, 3.72. Found: C, 38.23; H, 2.95; N, 3.65.

Bis-(4-pyridyl)benzene (Method A). P-Dibomobenzene (0.500g, 2.12 mmol) and tetrakis(triphenylphosphine) palladium(0) (0.131 g, 0.107 mmol) were dissolved in 50 mL of toluene. Under nitrogen, tributyl-(4-pyridyl)stannane (1.73 g, 4.70 mmol) was added over a period of 15 min. The reaction was heated at reflux for 30 h. After cooling to room temperature, the mixture was diluted with EtOAc (50 mL). Insolubles were filtered away, and the filtrate was extracted with 0.2 M HCl (2 x 50 mL). The acidic aqueous phases were combined and neutralized with Na_2CO_3. This solution was extracted with $CHCl_3$ (3 x 40 mL), and solvent evaporation of the combined organic phases yielded a pale yellow oil. The oil was dissolved in acetone, and upon addition of H_2O, a pale yellow precipitate formed. The solid was dissolved in CH_2Cl_2 and flash chromatographed with silica gel. Eluting with EtOAc : hexanes (50:50) removed the monocoupled product, and the bis-coupled product was eluted with EtOAc : MeOH (50:50). The solid product was obtained upon solvent evaporation (260 mg, 1.12 mmol, 53% yield, mp 198-200 °C, lit.[115,116] mp 202-204 °C). ^1H NMR ($CDCl_3$): δ 8.71 (4H, d, J = 5 Hz), 7.78 (4H, s), 7.57 (4H, dd, J = 1 and 4 Hz). Anal. Calcd. for $C_{16}H_{12}N_2$: C, 82.73; H, 5.21; N, 12.06. Found: C, 83.03; H, 5.36; N, 11.81.

Method B. P-Dibomobenzene (0.110g, 0.466 mmol) and *trans*-di(acetato)-bis[*o*-(di-*o*-tolylphosphino)benzyl]palladium[118,119] (0.20 g, 0.021 mmol) were dissolved in 30 mL of toluene. Under nitrogen, tributyl-(4-pyridyl)stannane (0.368 g, 1.00 mmol) was added over a period of 15 min. The reaction was heated at reflux for 19 h. After cooling to room temperature, the mixture was diluted with diethyl ether (70 mL). Insolubles were filtered away, and the filtrate was extracted with 0.2 M HCl (2 x 25 mL). The acidic aqueous phases were combined and neutralized with Na_2CO_3. This solution was extracted with $CHCl_3$ (3 x 40 mL), and solvent evaporation of the combined organic phases yielded a pale yellow solid with good purity by NMR (89 mg, 0.39 mmol, 82% yield, mp 198-200 °C).

1-Methyl-4-((4′-pyridyl)-phenyl)pyridinium Iodide (STRBPY) 5-2. Bis-(4-pyridyl)benzene (0.050 g, 0.215 mmol) was dissolved in CH_2Cl_2 (2 mL), $CHCl_3$ (2 mL), and hexanes (2 mL). Methyl iodide (14 μL, 0.23 mmol) was added with stirring. The mixture was placed in the refrigerator with continued stirring, and after several hours, the yellow solid product formed (15 mg, 0.040 mmol, 19% yield, mp 211-215 °C). ^1H NMR (DMSO-d_6): δ 9.05 (2H, d, J = 7 Hz), 8.72 (2H, d, J = 5 Hz), 8.60 (2H, d, J = 7 Hz), 8.25 (2H, d, J = 9 Hz), 8.10 (2H, d, J = 9 Hz), 7.86 (2H, d, J = 7 Hz), 4.35 (3H, s). Anal. Calcd. for $C_{17}H_{15}N_2I \bullet H_2O$: C,52.06; H,4.37; N,7.14. Found: C,52.19; H,4.43; N,7.03.

4,4′-Bipyridyl N-Oxide (BPYNOX) 5-3. Following a literature procedure, 4,4′-dipyridyl (1.00 g, 6.40 mmol) was dissolved in glacial acetic acid (17 mL). To this was added H_2O_2 (0.815 g, 30 % soln., 7.19 mmol). The mixture was heated at 70 °C for 24 h. After, cooling, the mixture was poured into H_2O (60 mL) and made alkaline with Na_2CO_3. A thorough extraction was done with $CHCl_3$, followed by drying of the organic phase over $Na2_sO_4$ and solvent evaporation. The pale yellow solid was recrystallized from acetone containing a trace of water and product resulted (160 mg, 0.929 mmol, 15% yield, mp 178-180 °C after drying at 100 °C in vacuo, lit.^{114} mp 180 °C). ^{1}H NMR (D$_2$O): δ 8.64 (2H, dd, J = 2 and 4 Hz), 8.41 (2H, dd, J = 2 and 5 Hz), 7.95 (2H, dd, J = 2 and 5 Hz), 7.75 (2H, dd, J = 1 and 4 Hz). Anal. Calcd. for $C_{10}H_8N_2O$: C, 69.75; H, 4.68; N, 16.27. Found: C, 70.00; H, 4.68; N, 16.31.

N-Methyl-4,4'-Bipyridinium Iodide N-Oxide (MEPOX) 5-4. Following a literature procedure, 5-3 (0.160, 0.929 mmol) and methyl iodide were dissolved in ethanol (12 mL). Under nitrogen, the mixture was refluxed for 30 min. Upon cooling, the yellow solid product precipitated and was collect (210 mg, 0.669 mmol, 72% yield, mp 230-233 °C, lit.^{114} mp 234 °C). ^{1}H NMR (D$_2$O): δ 8.91 (2H, d, J = 7 Hz), 8.53 (2H, d, J = 8 Hz), 8.40 (2H, d, J = 6 Hz), 8.13 (2H, d, J = 7 Hz), 4.44 (3H, s). Anal. Calcd. for $C_{11}H_{11}N_2O$: C,42.06; H,3.53; N,8.92. Found: C,41.90; H,3.65; N,8.79.

Stock Solutions of MEBPY (5-1). 5-1 (29.9 mg, 0.100 mmol) was placed in a 1 mL volumetric flask and was diluted to the mark with degassed D$_2$O, DMSO-d$_6$, or CD$_3$OD resulting in a 0.100 M solution. (For the experiment containing acetic acid, acetic acid-d$_1$ solution (100 μL) was added to the volumetric flask.)

Stock Solution of STRBPY (5-2). 5-2 (22.5 mg, 0.0600 mmol) was placed in a 1 mL volumetric flask and was diluted to the mark with degassed D_2O (600 µL) and DMSO-d_6 (400 µL) resulting in a 0.0600 M solution.

Stock Solution of BPYNOX (5-3). 5-3 (17.2 mg, 0.100 mmol) was placed in a 1 mL volumetric flask and was diluted to the mark with degassed D_2O resulting in a 0.100 M solution.

Stock Solution of MEPOX (5-4). 5-4 (21.8 mg, 0.0700 mmol) was placed in an NMR tube and was diluted with degassed D_2O (700 µL) resulting in a 0.100 M solution.

Stock Solution of MEPYR (5-5). 5-5 (22.1 mg, 0.100 mmol) was placed in a 1 mL volumetric flask and was diluted to the mark with degassed D_2O resulting in a 0.100 M solution.

Stock Solutions of $NiCl_2$. Flame dried $NiCl_2$ (38.89 mg, 0.300 mmol) was placed in a 1 mL volumetric flask and was diluted to the mark with degassed D_2O, DMSO-d_6, CD_3OD or a combination as necessary resulting in a 0.300 M solution.

Stock Solution of $NiBr_2$. Flame dried $NiBr_2$ (65.6 mg, 0.300 mmol) was placed in a 1 mL volumetric flask and was diluted to the mark with degassed D_2O resulting in a 0.300 M solution.

Stock Solution of $CoCl_2$. Flame dried $CoCl_2$ (39.0 mg, 0.300 mmol) was placed in a 1 mL volumetric flask and was diluted to the mark with degassed D_2O resulting in a 0.300 M solution.

General Procedure for T_1 Measurements. Stock solution of a substrate (700 µL) was placed in an NMR tube and T_1 measurements for proton or carbon were made. Afterwards, aliquots of the metal salt solution were added to increase the concentration of metal ion in solution, and relaxation data was collected after each addition. T_1 measurements made use of the inversion recovery routine available with the Gemini-300 and Unity-500. Samples were allowed to equilibrate in the probe at 25 °C for 15 min. All the measurements were made using 8-14 delay times with array being computer generated or manually entered depending on the constraints of the experiment. The computer software computes an exponential fit of peak intensities to obtain T_1. For each proton signal, T_1 values were calculated for several lines in the multiplet (or the one line of a singlet) and the values were averaged to give the final value. Nuclear distances and angles were measured for the compounds using Alchemy software and scale models based on a 2.5 Å bond length between the coordinating atom and the metal ion.

APPENDIX
T_1 RELAXATION DATA

The following tables summarize the relaxation time data for compounds discussed in Chapter 5. The error limits were determined from the original standard deviations observed from the experimental relaxation times. When multiplets were present in a spectrum, the relaxation time was calculated as the average of the times for each peak of the multiplet. In these cases, the error limits were then determined by the square-root of the sum of the squares of the standard deviations ($\sqrt{\Sigma x^2}$).[132] For the second-order rate constants (k_2), standard deviations of the slopes were determined but were not used as error limits. Instead, the error limits of the corrected rate constant values were used to determined maximum and minimum slope values in the k_2 plots. The differences in these maximum and minimum slopes and the observed slope gave the error limits for k_2.

Key

H = Proton

C = Carbon

δ = Chemical Shift in ppm

T_1 = Relaxation Time (s)

k_{solv} = Relaxation Rate Constant($1/T_1$)without paramagnet(s^{-1})

k_{obs} = Relaxation Rate Constant ($1/T_1$) with paramagnet(s^{-1})

k_{corr} = k_{obs} - k_{solv} (s^{-1})

k_2 = Apparent second-order rate constant(M^{-1} s^{-1})

Error = Standard deviation or uncertainty in the observed or calculated value.

R = Distance from Metal-center to Atom(Å)

Table A-1: T_1 Relaxation Times and Rate Constants for MEBPY in D_2O with $NiCl_2$ at 25 °C.

Experiment: MEBPY with $NiCl_2$ in D_2O

Correction Values: [MEBPY]= 0.100 M [Ni^{+2}] = 0 M

Proton	δ	T_1 (s)	Error	k_{solv} (s^{-1})	Error
H-2'	8.79	3.83	0.31	0.261	0.021
H-3'	7.94	2.98	0.28	0.336	0.032
H-3	8.42	2.84	0.23	0.352	0.029
H-2	8.95	3.16	0.18	0.316	0.018
Me	4.50	1.53	0.040	0.654	0.017

Experiment 1: [MEBPY]= 0.0980 M [Ni^{+2}] = 0.00588 M

Proton	δ	T_1 (s)	Error	k_{obs} (s^{-1})	k_{corr} (s^{-1})	Error
H-2'	8.79	0.158	0.009	6.33	6.07	0.36
H-3'	7.94	0.225	0.011	4.44	4.11	0.23
H-3	8.42	0.431	0.021	2.32	1.97	0.12
H-2	8.95	1.04	0.04	0.962	0.645	0.038
Me	4.50	0.956	0.015	1.05	0.392	0.024

Experiment 2: [MEBPY]= 0.0966 M [Ni^{+2}] = 0.0103 M

Proton	δ	T_1 (s)	Error	k_{obs} (s^{-1})	k_{corr} (s^{-1})	Error
H-2'	8.78	0.0859	0.0014	11.6	11.4	0.2
H-3'	7.94	0.127	0.001	7.87	7.54	0.06
H-3	8.41	0.268	0.008	3.73	3.38	0.11
H-2	8.94	0.712	0.036	1.40	1.09	0.07
Me	4.49	0.749	0.028	1.34	0.682	0.054

Experiment 3: [MEBPY]= 0.0952 M [Ni^{+2}] = 0.0143 M

Proton	δ	T_1 (s)	Error	k_{obs} (s^{-1})	k_{corr} (s^{-1})	Error
H-2'	8.79	0.0688	0.0016	14.5	14.3	0.3
H-3'	7.94	0.0945	0.0024	10.6	10.3	0.3
H-3	8.41	0.192	0.010	5.21	4.86	0.27
H-2	8.94	0.526	0.015	1.90	1.59	0.06
Me	4.49	0.621	0.007	1.61	0.957	0.024

Table A-1- Cont.

Experiment 4: [MEBPY]= 0.0926 M [Ni^{+2}] = 0.0222 M

Proton	δ	T_1 (s)	Error	k_{obs} (s^{-1})	k_{corr} (s^{-1})	Error
H-2'	8.78	0.0442	0.0005	22.6	22.4	0.2
H-3'	7.93	0.0604	0.0016	16.6	16.2	0.4
H-3	8.41	0.127	0.005	7.87	7.52	0.30
H-2	8.93	0.348	0.003	2.87	2.56	0.03
Me	4.48	0.460	0.003	2.17	1.52	0.02

Experiment 5: [MEBPY]= 0.0909 M [Ni^{+2}] = 0.0273 M

Proton	δ	T_1 (s)	Error	k_{obs} (s^{-1})	k_{corr} (s^{-1})	Error
H-2'	8.77	0.0435	0.0026	23.0	22.7	1.4
H-3'	7.92	0.0507	0.0004	19.7	19.4	0.2
H-3	8.40	0.109	0.002	9.17	8.82	0.13
H-2	8.91	0.289	0.004	3.46	3.14	0.05
Me	4.47	0.383	0.004	2.61	1.96	0.03

Experiment 6: [MEBPY]= 0.0824 M [Ni^{+2}] = 0.0529 M

Proton	δ	T_1 (s)	Error	k_{obs} (s^{-1})	k_{corr} (s^{-1})	Error
H-2'	8.76	0.0285	0.0027	35.1	34.8	3.4
H-3'	7.90	0.0251	0.0013	39.84	39.51	2.1
H-3	8.38	0.0583	0.0036	17.2	16.8	1.1
H-2	8.89	0.174	0.007	5.74	5.43	0.22
Me	4.44	0.247	0.008	4.05	3.40	0.13

Table A-2: Second-Order Rate Constants (k_2) for MEBPY in D_2O with $NiCl_2$ at 25 °C.

Experiment: MEBPY with $NiCl_2$ in D_2O

Proton	Slope (k_2)	Error	Intercept	Corr. Coef.	# of Pnts.	R (A)
H-2'	979	56	0.631	0.998	4	3.1
H-3'	750	50	-0.442	0.999	5	5.1
H-3	314	23	0.263	0.999	5	6.8
H-2	102	6	0.14	0.997	5	9.1
Me	64.5	3.9	0.0571	0.998	5	10.8

Table A-3: T_1 Relaxation Times and Rate Constants for MEBPY in D_2O with $NiCl_2$ and Acetic Acid at 25 °C.

Correction Values:		[MEBPY]=	0.100 M	$[Ni^{+2}]$ =	0 M	[Acid]=	0.0100 M
Proton	Shift	T_1 (s)	Error	k_{solv} (s^{-1})	Error		
H-2'	8.80	2.49	0.66	0.402	0.106		
H-3'	7.98	2.80	0.86	0.357	0.110		
H-3	8.42	2.70	0.53	0.370	0.073		
H-2	8.95	3.03	0.63	0.330	0.068		
Me	4.49	1.89	0.37	0.529	0.103		
Experiment 1:		[MEBPY]=	0.0980 M	$[Ni^{+2}]$ =	0.00588 M	[Acid]=	0.00980 M
Proton	Shift	T_1 (s)	Error	k_{obs} (s^{-1})	k_{corr} (s^{-1})	Error	
H-2'	8.81	0.154	0.001	6.49	6.09	0.12	
H-3'	7.99	0.218	0.002	4.59	4.23	0.12	
H-3	8.43	0.439	0.006	2.28	1.91	0.08	
H-2	8.96	1.04	0.01	0.962	0.632	0.069	
Me	4.50	0.947	0.011	1.06	0.527	0.104	
Experiment 2:		[MEBPY]=	0.0952 M	$[Ni^{+2}]$ =	0.0143 M	[Acid]=	0.00952 M
Proton	Shift	T_1 (s)	Error	k_{obs} (s^{-1})	k_{corr} (s^{-1})	Error	
H-2'	8.81	0.0674	0.0008	14.8	14.4	0.2	
H-3'	7.99	0.0929	0.0007	10.8	10.4	0.1	
H-3	8.43	0.203	0.004	4.93	4.56	0.13	
H-2	8.95	0.540	0.009	1.85	1.52	0.07	
Me	4.49	0.626	0.014	1.60	1.07	0.11	
Experiment 3:		[MEBPY]=	0.0926 M	$[Ni^{+2}]$ =	0.0222 M	[Acid]=	0.00926 M
Proton	Shift	T_1 (s)	Error	k_{obs} (s^{-1})	k_{corr} (s^{-1})	Error	
H-2'	8.81	0.0460	0.0012	21.7	21.3	0.6	
H-3'	7.99	0.0596	0.0004	16.8	16.4	0.2	
H-3	8.42	0.131	0.001	7.63	7.26	0.08	
H-2	8.95	0.360	0.006	2.78	2.45	0.08	
Me	4.48	0.453	0.008	2.21	1.68	0.11	
Experiment 4:		[MEBPY]=	0.0909 M	$[Ni^{+2}]$ =	0.0273 M	[Acid]=	0.00909 M
Proton	Shift	T_1 (s)	Error	k_{obs} (s^{-1})	k_{corr} (s^{-1})	Error	
H-2'	8.81	0.0397	0.0016	25.2	24.8	1.0	
H-3'	7.99	0.0507	0.0002	19.7	19.4	0.1	
H-3	8.42	0.112	0.001	8.93	8.56	0.13	
H-2	8.94	0.309	0.001	3.24	2.91	0.07	
Me	4.48	0.404	0.002	2.48	1.95	0.11	

Table A-3—Cont.

Experiment 5: [MEBPY]= 0.0824 M [Ni^{+2}] = 0.0529 M [Acid]= 0.00824 M

Proton	Shift	T_1 (s)	Error	k_{obs} (s^{-1})	k_{corr} (s^{-1})	Error
H-2'	8.79	0.0315	0.0040	31.8	31.3	4.0
H-3'	7.98	0.0276	0.0002	36.2	35.9	0.3
H-3	8.40	0.0632	0.0010	15.8	15.5	0.3
H-2	8.91	0.183	0.002	5.46	5.13	0.10
Me	4.45	0.245	0.003	4.08	3.55	0.12

Table A-4: Second-Order Rate Constants (k_2) for MEBPY in D_2O with $NiCl_2$ and Acetic Acid at 25 °C.

Experiment: MEBPY with $NiCl_2$ in D_2O with Acid

Proton	Slope (k_2)	Error	Intercept	Corr. Coef.	# of Pnts.	R (A)
H-2'	879	59	1.35	0.998	5	3.1
H-3'	668	15	0.876	0.999	5	5.1
H-3	286	10	0.536	0.998	5	6.8
H-2	95.0	4.4	0.199	0.997	5	9.1
Me	64.2	4.9	0.182	0.999	5	10.8

Table A-5: T_1 Relaxation Times and Rate Constants for MEBPY in D_2O with $NiBr_2$ at 25 °C.

Experiment: MEBPY with $NiBr_2$ in D_2O

Correction Values: [MEBPY]= 0.100 M [Ni^{+2}] = 0 M

Proton	Shift	T_1 (s)	Error	k_{solv} (s^{-1})	Error
H-2'	8.79	3.83	0.31	0.261	0.021
H-3'	7.94	2.98	0.28	0.336	0.032
H-3	8.43	2.84	0.23	0.352	0.029
H-2	8.96	3.16	0.18	0.316	0.018
Me	4.50	1.53	0.04	0.654	0.017

Experiment 1: [MEBPY]= 0.0980 M [Ni^{+2}] = 0.00588 M

Proton	Shift	T_1 (s)	Error	k_{obs} (s^{-1})	k_{corr} (s^{-1})	Error
H-2'	8.79	0.134	0.003	7.46	7.20	0.14
H-3'	7.94	0.187	0.002	5.35	5.01	0.07
H-3	8.42	0.377	0.006	2.65	2.30	0.05
H-2	8.96	0.954	0.029	1.05	0.732	0.037
Me	4.50	0.913	0.033	1.10	0.442	0.044

Experiment 2: [MEBPY]= 0.0952 M [Ni^{+2}] = 0.0143 M

Proton	Shift	T_1 (s)	Error	k_{obs} (s^{-1})	k_{corr} (s^{-1})	Error
H-2'	8.78	0.0766	0.0005	13.1	12.8	0.1
H-3'	7.94	0.105	0.001	9.52	9.19	0.04
H-3	8.42	0.183	0.002	5.46	5.11	0.05
H-2	8.95	0.460	0.005	2.17	1.86	0.03
Me	4.49	0.560	0.005	1.79	1.13	0.02

Table A-5—Cont.

Experiment 3: [MEBPY]= 0.0935 M [Ni^{+2}] = 0.0196 M

Proton	Shift	T_1 (s)	Error	k_{obs} (s^{-1})	k_{corr} (s^{-1})	Error
H-2'	8.78	0.0505	0.0005	19.8	19.5	0.2
H-3'	7.94	0.0680	0.0002	14.7	14.4	0.1
H-3	8.41	0.124	0.002	8.07	7.71	0.13
H-2	8.94	0.311	0.002	3.22	2.90	0.03
Me	4.49	0.409	0.002	2.45	1.79	0.02

Experiment 4: [MEBPY]= 0.0909 M [Ni^{+2}] = 0.0273 M

Proton	Shift	T_1 (s)	Error	k_{obs} (s^{-1})	k_{corr} (s^{-1})	Error
H-2'	8.77	0.0350	0.0008	28.6	28.3	0.6
H-3'	7.92	0.0448	0.0003	22.3	22.0	0.1
H-3	8.40	0.0851	0.0022	11.8	11.4	0.3
H-2	8.92	0.220	0.002	4.55	4.23	0.05
Me	4.47	0.302	0.003	3.31	2.66	0.04

Table A-6: Second-Order Rate Constants (k_2) for MEBPY in D_2O with $NiBr_2$ at 25 °C.

Experiment: MEBPY with $NiBr_2$ in D_2O

Proton	Slope (k_2)	Error	Intercept	Corr. Coef.	# of Pnts.	R (A)
H-2'	999	22	-0.202	0.990	4	3.1
H-3'	800	17	-0.0718	0.996	3	5.1
H-3	313	93	-0.543	0.995	4	6.8
H-2	165	6	-0.336	0.997	4	9.1
Me	105	4	-0.248	0.997	4	10.8

Table A-7: T_1 Relaxation Times and Rate Constants for MEBPY in DMSO-d_6 with $NiCl_2$ at 25 °C.

Experiment: MEBPY with $NiCl_2$ in DMSO

Correction Values: [MEBPY]= 0.100 M [Ni^{+2}] = 0 M

Proton	Shift	T_1 (s)	Error	k_{solv} (s^{-1})	Error
H-2'	8.86	2.81	0.15	0.356	0.019
H-3'	8.04	1.58	0.06	0.633	0.023
H-3	8.62	1.47	0.03	0.680	0.015
H-2	9.16	1.74	0.06	0.575	0.019
Me	4.40	0.868	0.037	1.15	0.05

Experiment 1: [MEBPY]= 0.0994 M [Ni^{+2}] = 0.00170 M

Proton	Shift	T_1 (s)	Error	k_{obs} (s^{-1})	k_{corr} (s^{-1})	Error
H-2'	8.79	0.0546	0.0008	18.3	18.0	0.3
H-3'	7.94	0.248	0.003	4.03	3.40	0.06
H-3	8.42	0.694	0.018	1.44	0.761	0.040
H-2	8.95	1.25	0.04	0.800	0.225	0.033
Me	4.50	0.750	0.087	1.33	0.181	0.162

Table A-7—Cont.

Experiment 2: [MEBPY]= 0.0990 M $[Ni^{+2}]$ = 0.00297 M

Proton	Shift	T_1 (s)	Error	k_s (s^{-1})	k_{corr} (s^{-1})	Error
H-2'	8.78	0.0225	0.0009	44.4	44.1	1.8
H-3'	7.94	0.114	0.002	8.77	8.14	0.13
H-3	8.41	0.415	0.013	2.41	1.73	0.08
H-2	8.94	0.893	0.030	1.12	0.545	0.042
Me	4.49	0.637	0.009	1.57	0.418	0.054

Experiment 3: [MEBPY]= 0.0986 M $[Ni^{+2}]$ = 0.00423 M

Proton	Shift	T_1 (s)	Error	k_{obs} (s^{-1})	k_{corr} (s^{-1})	Error
H-2'	8.79	0.0136	0.0007	73.5	73.2	3.6
H-3'	7.94	0.0704	0.0011	14.2	13.6	0.2
H-3	8.41	0.280	0.016	3.57	2.89	0.21
H-2	8.94	0.720	0.043	1.39	0.814	0.085
Me	4.49	0.577	0.016	1.73	0.581	0.069

Experiment 4: [MEBPY]= 0.0983 M $[Ni^{+2}]$ = 0.00506 M

Proton	Shift	T_1 (s)	Error	k_{obs} (s^{-1})	k_{corr} (s^{-1})	Error
H-2'	8.78	0.0104	0.0006	96.2	95.8	5.6
H-3'	7.93	0.0530	0.0009	18.9	18.2	0.3
H-3	8.41	0.206	0.017	4.85	4.17	0.40
H-2	8.93	0.606	0.034	1.65	1.08	0.095
Me	4.48	0.536	0.016	1.87	0.714	0.073

Experiment 5: [MEBPY]= 0.0979 M $[Ni^{+2}]$ = 0.00629 M

Proton	Shift	T_1 (s)	Error	k_{obs} (s^{-1})	k_{corr} (s^{-1})	Error
H-2'	8.77	0.00873	0.00088	114.5	114.2	11.6
H-3'	7.92	0.0403	0.0011	24.81	24.18	0.65
H-3	8.40	0.161	0.015	6.21	5.53	0.59
H-2	8.91	0.493	0.037	2.03	1.45	0.15
Me	4.47	0.488	0.014	2.05	0.897	0.077

Table A-8: Second-Order Rate Constants (k_2) for MEBPY in DMSO-d_6 with $NiCl_2$ at 25 °C.

Experiment: MEBPY with $NiCl_2$ in DMSO

Proton	Slope (k_2)	Error	Intercept	Corr. Coef.	# of Pnts.	R (A)
H-2'	21600	2030	-18.5	0.997	5	3.1
H-3'	4570	114	-4.98	0.997	5	5.1
H-3	1060	117	-1.26	0.993	5	6.8
H-2	264	45	-0.246	0.997	5	9.1
Me	153	52	-0.0634	0.998	5	10.8

Table A-9: T_1 Relaxation Times and Rate Constants for MEBPY in CD_3OD with $NiCl_2$ at 25 °C.

Experiment: MEBPY with $NiCl_2$ in CD_3OD

Correction Values: [MEBPY]= 0.100 M $[Ni^{+2}]$ = 0 M

Proton	Shift	T_1 (s)	Error	k_{solv} (s^{-1})	Error
H-2'	8.82	3.79	0.15	0.264	0.010
H-3'	8.00	2.99	0.11	0.334	0.012
H-3	8.52	3.07	0.02	0.326	0.002
H-2	9.06	3.42	0.05	0.292	0.004
Me	4.49	1.81	0.07	0.552	0.021

Experiment 1: [MEBPY]= 0.0996 M $[Ni^{+2}]$ = 0.00128 M

Proton	Shift	T_1 (s)	Error	k_{obs} (s^{-1})	k_{corr} (s^{-1})	Error
H-2'	8.82	0.0992	0.0011	10.1	9.82	0.11
H-3'	8.00	0.318	0.003	3.15	2.81	0.03
H-3	8.52	0.928	0.008	1.08	0.725	0.009
H-2	9.06	2.07	0.03	0.484	0.191	0.008
Me	4.49	1.45	0.03	0.692	0.139	0.025

Experiment 2: [MEBPY]= 0.0990 M $[Ni^{+2}]$ = 0.00297 M

Proton	Shift	T_1 (s)	Error	k_s (s^{-1})	k_{corr} (s^{-1})	Error
H-2'	8.82	0.0343	0.0002	29.2	28.9	0.2
H-3'	8.00	0.135	0.001	7.41	7.07	0.02
H-3	8.52	0.485	0.001	2.06	1.71	0.01
H-2	9.06	1.27	0.02	0.787	0.495	0.014
Me	4.49	1.10	0.01	0.912	0.360	0.022

Experiment 3: [MEBPY]= 0.0983 M $[Ni^{+2}]$ = 0.00506 M

Proton	Shift	T_1 (s)	Error	k_{obs} (s^{-1})	k_{corr} (s^{-1})	Error
H-2'	8.82	0.0166	0.0001	60.2	60.0	0.4
H-3'	8.01	0.0732	0.0004	13.7	13.3	0.1
H-3	8.53	0.295	0.001	3.39	3.04	0.01
H-2	9.05	0.843	0.021	1.19	0.894	0.030
Me	4.49	0.872	0.008	1.15	0.594	0.024

Table A-10: Second-Order Rate Constants (k_2) for MEBPY in CD_3OD with $NiCl_2$ at 25 °C.

Experiment: MEBPY with $NiCl_2$ in CD_3OD

Proton	Slope (k_2)	Error	Intercept	Corr. Coef.	# of Pnts.	R (A)
H-2'	13300	1600	-8.48	0.997	3	3.1
H-3'	2790	36	0.925	0.999	3	5.1
H-3	613	6	0.0774	0.993	3	6.8
H-2	186	10	-0.0511	0.999	3	9.1
Me	120	12	0.0082	0.999	3	10.8

Table A-11: T_1 Relaxation Times and Rate Constants for MEBPY in D_2O with $CoCl_2$ at 25 °C.

Experiment: MEBPY with $CoCl_2$ in D_2O

Correction Values: [MEBPY]= 0.100 M [Co^{+2}] = 0 M

Proton	Shift	T_1 (s)	Error	k_{solv} (s^{-1})	Error
H-2'	8.79	3.83	0.31	0.261	0.021
H-3'	7.94	2.98	0.28	0.336	0.032
H-3	8.42	2.84	0.23	0.352	0.029
H-2	8.95	3.16	0.18	0.316	0.018
Me	4.50	1.53	0.04	0.654	0.017

Experiment 1: [MEBPY]= 0.0994 M [Co^{+2}] = 0.00170 M

Proton	Shift	T_1 (s)	Error	k_{obs} (s^{-1})	k_{corr} (s^{-1})	Error
H-2'	8.79	0.283	0.001	3.53	3.27	0.02
H-3'	7.94	1.76	0.01	0.568	0.233	0.032
H-3	8.42	2.40	0.01	0.417	0.065	0.029
H-2	8.95	2.78	0.04	0.360	0.043	0.019
Me	4.50	1.38	0.02	0.725	0.071	0.020

Experiment 2: [MEBPY]= 0.0986 M [Co^{+2}] = 0.00423 M

Proton	Shift	T_1 (s)	Error	k_{obs} (s^{-1})	k_{corr} (s^{-1})	Error
H-2'	8.78	0.129	0.003	7.75	7.49	0.18
H-3'	7.94	1.15	0.01	0.870	0.534	0.032
H-3	8.41	1.89	0.07	0.529	0.177	0.034
H-2	8.94	2.29	0.15	0.437	0.120	0.034
Me	4.49	1.25	0.01	0.801	0.148	0.018

Experiment 3: [MEBPY]= 0.0976 M [Co^{+2}] = 0.00711 M

Proton	Shift	T_1 (s)	Error	k_{obs} (s^{-1})	k_{corr} (s^{-1})	Error
H-2'	8.79	0.0903	0.0075	11.1	10.8	0.9
H-3'	7.94	0.828	0.0096	1.21	0.872	0.035
H-3	8.41	1.54	0.09	0.649	0.297	0.045
H-2	8.94	1.94	0.10	0.515	0.199	0.032
Me	4.49	1.22	0.01	0.820	0.166	0.018

Table A-12: Second-Order Rate Constants (k_2) for MEBPY in D_2O with $CoCl_2$ at 25 °C.

Experiment: MEBPY with $CoCl_2$ in D_2O

Proton	Slope (k_2)	Error	Intercept	Corr. Coef.	# of Pnts.	R (A)
H-2'	1390	180	1.16	0.994	3	3.1
H-3'	118	12	0.0033	0.999	3	5.1
H-3	42.9	14.2	0.0661	0.999	3	6.8
H-2	28.8	9.5	0.00453	0.999	3	9.1
Me	17.3	7.4	0.0531	0.928	3	10.8

Table A-13: T_1 Relaxation Times and Rate Constants for MEBPY in D_2O with $NiBr_2$ at 25 °C.

Experiment: MEBPY with $NiBr_2$ in D_2O

Experiment 1: [MEBPY]= 0.0993 M $[Ni^{+2}]$ = 0.00213 M

Carbon	Shift	T_1 (s)	Error	k_{obs} (s^{-1})	Error
C-2'	154.03	0.423	0.021	2.37	0.12
C-3'	126.54	0.535	0.015	1.87	0.05
C-4'	146.58	0.903	0.061	1.11	0.07
C-4	157.44	2.39	0.22	0.418	0.038
C-3	129.83	2.07	0.06	0.484	0.014
C-2	149.70	2.70	0.21	0.371	0.029
C-Me	52.00	2.30	0.14	0.435	0.026

Experiment 2: [MEBPY]= 0.0983 M $[Ni^{+2}]$ = 0.00506 M

Carbon	Shift	T_1 (s)	Error	k_{obs} (s^{-1})	Error
C-2'	154.03	0.198	0.011	5.05	0.28
C-3'	126.54	0.245	0.012	4.09	0.20
C-4'	146.58	0.440	0.029	2.27	0.15
C-4	157.44	1.27	0.29	0.787	0.180
C-3	129.83	1.47	0.08	0.681	0.037
C-2	149.70	2.23	0.20	0.449	0.040
C-Me	52.00	1.61	0.25	0.620	0.096

Experiment 3: [MEBPY]= 0.0970 M $[Ni^{+2}]$ = 0.00914 M

Carbon	Shift	T_1 (s)	Error	k_{obs} (s^{-1})	Error
C-2'	154.03	0.119	0.012	8.44	0.85
C-3'	126.54	0.144	0.007	6.96	0.34
C-4'	146.58	0.241	0.044	4.15	0.76
C-4	157.44	1.06	0.22	0.941	0.195
C-3	129.83	1.22	0.05	0.822	0.034
C-2	149.70	1.62	0.13	0.617	0.050
C-Me	52.00	2.34	0.28	0.428	0.051

Table A-14: Second-Order Rate Constants (k_2) for MEBPY in D_2O with $NiBr_2$ at 25 °C.

Experiment: MEBPY with $NiBr_2$ in D_2O

Carbon	Slope (k_2)	Error	Intercept	Corr. Coef.	# of Pnts.	R (A)
C-2'	864	138	0.585	0.999	3	3.0
C-3'	725	58	0.362	0.999	3	4.3
C-4'	435	122	0.14	0.999	3	4.8
C-4	72.3	35.4	0.322	0.947	3	6.3
C-3	47.4	8.1	0.405	0.982	3	7.1
C-2	35.5	11.7	0.286	0.994	3	8.4
C-Me	63.1	17.7	0.301	0.999	3	10.4

Table A-15: T_1 Relaxation Times and Rate Constants for STRBPY in D_2O with $NiCl_2$ at 25 °C.

Experiment: STRBPY with $NiCl_2$ in D_2O/DMSO

Correction Values: [STRBPY] = 0.060 M [Ni^{+2}] = 0 M

Proton	Shift	T_1 (s)	Error	k_{solv} (s^{-1})	Error
H-2"	8.75	0.932	0.025	1.07	0.03
H-3"	7.92	0.881	0.023	1.14	0.03
H-3'	8.11	0.884	0.037	1.13	0.05
H-2'	8.20	0.829	0.027	1.21	0.04
H-3	8.47	0.847	0.026	1.18	0.04
H-2	8.92	1.07	0.04	0.935	0.033
Me	4.50	0.704	0.063	1.42	0.13

Experiment 1: [STRBPY] = 0.0593 M [Ni^{+2}] = 0.00356 M

Proton	Shift	T_1 (s)	Error	k_{obs} (s^{-1})	k_{corr} (s^{-1})	Error
H-2"	8.75	0.150	0.002	6.67	5.59	0.10
H-3"	7.92	0.205	0.001	4.88	3.74	0.04
H-3'	8.11	0.301	0.004	3.32	2.19	0.07
H-2'	8.20	0.457	0.014	2.19	0.982	0.077
H-3	8.47	0.567	0.008	1.76	0.583	0.045
H-2	8.92	0.640	0.012	1.56	0.628	0.045
Me	4.50	0.411	0.007	2.43	1.01	0.13

Experiment 2: [STRBPY] = 0.0583 M [Ni^{+2}] = 0.00870 M

Proton	Shift	T_1 (s)	Error	k_{obs} (s^{-1})	k_{corr} (s^{-1})	Error
H-2"	8.75	0.0682	0.0010	14.7	13.6	0.2
H-3"	7.92	0.0944	0.0007	10.6	9.5	0.1
H-3'	8.11	0.152	0.004	6.58	5.45	0.18
H-2'	8.20	0.262	0.009	3.82	2.61	0.14
H-3	8.47	0.382	0.017	2.62	1.44	0.12
H-2	8.92	0.399	0.012	2.51	1.57	0.08
Me	4.50	0.281	0.003	3.56	2.14	0.13

Experiment 3: [STRBPY] = 0.0573 M [Ni^{+2}] = 0.0137 M

Proton	Shift	T_1 (s)	Error	k_{obs} (s^{-1})	k_{corr} (s^{-1})	Error
H-2"	8.75	0.0455	0.0016	22.0	21.0	0.8
H-3"	7.92	0.0654	0.0014	15.3	14.2	0.3
H-3'	8.11	0.114	0.003	8.77	7.64	0.27
H-2'	8.20	0.177	0.002	5.65	4.44	0.07
H-3	8.47	0.281	0.003	3.56	2.38	0.05
H-2	8.92	0.291	0.005	3.44	2.50	0.07
Me	4.50	0.211	0.004	4.74	3.32	0.15

Table A-15—Cont.

Experiment 4: [STRBPY] = 0.0566 M [Ni^{+2}] = 0.0169 M

Proton	Shift	T_1 (s)	Error	k_{obs} (s^{-1})	k_{corr} (s^{-1})	Error
H-2"	8.75	0.0379	0.0011	26.4	25.3	0.8
H-3"	7.92	0.0544	0.0015	18.4	17.3	0.5
H-3'	8.11	0.0935	0.0025	10.7	9.56	0.29
H-2'	8.20	0.155	0.002	6.45	5.25	0.11
H-3	8.47	0.241	0.005	4.15	2.97	0.09
H-2	8.92	0.251	0.004	3.98	3.05	0.07
Me	4.50	0.188	0.003	5.32	3.90	015

Experiment 5: [STRBPY] = 0.0533 M [Ni^{+2}] = 0.0333 M

Proton	Shift	T_1 (s)	Error	k_{obs} (s^{-1})	k_{corr} (s^{-1})	Error
H-2"	8.75	0.0264	0.0029	37.9	36.8	4.1
H-3"	7.92	0.0395	0.0030	25.3	24.2	1.9
H-3'	8.11	0.0633	0.0022	15.8	14.7	0.6
H-2'	8.20	0.099	0.0013	10.1	8.90	0.14
H-3	8.47	0.165	0.004	6.06	4.88	0.13
H-2	8.92	0.173	0.002	5.78	4.85	0.07
Me	4.50	0.124	0.003	8.07	6.64	0.24

Experiment 6: [STRBPY]= 0.0533 M [Ni^{+2}] = 0.0333 M

Proton	Shift	T_1 (s)	Error	k_{obs} (s^{-1})	k_{corr} (s^{-1})	Error
H-2"	8.75	0.0225	0.0004	44.4	43.4	0.7
H-3"	7.92	0.0374	0.0013	26.7	25.6	0.9
H-3'	8.11	0.0505	0.0014	19.8	18.7	0.6
H-2'	8.20	0.0968	0.0023	10.3	9.12	0.25
H-3	8.47	0.147	0.002	6.80	5.62	0.08
H-2	8.92	0.134	0.002	7.46	6.53	0.11
Me	4.50	0.106	0.002	9.43	8.01	0.24

Table A-16: Second-Order Rate Constants (k_2) for STRBPY in D_2O with $NiCl_2$ at 25 °C.

Experiment: STRBPY with $NiCl_2$ in D_2O/DMSO

Proton	Slope (k_2)	Error	Intercept	Corr. Coef.	# of Pnts.	R (A)
H-2"	1250	46	2.66	0.996	5	3.1
H-3"	1010	67	0.362	0.999	4	5.1
H-3'	549	26	0.356	0.994	5	6.8
H-2'	271	13	0.335	0.999	5	9.1
H-3	170	5	0.0134	0.999	5	10.8
H-2	199	6	-0.178	0.999	5	13.1
Me	236	13	0.0842	0.999	5	14.9

Table A-17: T_1 Relaxation Times and Rate Constants for MEPYR in D_2O with $NiCl_2$ at 25 °C.

Experiment: MEPYR with $NiCl_2$ in D_2O

Correction Values:		[MEPYR]=	0.100 M	$[Ni^{+2}]$ =	0 M		
Proton	Shift	T_1 (s)	Error	k_{solv} (s^{-1})	Error		
H-2	8.84	13.68	1.48	0.073	0.008		
H-3	8.11	15.32	2.19	0.065	0.009		
H-4	8.60	21.14	2.57	0.047	0.006		
Me	4.45	7.246	0.47	0.138	0.009		
Experiment 1:		[MEPYR]=	0.0980 M	$[Ni^{+2}]$ =	0.00588 M		
Proton	Shift	T_1 (s)	Error	k_{obs} (s^{-1})	k_{corr} (s^{-1})	Error	
H-2	8.79	3.83	0.23	0.261	0.188	0.018	
H-3	7.94	3.92	0.29	0.255	0.190	0.021	
H-4	8.42	3.94	0.230	0.254	0.207	0.020	
Me	4.50	3.22	0.13	0.311	0.173	0.015	
Experiment 2:		[MEPYR]=	0.0952 M	$[Ni^{+2}]$ =	0.0143 M		
Proton	Shift	T_1 (s)	Error	k_{obs} (s^{-1})	k_{corr} (s^{-1})	Error	
H-2	8.78	2.02	0.03	0.495	0.422	0.012	
H-3	7.94	2.05	0.07	0.488	0.423	0.019	
H-4	8.41	2.03	0.04	0.493	0.445	0.011	
Me	4.49	1.87	0.02	0.535	0.397	0.010	
Experiment 3:		[MEPYR]=	0.0926 M	$[Ni^{+2}]$ =	0.0222 M		
Proton	Shift	T_1 (s)	Error	k_{obs} (s^{-1})	k_{corr} (s^{-1})	Error	Error
H-2	8.79	1.28	0.07	0.781	0.708	0.044	6.18
H-3	7.94	1.31	0.04	0.763	0.698	0.026	3.67
H-4	8.41	1.30	0.04	0.769	0.722	0.022	3.00
Me	4.49	1.29	0.03	0.775	0.637	0.021	3.27

Table A-18: Second-Order Rate Constants (k_2) for MEPYR in D_2O with $NiCl_2$ at 25 °C.

Experiment: MEPYR with $NiCl_2$ in D_2O

Proton	Slope (k_2)	Error	Intercept	Corr. Coef.	# of Pnts.	R (A)
H-2	31.8	3.8	-0.102	0.997	3	UNK
H-3	31.1	2.9	-0.0022	0.998	3	UNK
H-4	31.5	5.7	0.0127	0.998	3	UNK
Me	28.4	2.3	0.00098	0.999	3	UNK

Table A-19: T_1 Relaxation Times and Rate Constants for MEPOX in D_2O with $NiCl_2$ at 25 °C.

Experiment: MEPOX with $NiCl_2$ in D_2O

Correction Values: [MEPOX]= 0.100 M [Ni^{+2}] = 0 M

Proton	Shift	T_1 (s)	Error	k_{solv} (s^{-1})	Error
H-2	8.60	4.25	0.53	0.235	0.029
H-3	8.21	2.87	0.62	0.348	0.076
H-3'	8.47	2.69	0.19	0.372	0.026
H-2'	8.98	3.22	0.19	0.311	0.019
Me	4.50	1.58	0.08	0.633	0.033

Experiment 1: [MEPOX]= 0.0980 M [Ni^{+2}] = 0.00588 M

Proton	Shift	T_1 (s)	Error	k_{obs} (s^{-1})	k_{corr} (s^{-1})	Error
H-2'	8.59	0.745	0.051	1.34	1.11	0.10
H-3'	8.20	1.43	0.08	0.699	0.351	0.086
H-3	8.47	1.61	0.08	0.621	0.249	0.041
H-2	8.98	1.80	0.08	0.556	0.245	0.030
Me	4.51	0.953	0.087	1.05	0.416	0.101

Experiment 2: [MEPOX]= 0.0952 M [Ni^{+2}] = 0.0143 M

Proton	Shift	T_1 (s)	Error	k_{obs} (s^{-1})	k_{corr} (s^{-1})	Error
H-2'	8.58	0.361	0.006	2.77	2.54	0.05
H-3'	8.19	1.04	0.07	0.962	0.613	0.100
H-3	8.46	1.62	0.39	0.617	0.246	0.152
H-2	8.97	1.92	0.83	0.521	0.210	0.200
Me	4.51	1.48	0.05	0.676	0.043	0.041

Experiment 3: [MEPOX]= 0.0926 M [Ni^{+2}] = 0.0222 M

Proton	Shift	T_1 (s)	Error	k_{obs} (s^{-1})	k_{corr} (s^{-1})	Error
H-2'	8.57	0.239	0.001	4.18	3.95	0.04
H-3'	8.19	0.683	0.007	1.46	1.12	0.08
H-3	8.46	0.873	0.012	1.15	0.774	0.030
H-2	8.97	0.942	0.016	1.06	0.751	0.026
Me	4.50	0.704	0.009	1.42	0.788	0.038

Experiment 4: [MEPOX]= 0.0909 M [Ni^{+2}] = 0.0273 M

Proton	Shift	T_1 (s)	Error	k_{obs} (s^{-1})	k_{corr} (s^{-1})	Error
H-2'	8.56	0.201	0.002	4.98	4.74	0.07
H-3'	8.19	0.590	0.011	1.70	1.35	0.08
H-3	8.45	0.731	0.017	1.37	0.996	0.041
H-2	8.97	0.782	0.018	1.28	0.968	0.035
Me	4.50	0.590	0.014	1.70	1.06	0.05

Table A-19—Cont.

Experiment 5: [MEPOX]= 0.0824 M $[Ni^{+2}]$ = 0.0529 M

Proton	Shift	T_1 (s)	Error	k_{obs} (s^{-1})	k_{corr} (s^{-1})	Error
H-2'	8.54	0.0940	0.0011	10.6	10.4	0.1
H-3'	8.19	0.305	0.005	3.28	2.93	0.09
H-3	8.43	0.353	0.021	2.83	2.46	0.17
H-2	8.95	0.451	0.013	2.22	1.91	0.06
Me	4.48	0.384	0.008	2.60	1.97	0.07

Table A-20: Second-Order Rate Constants (k_2) for MEPOX in D_2O with $NiCl_2$ at 25 °C.

Experiment: MEPOX with $NiCl_2$ in D_2O

Proton	Slope (k_2)	Error	Intercept	Corr. Coef.	# of Pnts.	R (A)
H-2	199	8	0.327	0.997	5	4.3
H-3	56.3	5.3	-0.107	0.996	5	6.5
H-3'	48.0	5.3	0.18	0.988	4	8.2
H-2'	35.7	2.4	0.00135	0.999	4	10.6
Me	33.7	4.0	0.145	0.993	4	12.3

Table A-21: T_1 Relaxation Times and Rate Constants for BPYNOX in D_2O with $NiCl_2$ at 25 °C.

Experiment: BPYNOX with $NiCl_2$ in D_2O

Correction Values: [BPYNOX] = 0.100 M $[Ni^{+2}]$ = 0 M

Proton	Shift	T_1 (s)	Error	k_{solv} (s^{-1})	Error
H-2'	8.61	2.27	0.2989	0.441	0.058
H-3'	7.70	2.77	0.8371	0.361	0.109
H-3	7.89	2.82	0.9642	0.355	0.121
H-2	8.40	4.1	1.2801	0.244	0.076

Experiment 1: [BPYNOX] = 0.0980 M $[Ni^{+2}]$ = 0.00588 M

Proton	Shift	T_1 (s)	Error	k_{obs} (s^{-1})	k_{corr} (s^{-1})	Error
H-2'	8.61	0.0544	0.0004	18.4	17.9	0.2
H-3'	7.71	0.111	0.001	9.01	8.65	0.13
H-3	7.91	0.191	0.002	5.24	4.88	0.13
H-2	8.38	0.144	0.003	6.94	6.70	0.16

Experiment 2: [BPYNOX] = 0.0952 M $[Ni^{+2}]$ = 0.0143 M

Proton	Shift	T_1 (s)	Error	k_{obs} (s^{-1})	k_{corr} (s^{-1})	Error
H-2'	8.61	0.0275	0.0003	36.4	35.9	0.5
H-3'	7.71	0.0505	0.0006	19.8	19.4	0.3
H-3	7.91	0.0888	0.0008	11.3	10.9	0.2
H-2	8.37	0.0669	0.0012	15.0	14.7	0.3

Table A-21—Cont.

Experiment 3: [BPYNOX] = 0.0926 M $[Ni^{+2}]$ = 0.0222 M

Proton	Shift	T_1 (s)	Error	k_{obs} (s^{-1})	k_{corr} (s^{-1})	Error
H-2'	8.61	0.0187	0.0002	53.5	53.0	0.6
H-3'	7.71	0.033	0.0003	30.3	29.9	0.3
H-3	7.93	0.0648	0.0014	15.4	15.1	0.4
H-2	8.36	0.0440	0.0008	22.7	22.5	0.5

Experiment 4: [BPYNOX] = 0.0909 M $[Ni^{+2}]$ = 0.0273 M

Proton	Shift	T_1 (s)	Error	k_{obs} (s^{-1})	k_{corr} (s^{-1})	Error
H-2'	8.62	0.0178	0.0004	56.2	55.7	1.3
H-3'	7.72	0.0257	0.0002	38.9	38.6	0.4
H-3	7.94	0.0538	0.0012	18.6	18.2	0.4
H-2	8.38	0.0412	0.0008	24.3	24.0	0.5

Table A-22: Second-Order Rate Constants (k_2) for BPYNOX in D_2O with $NiCl_2$ at 25 °C.

Experiment: BPYNOX with $NiCl_2$ in D_2O

Proton	Slope (k_2)	Error	Intercept	Corr. Coef.	# of Pnts.	R (A)
H-2'	2150	495	5.25	0.999	3	0.685
H-3'	1380	137	0.101	0.998	4	0.041
H-3	615	98	1.57	0.998	4	0.393
H-2	967	193	0.97	0.999	3	0.146

Table A-23: T_1 Relaxation Times and Rate Constants for MEBPY in D_2O with $NiBr_2$, Temperature Dependence.

Experiment: MEBPY with $NiBr_2$ in D_2O Temp. Study

Correction Values: [MEBPY]= 0.0952 M $[Ni^{+2}]$ = 0.0143 M

Proton	Shift	T_1 (s)	Error	k_{solv} (s^{-1})	Error
H-2'	8.81	4.11	0.19	0.243	0.011
H-3'	7.95	3.44	0.15	0.291	0.012
H-3	8.43	3.37	0.01	0.297	0.001
H-2	8.96	3.60	0.06	0.278	0.004
Me	4.52	1.68	0.06	0.595	0.020

Experiment 30 C: [MEBPY]= 0.0952 M $[Ni^{+2}]$ = 0.0143 M

Proton	Shift	T_1 (s)	Error	k_{obs} (s^{-1})	k_{corr} (s^{-1})	Error
H-2'	8.82	0.0731	0.0004	13.7	13.4	0.1
H-3'	7.97	0.106	0.001	9.43	9.14	0.03
H-3	8.44	0.222	0.001	4.51	4.21	0.03
H-2	8.97	0.613	0.001	1.63	1.35	0.01
Me	4.52	0.706	0.003	1.42	0.821	0.021

Table A-23—Cont.

Correction Values: [MEBPY]= 0.0952 M $[\mathrm{Ni}^{+2}]$ = 0.0143 M

Proton	Shift	T_1 (s)	Error	k_{solv} (s^{-1})	Error
H-2'	8.92	4.73	0.13	0.211	0.006
H-3'	8.06	4.16	0.12	0.240	0.007
H-3	8.54	4.16	0.02	0.240	0.001
H-2	9.07	4.45	0.11	0.225	0.006
Me	4.62	2.08	0.10	0.481	0.022

Experiment 40 C: [MEBPY]= 0.0952 M $[\mathrm{Ni}^{+2}]$ = 0.0143 M

Proton	Shift	T_1 (s)	Error	k_{obs} (s^{-1})	k_{corr} (s^{-1})	Error
H-2'	8.79	0.0425	0.0002	23.5	23.3	0.1
H-3'	7.94	0.0798	0.0002	12.5	12.3	0.1
H-3	8.41	0.243	0.001	4.12	3.88	0.01
H-2	8.93	0.757	0.003	1.32	1.10	0.01
Me	4.49	0.864	0.004	1.16	0.677	0.023

Correction Values: [MEBPY]= 0.0952 M $[\mathrm{Ni}^{+2}]$ = 0.0143 M

Proton	Shift	T_1 (s)	Error	k_{solv} (s^{-1})	Error
H-2'	9.03	5.09	0.07	0.196	0.003
H-3'	8.16	4.87	0.16	0.205	0.007
H-3	8.64	4.91	0.06	0.204	0.002
H-2	9.16	5.12	0.13	0.195	0.005
Me	4.72	2.32	0.05	0.431	0.010

Experiment 50 C: [MEBPY]= 0.0952 M $[\mathrm{Ni}^{+2}]$ = 0.0143 M

Proton	Shift	T_1 (s)	Error	k_{obs} (s^{-1})	k_{corr} (s^{-1})	Error
H-2'	8.79	0.0256	0.0002	39.1	38.9	0.3
H-3'	7.94	0.0740	0.0002	13.5	13.3	0.1
H-3	8.42	0.288	0.0004	3.47	3.27	0.01
H-2	8.95	0.940	0.010	1.06	0.869	0.013
Me	4.50	1.03	0.01	0.971	0.540	0.013

REFERENCES

1. *Beilsteins Handbuch der Organische Chemie, Supplement III/IV, Vol. 27/3;* Springer-Verlag: New York, 1983.

2. Karrer, P.; Krishna, H. *Helv. Chim. Acta* **1950**, *33*, 555.

3. Karrer, P.; Krishna, H. *Helv. Chim. Acta* **1952**, *35*, 459.

4. Matsukawa, T.; Hirano, H.; Iwatsu, T.; Yurugi, S. *J. Vitaminol.* **1957**, *3*, 213.

5. Matsukawa, T.; Matsukawa, T.; Hirano, H.; Iwatsu, T.; Yurugi, S. *J. Vitaminol.* **1957**, *3*, 213.

6. Matsukawa, T.; Iwatsu, T. *J. Vitaminol.* **1955**, *1*, 305.

7. Hirano, H.; Iwatsu, T.; Yurugi, S. *Yakugalu. Zasshi.* **1957**, *77*, 241.

8. Iwatsu, T. *Yakugalu. Zasshi.* **1955**, *75*, 677.

9. Bonvicino, G.; Hennessy, D. *J. Am. Chem. Soc.* **1957**, *79*, 6325.

10. Derome, A. *Modern NMR Techniques for Chemistry Research;* Pergamon Press: New York, 1987.

11. Silverstein, R.; Bassler, G.; Morrill, T. *Spectrometric Identification of Organic Compounds;* J. Wiley & Sons: New York, 1991.

12. Lambert, J.; Shurvell, H.; Lightner, D.; Cooks, R. *Introduction to Organic Spectroscopy;* Macmillan Publishing Company: New York, 1987.

13. Drago, R. *Physical Methods for Chemists;* Saunders College Publishing: Ft. Worth, TX, 1992.

14. Solomon, I. *Phys. Rev.* **1955**, *99*, 559.

15. Bloembergen, N. *J. Chem. Phys.* **1957**, *27*, 575.

16. De Boer, E.; Van Wlligen, H. *Prog. Nucl. Magn. Reson. Spectrosc.* **1967**, *2*, 111.

17. Eaton, D.; Phillips, W. *Adv. Magn. Reson.* **1965**, *1*, 103.

18. Kowalewski, J.; Nordenskiold, L.; Benetis, N.; Westland, P. *Prog. Nucl. Magn. Reson. Spectrosc.* **1985**, *17*, 141.

19. Chachaty, C. *Prog. Nucl. Magn. Reson. Spectrosc.* **1987**, *19*, 183.

20. Sloan, D.; Mildvan, A. *Biochemistry* **1974**, *13*, 1711.

21. Sloan, D.; Mildvan, A. *J. Biol. Chem.* **1976**, *251*, 2412.

22. Sloan, D.; Loeb, L.; Mildvan, A.; Feldmann, R. *J. Biol. Chem.* **1975**, *250*, 8913.

23. Doddrell, D.; Gregson, A. *Chem. Phys. Lett.* **1974**, *29*, 512.

24. Doddrell, D.; Pegg, D.; Bendall, M.; Gottlieb, P; Gregson, A.; Anker, M. *Chem. Phys. Lett.* **1976**, *39*, 65.

25. Doddrell, D.; Healy, P.; Bendall, M. *J. Magn. Reson.* **1978**, *29*, 163.

26. Fan, S.; Storer, A.; Hammes, G. *J. Am. Chem. Soc.* **1977**, *99*, 8293.

27. Bertini, I.; Luchinat, C. *NMR of Paramagnetic Molecules in Biological Systems*; The Benjamin/Cumming Publishing Company, Inc.: Menlo Park, CA, 1986.

28. Trecourt, F.; Mallet, M.; Marsais, F.; Queguiner, G. *J. Org. Chem.* **1988**, *53*, 1367.

29. Stille, J. *Angew. Chem., Int. Ed. Engl.* **1986**, *25*, 508.

30. Suzuki, A. *Acc. Chem. Res.* **1982**, *15*, 178.

31. Stille, J. *The Chemistry of the Metal-Carbon Bond*; John Wiley: New York, 1985.

32. Collman, J.; Hegedus, L.; Norton, J.; Finke, R. *Principles and Applications of Organotransition Metal Chemistry;* University Science Books: Mill Vallye, CA, 1987.

33. Negeishi, E.; Takahashi, T.; Baba, S.; Van Horn, D.; Okukado, N. *J. Am. Chem. Soc.* **1987**, *109*, 2393.

34. Amatore, C.; Pfluger, F. *Organometallics* **1990**, *9*, 2276.

35. Portnoy, M.; Milstein, D. *Organometallics* **1993**, *12*, 1655.

36. Fauvaque, J.; Pluger, F.; Troupel, M. *J. Organomet. Chem.* **1971**, *28*, 287.

37. Fitton, P.; Rick, E. *J. Organomet. Chem.* **1971**, *28*, 287.

38. Atwood, J. *Inorganic and Organometallic Reaction Mechanisms;* Brooks-Cole: Monterey, CA, 1985.

39. Farina, V.; Krishnan, B. *J. Am. Chem. Soc.* **1991**, *113*, 9585.

40. Ohe, T.; Miyaura, N.; Suzuki, A. *J. Org. Chem.* **1993**, *58*, 2201.

41. Heck, R. *Palladium Reagents in Organic Synthesis;* Academic Press: New York, 1985.

42. Isobe, K.; Kawaguchi, S. *Heterocycles* **1981**, *16*, 1603.

43. Amatore, C.; Jutand, A.; Suarez, A. *J. Am. Chem. Soc.* **1993**, *115*, 9531.

44. Grushin, V.; Alper, H. *Chem. Rev.* **1994**, *94*, 1047.

45. Thompson, W.; Jones, J.; Lyle, P.; Theis, J. *J. Org. Chem.* **1988**, *53*, 2052.

46. Wright, S.; Hageman, D.; McLure, L. *J. Org. Chem.* **1994**, *59*, 6095.

47. Zoltewicz, J.; Uray, G. *Bioorg. Chem.* **1994**, *22*, 1.

48. Hadjiliadis, N.; Markopoulos, J. *J. Chem. Soc., Dalton Trans.* **1981**, 1635.

49. Eliel, E.; Wilen, S. *Stereochemistry of Organic Compounds;* J. Wiley & Sons: New York, 1994.

50. Etter, M. *Acc. Chem. Res.* **1990**, *23*, 120.

51. Takamizawa, A.; Hirai, K.; Ishiba, T.; Makino, I. *Chem. Pharm. Bull.* **1971**, *19*, 759.

52. Siro, M.; Nakai, H.; Makino, I.; Takamizawa, A. *Acta. Crystallogr.* **1978**, *B34*, 3424.

53. Kemp, D.; O'Brien, J. *J. Am. Chem. Soc.* **1970**, *92*, 2554.

54. Clarke, G.; Sykes, P. *J. Chem. Soc.* **1967**, 1411.

55. Crabb, T.; Katritzky, A. *Adv. Heterocycl. Chem.* **1984**, *36*, 1.

56. Leeper, F.; Lowe, P. *Heterocycles* **1983**, *20*, 65.

57. Bau, R.; Hyun, Y.; Lim, J.; Choi, H.; Yannopoulos, A.; Hadjiliadis, N. *Inorg. Chim. Acta* **1988**, *150*, 107.

58. Brown, H.; Bell, H. *J. Org. Chem.* **1962**, 1928.

59. Schlesinger, H.; Brown, H.; Hoekstra, H.; Rapp, L. *J. Am. Chem. Soc.* **1953**, *75*, 199.

60. Lane, C. *Synthesis* **1975**, 135.

61. Cain, A.; Sullivan, G.; Roberts, J. *J. Am. Chem. Soc.* **1977**, *99*, 6423.

62. Kirby, A. *Adv. Phys. Org. Chem.* **1980**, *17*, 183.

63. Maier, G.; Metzler, D. *J. Am. Chem. Soc.* **1957**, *79*, 4387.

64. Chahine, J.; Dubois, J. *J. Chem. Soc., Perkin Trans. 2* **1989**, 25.

65. Chahine, J. *Adv. J. Chem. Soc., Perkin Trans. 2* **1990**, 1045.

66. Washabaugh, M.; Yang, C.; Hollenbach, A.; Chen, P. *Bioorg. Chem.* **1993**, *21*, 170.

67. Beak, P.; Snieckus, V. *Acc. Chem. Res.* **1982**, *15*, 306

68. Gilman, H. *J. Am. Chem. Soc.* **1951**, *73*, 32. Gilman, H.; Young, ; *J. Am. Chem. Soc.* **1934**, *56*, 1415.

69. Maggi, R.; Schlosser, M. *J. Org. Chem.* **1996**, *61*, 5430.

70. Snieckus, V. *Chem. Rev.* **1990**, *90*, 879.

71. Queguiner, G.; Marsais, F.; Snieckus, V.; Epsztajn, J. *Adv. Heterocycl. Chem.* **1991**, *52*, 189.

72. Rewcastle, G. W.; Katritzky, A. R. *Adv. Heterocycl. Chem.* **1993**, *56*, 157.

73. Kremer, T.; Junge, M.; Schleyer, P. v. R. *Organometallics* **1996**, *15*, 3345.

74. Farina, V. *Pure. Appl. Chem* **1996**, *68*, 73.

75. Turck, A.; Ple, N.; Tallon, V.; Queguiner, G. *Tetrahedron* **1995**, *51*, 13045.

76. Spotswood, T. M.; Tanzer, C. I. *Aust. J. Chem.* **1967**, *20*, 1227.

77. Mitchell, T. N. *Organ. Magn. Reson.* **1975**, *7*, 610.

78. Kaushal, P.; Mok, P. L. H.; Roberts, B. P. *J. Chem. Soc., Perkin Trans. 2* **1990**, 1663.

79. Osborne, A. G.; Green, R.; Sadler, I. H.; Reed, D. *Magn. Reson. Chem.* **1989**, *27*, 4.

80. Constable, E. C.; Seddon, K. R. *J. Chem. Soc., Chem. Commun.* **1982**, 34.

81. Ward, M. D. *J. Chem. Soc., Dalton Trans.* **1994**, 3095.

82. Zoltewicz, J.; Dill, C. *Tetrahedron* **1996**, *52*, 14469.

83. Constable, E. *Adv. Heterocycl. Chem.* **1989**, *34*, 1.

84. Constable, E. *Tetrahedron* **1992**, *48*, 10013.

85. Bardwell, D.; Barogelletti, F.; Cleary, R.; Flamigni, L.; Guardigili, M.; Jeffery, J.; Ward, M. *Inorg. Chem.* **1995**, *34*, 2438.

86. Gallo, R.; Roussel, C.; Berg, U. *Adv. Heterocycl. Chem.* **1988**, *43*, 173.

87. Zoltewicz, J.; Deady, L. *Adv. Heterocycl. Chem.* **1978,** *22,* 71.

88. Grimmett, M.; Keene, B. *Adv. Heterocycl. Chem.* **1988,** *43,* 127.

89. Moran, D.; Morton, G.; Albright, J. *J. Heterocycl. Chem.* **1986,** *23,* 1071.

90. Zoltewicz, J.; Bloom, L.; Kem, W. *J. Org. Chem.* **1992,** *57,* 2392.

91. Zoltewicz, J.; Cruskie, M.; Dill, C. *J. Org. Chem.* **1995** *60,* 264.

92. Terashima, M; Ishikura, M. *Adv. Heterocycl. Chem.* **1989** *46,* 143.

93. Abramovitch, R.; Barton, D.; Finet, J. *Tetrahedron* **1988,** *44,* 3039.

94. Undheim, K.; Benneche, T. *Heterocycles* **1990** *30,* 1155.

95. Gronowitz, S.; Bobosik, V.; Lawitz, K. *Chem. Scripta* **1984,** *23,* 120.

96. Benneche, T. *Acta Chem. Scand.* **1990,** *44,* 927.

97. Yamamoto, Y.; Yanagi, A. *Chem. Pharm. Bull.* **1982,** *30,* 2003.

98. Illuminati, G. *Adv. Heterocycl. Chem.* **1964,** *3,* 285.

99. Oae, S.; Furukawa, N. *Adv. Heterocycl. Chem.* **1989,** *48,*1.

100. Bunting, J. *Adv. Heterocycl. Chem.* **1979,** *25,* 1.

101. Krumholtz, P. *J. Am. Chem. Soc.* **1951,** *73,* 3487.

102. Zoltewicz, J.; Cross, R. *J. Chem. Soc., Perkin Trans.* 2 **1974,** 1363.

103. Ishikura, M.; Kamada, M.; Terashima, M. *Heterocycles* **1984,** *22,* 265.

104. Shepherd, R.; Fedrick, J. *Adv. Heterocycl. Chem.* **1965**, *4*, 145.

105. Bunting, J. *Tetrahedron* **1987**, *43*, 4277.

106. Bunting, J.; Chew, V.; Sindhuatmadja, S. *Can. J. Chem.* **1981**, *59*, 3195.

107. Ishikura, M.; Kamada, M.; Terashima, M. *Synthesis* **1984**, 936.

108. Zoltewicz, J.; Cruskie, M. *J. Org. Chem.* **1995**, *60*, 3487.

109. Bertini, I.; Luchinat, C.; Scozzafava, A. *Inorg. Chim. Acta* **1976**, *19*, 201.

110. Cramer, R.; Drago, R. *J. Am. Chem. Soc.* **1970**, *92*, 66.

111. Doddrell, D.; Roberts, J. *J. Am. Chem. Soc.* **1970**, *92*, 6839.

112. Zoltewicz, J.; Bloom, L. *J. Phys. Chem.* **1992**, *96*, 5156.

113. Johansen, O.; *Aust. J. Chem.* **1981**, *34*, 981.

114. Fielden, R.; Summers, L. *J. Het. Chem.* **1974**, *11*, 299.

115. Ishikura, M.; Ohta, T.; Terashima, M. *Chem. Pharm. Bull.* **1985**, *33*, 4755.

116. Takahashi, K.; Nihira, T.; Akiyama, K.; Ikegami, Y.; Fukuyo, E. *J. Chem. Soc., Chem. Commun.* **1992**, 620.

117. Yamamoto, Y.; Yanagi, A. *Chem. Pharm. Bull.* **1982**, 30, 1731.

118. Beller, M.; Fischer, H.; Herrmann, W.; Ofele, K.; Brossmer, C. *Angew. Chem. Int. Ed. Engl.* **1995**, *34*, 1844.

119. Herrmann, W.; Brossmer, C.; Ofele, K.; Reisinger, C.; Priermeier, T.; Beller, M.; Fischer, H. *Angew. Chem. Int. Ed. Engl.* **1995**, *34*, 1844.

120. Hunt, J.; Friedman, H. *Prog. Inorg. Chem.* **1983**, *30*, 359.

121. Desai, A.; Dodger, H.; Hunt, J. *J. Am. Chem. Soc.* **1969,** *91,* 5001.

122. Imhof, V.; Drago, R. *Inorg. Chem.* **1965,** *3,* 429.

123. Van Leeuwen, P. *Recl. Trav. Chim. Pays-Bas* **1967,** *86,* 247.

124. Reynolds, W. *Prog. Inorg. Chem.* **1970,** *12,* 1.

125. Schlafer, H.; Papitz, H. *Angew. Chem.* **1960,** *72,* 618.

126. Karayannis, N.; Pytlewski, L.; Mikulski, C. *Coord. Chem. Rev.* **1973,** *11,* 93.

127. Vegas, A.; Perez-Salazar, A.; Silio, F. *Acta. Crystallogr., Sect. B* **1979,** *35,* 3062.

128. Happe, J.; Ward, R. *J. Chem. Phys.* **1963,** *39,* 1211.

129. Faraglia, G.; Rossotti, F.; Rossotti, H. *Inorg. Chim. Acta* **1970,** *4,* 488.

130. Ronfard-Haret, J.; Chachaty, C. *J. Phys. Chem.* **1978,** *82,* 1541.

131. Sheldrick, G. **1995,** SHELXTL5. Siemens Analytical Instrumentation. Madison, WS.

132. Barry, B. *Errors In Practical Measurement in Science, Engineering, and Technology;* J. Wiley & Sons: New York, 1978.

BIOGRAPHICAL SKETCH

Carlton D. Dill was born on August 16, 1970 in Columbus, Georgia to Mr. and Mrs. Thomas R. Dill. Much of his young life was spent in Auburn, Alabama prior to moving to Kernersville, North Carolina in 1981. In North Carolina, Carlton attended East Forsyth High School, graduating in 1988. While in high school he was a member of the National Honors Society and a six-time letterman in cross-country and track.

In the fall of 1988, Carlton received a Chancellor's Scholarship from Appalachian State University in Boone, North Carolina. While there, he received the CRC Press Freshman Chemistry Award and the Senior Chemistry Award. He received the degree of Bachelor of Science in chemistry with a minor in mathematics in May, 1992.

In August of 1992, Carlton enrolled at the University of Florida to pursue the degree of Doctor of Philosophy in organic chemistry. He has received a teaching award as an instructor in the organic teaching laboratories. After the completion of his degree, he will be pursuing other interests in the field of chemistry.

I certify that I have read this study and that in my opinion it conforms to acceptable standards of scholarly presentation and is fully adequate, in scope and quality, as a dissertation for the degree of Doctor of Philosophy.

J. A. Zoltewicz

John A. Zoltewicz, Chairman
Professor of Chemistry

I certify that I have read this study and that in my opinion it conforms to acceptable standards of scholarly presentation and is fully adequate, in scope and quality, as a dissertation for the degree of Doctor of Philosophy.

Eric Enholm

J. Eric Enholm
Associate Professor of Chemistry

I certify that I have read this study and that in my opinion it conforms to acceptable standards of scholarly presentation and is fully adequate, in scope and quality, as a dissertation for the degree of Doctor of Philosophy.

Kirk S. Sch

Kirk S. Schanze
Associate Professor of Chemistry

I certify that I have read this study and that in my opinion it conforms to acceptable standards of scholarly presentation and is fully adequate, in scope and quality, as a dissertation for the degree of Doctor of Philosophy.

Robert Hanrahan

Robert J. Hanrahan
Professor of Chemistry

I certify that I have read this study and that in my opinion it conforms to acceptable standards of scholarly presentation and is fully adequate, in scope and quality, as a dissertation for the degree of Doctor of Philosophy.

William R Kem

William R. Kem
Professor of Pharmacology
and Therapeutics

This dissertation was submitted to the Graduate Faculty of the Department of Chemistry in the College of Liberal Arts and Sciences and to the Graduate School and was accepted as partial fulfillment of the requirements for the degree of Doctor of Philosophy.

August, 1997

Dean, Graduate School

LD
1780
1997
.D578

UNIVERSITY OF FLORIDA
3 1262 08555 0522